REPORT DOCUMENTATION PAGE

Form Approved
OMB No. 0704-0188

Public reporting burden for this collection of information is estimated to average 1 hour per response, including the time for reviewing instructions, searching existing data sources, gathering and maintaining the data needed, and completing and reviewing the collection of information. Send comments regarding this burden estimate or any other aspect of this collection of information, including suggestions for reducing this burden, to Washington Headquarters Services, Directorate for Information Operations and Reports, 1215 Jefferson Davis Highway, Suite 1204, Arlington, VA 22202-4302, and to the Office of Management and Budget, Paperwork Reduction Project (0704-0188), Washington, DC 20503.

1. AGENCY USE ONLY (Leave blank)	2. REPORT DATE	3. REPORT TYPE AND DATES COVERED
	4/30/96	Final 9/1/94 - 2/29/96

4. TITLE AND SUBTITLE Threshold and Suprathreshold Lateral Spatial Interactions in Brightness, Contrast and Stereoscopic Depth Perception

5. FUNDING NUMBERS

F49620-94-1-0445
(G)
3484/HS
61103D

6. AUTHOR(S)
Mark E. McCourt and Barbara Blakeslee

7. PERFORMING ORGANIZATION NAME(S) AND ADDRESS(ES)
North Dakota State University
Fargo, ND 58105-5075

8. PERFORMING ORGANIZATION REPORT NUMBER

AFOSR-TR-96
0255

9. SPONSORING / MONITORING AGENCY NAME(S) AND ADDRESS(ES)
AFOSR/NL
110 Duncan Avenue B115
Bollins AFB DC 20332-0001
Capt William P. Roach

11. SUPPLEMENTARY NOTES

12a. DISTRIBUTION / AVAILABILITY STATEMENT

Approved for public release;
distribution unlimited.

19960618 020

13. ABSTRACT *(Maximum 200 words)*

We measured the effects of stereoscopic and pictorial depth separation on a variety of phenomena involving lateral interactions in the luminance and contrast domains (e.g., grating induction, perceptual transparency, simulataneous brightness contrast and contrast-contrast). In addition, the early visual mechanisms underlying the formation of illusory contours were assessed by measuring the effects of illusory contours on the visibility of spatiotemporally limited targets (i.e., Gabor patches); and by measuring the effects of filtered noise textures on the strength of illusory contours. Finally, the temporal characteristics of the mechanisms underlying grating induction and simultaneous brightness contrast were measured.

14. SUBJECT TERMS	15. NUMBER OF PAGES
Vision, Threshold, Suprathreshold, Brightness, Contrast, Stereoscopic Depth	16. PRICE CODE

17. SECURITY CLASSIFICATION OF REPORT	18. SECURITY CLASSIFICATION OF THIS PAGE	19. SECURITY CLASSIFICATION OF ABSTRACT	20. LIMITATION OF ABSTRACT
U	U	U	U

29 MAY 1996

Final Technical Report (from 9/30/94-2/28/96)

1. Cover Sheet

P.I. Mark E. McCourt, Ph.D.
Department of Psychology
North Dakota State University
Fargo, ND 58105-5075

(701) 231-8625 (voice)
(701) 231-8426 (FAX)
mccourt@plains.nodak.edu

Grant #: F49620-94-1-0445

2. Objectives:

One objective of the proposed research was to quantitatively measure the effect of stereoscopic and pictorial depth separation on two well-known lateral interactions in the luminance and contrast domains: grating induction and contrast-contrast, respectively. A second objective was to measure the magnitude and character of lateral interactions within the domain of stereoscopic depth processing, and to compare the quantitative features of such depth interactions with those occurring in the luminance and contrast domains. The careful measurement of the similarities and/or differences in such interactions across the different domains will help unravel the important question of whether these lateral interaction effects reveal general or domain-specific processing strategies within the visual system. The planned experiments will enhance the understanding of the mechanistic bases of lateral interactions and their functional roles in normal visual perception.

Add: To quantitatively measure the effect of stereoscopic and pictorial depth separation on other induced brightness phenomena, such as simultaneous brightness contrast and transparency.

Add: To quantify the temporal characteristics of the mechanisms underlying grating induction and simultaneous brightness contrast.

Add: To explore and quantify the mechanisms of illusory contour formation by measuring 1) the effects of illusory contours on the visibility of spatiotemporally limited targets (i.e., Gabor patches); and 2) the effects of filtered noise textures on the strength of illusory contours.

The latter objectives are a natural outgrowth of the original objectives, which were to describe, using psychophysical methods, the mechanisms responsible for a wide range of lateral spatial interactions in the human visual system.

3. Status of Effort:

The equipment necessary to conduct these experiments (a psychophysical

display workstation from Vision Research Graphics) was ordered following final approval of the grant, on 11/1/94. The manufacturer delivered the equipment on 1/14/95. The programming necessary to produce the stimuli necessary to conduct the proposed experiments was written and debugged by 2/15/95. Given the abbreviated time to complete the stated goals, progress toward the stated objectives has been steady and good. A 6-month no-cost extension was granted in order to complete the remaining sets of proposed experiments.

4. Accomplishments/New Findings:

Summary:

We measured the effects of stereoscopic and pictorial depth separation on a variety of phenomena involving lateral interactions in the luminance and contrast domains (e.g., grating induction, perceptual transparency, simultaneous brightness contrast and contrast-contrast). In addition, the early visual mechanisms underlying the formation of illusory contours were assessed by measuring the effects of illusory contours on the visibility of spatiotemporally limited targets (i.e., Gabor patches); and by measuring the effects of filtered noise textures on the strength of illusory contours. Finally, the temporal characteristics of the mechanisms underlying grating induction and simultaneous brightness contrast were measured.

Specific findings:

Study 1: Comparison of spatial frequency response and spatial summation of suprathreshold lateral interactions: Grating induction and contrast-contrast (see attached manuscript).

Two suprathreshold lateral spatial interaction effects, grating induction [M.E. McCourt, Vis. Res., 22, 119, 1982] and contrast-contrast [C. Chubb, G. Sperling and J.A. Solomon, Proc. Natl. Acad. Sci., 86, 9631, 1989], were compared regarding their dependence upon inducing grating spatial frequency, "standard" grating contrast, and inducing grating extent. Both effects cause the contrast of "standard" gratings to be matched nonveridically. The magnitudes of each effect were measured in a common unit which indexed the nonveridicality of contrast matches across a large range of "standard" grating contrasts (±0.80). Grating induction possessed a low-pass spatial frequency response whereas that for contrast-contrast was high-pass; the two effects are equipotent at an inducing grating frequency of 1.0 c/d. At their optimal spatial frequencies grating induction magnitude was approximately 140% that of contrast-contrast. At an inducing grating contrast of 0.75, departures from veridical matching varied with "standard" grating contrast such that at low spatial frequencies (0.03125-0.125 c/d) grating induction produced a skewed unimodal pattern of nonveridical matching (peaking at "standard" grating contrasts of 0.60) which smoothly assumed a bimodal shape at intermediate spatial frequencies (0.25-2.0 c/d), peaking at "standard" grating contrasts of -0.20 and +0.60. Above 2.0 c/d grating induction magnitude grew

very weak. Contrast-contrast produced a symmetrical pattern of nonveridical contrast matching which was invariant with inducing grating spatial frequency; matching nonveridicality was maximal at "standard" grating contrasts of ±0.60.

Grating induction and contrast-contrast magnitudes decreased as inducing grating height decreased, implying that spatially extended mechanisms underlie both effects. At their optimal spatial frequencies the half-height summation space-constants for the two effects were 6° for grating induction, and 1.2° for contrast-contrast. As inducing grating spatial frequency increased to 4.0 c/d critical summation regions for grating induction decreased, while they increased for contrast-contrast. The integration regions of the two effects varied considerably with the contrast ratio of the inducing and "standard" grating, implying that submechanisms with differing spatial geometries are recruited with changing stimulus contrast.

Study 2: Facilitation of luminance grating detection by induced gratings (see attached preprint).

Grating induction causes a homogeneous test field surrounded by sinewave gratings to possess an induced counterphase grating [M.E. McCourt, Vis. Res., 22, 119, 1982]. Because there is currently no consensus about the stage of visual processing at which illusory phenomena such as simultaneous brightness contrast are signaled, the masking efficacy of induced gratings was assessed by measuring contrast detection thresholds for targets (sinewave luminance gratings) added in phase to both real and induced gratings which were matched in apparent contrast. At spatial frequencies below approximately 0.5 c/d target detection and discrimination were comparably facilitated by both real and induced low-contrast pedestals (0.5-2%). At higher spatial frequencies (above 1.0 c/d) facilitation continued to be observed for targets added in-phase to real grating pedestals, but occurred only for targets added out-of-phase with induced pedestal gratings. Higher inducing frequencies by themselves were not responsible for the observed phase shift of facilitation, however, since both real and induced pedestals produced similar target contrast discrimination functions when inducing frequency was varied by manipulating viewing distance (which holds the ratio of inducing grating period and test field height constant). The results imply the existence of at least two types of lateral interactive processes: one producing in-phase facilitation, and a second producing out-of-phase facilitation. The relative contribution of each process depends upon the ratio of inducing grating period and test field height.

Study 3: The differential effects of type 1 and type 2 illusory contours on spatial pattern detection and discrimination (see attached manuscript).

Illusory contours (IC's), like luminance-defined contours, possess neurophysiological correlates and interact with physical stimuli. IC's produced by either offset gratings (Type 1 IC's), or by Kanizsa-type inducers (Type 2 IC's), elicit neural responses in primate visual cortical areas V1 and V2, respectively. The effects

of Type 1 and Type 2 IC's on contrast discrimination thresholds for Gabor targets were assessed in order to infer the properties of the neural mechanisms which produce these contours in human observers. Type 1 and 2 IC strength was equated for all observers using a matching procedure. Increment thresholds for Gabor targets presented on Type 1 and 2 IC's were measured in four observers as a function of pedestal contrast (0-16%), spatial frequency (1.25-10 cpd, constant octave bandwidth) and orientation (0-90o relative to IC orientation). Relative to control conditions which possessed inducers but lacked IC's, Type 1 IC's masked, whereas Type 2 IC's facilitated target detection and discrimination at low (<5%) pedestal contrasts. At higher pedestal contrasts this relationship was reversed. Both Type 1 and Type 2 IC's interacted maximally with targets of approximately 5 c/d which were oriented parallel to the IC's. Both Type 1 and Type 2 IC's interacted maximally with Gabor targets whose spatial parameters are those which optimally stimulate primary visual cortical neurons. This finding suggests that Type 1 and Type 2 IC's share a common mechanism of early contrast transduction. Type 1 and 2 IC's equated in strength have opposite effects, however, on the detection and discrimination of Gabor targets. This latter finding suggests a dissimilarity in the pooling mechanisms which underlie the formation of Type 1 and 2 illusory contours.

Study 4: The effect of perceptual transparency on brightness perception (see attached manuscript).

Subjects matched the brightness of test patches located within a larger surround, where the surround was made to appear either different in reflectance from neighboring regions, or of the same reflectance but viewed beneath a transparent film. In both conditions the luminance and spatial extent of the immediate surround was equivalent, thus controlling for the effects of surround luminance and configuration. Perceived transparency had a significant effect on brightness: test patch brightness was significantly elevated when the perception of transparency was supported by stereo depth cues. The effect was, however, mediated by the virtual transmittance of the transparent overlay, increasing in magnitude with decreasing transmittance. Further, the effect of transparency on brightness was greatest for test patch luminances near to those of their immediate backgrounds. The implications of these results for the understanding of configurational effects on brightness is discussed.

Study 5: Temporal determinants of grating induction: Modulation transfer function and impulse response measures in stabilized and unstabilized viewing.

Grating induction [M.E. McCourt, Vis. Res., 22, 119, 1982] is a brightness effect which, like classical brightness contrast, is dependent on suprathreshold lateral interactions. Classical brightness contrast is a sluggish process, possessing a cut-off frequency of approximately 2.5 Hz [R.L. DeValois, M.A. Webster, K.K. DeValois and B. Lingelbach, Vision Research, 26, 887, 1986] which decreases with increasing target area [A.F. Rossi and M.A. Paradiso, Investigative Ophthalmology & Visual Science (Suppl.), 35, 9. 1994]. An edge-generated brightness fill-in process has been proposed

to underlie classical brightness contrast [M.A. Paradiso and K. Nakayama, Vision Research, 31, 1221, 1991].

Grating induction does not depend on sharp edges [M.E.McCourt and B. Blakeslee, Vision Research, 33, 2499, 1993] possesses a different dependence on stimulus contrast and luminance, and so may arise from entirely different lateral spatiotemporal interactions. The temporal properties of grating induction were assessed in order to further determine whether the lateral interactions underlying these effects are similar.

In Experiment 1 inducing grating drift frequency was varied from 0.24 to16.4 Hz under retinally stabilized viewing. Method of adjustment (25 canceling settings per frequency) was used to assess induction magnitude at each temporal frequency. In Experiment 2 The duration of tachistoscopic presentation of the induction display was varied from 16.7 to 4000 ms. Method of constant stimuli (10 phase judgments at each "standard" grating contrast) was used to determine induction magnitude at each stimulus duration. Inducing grating height was 16° (Experiment 1) or 32° (Experiment 2). Test field heights were 0.5° and 1.0°. In both experiments inducing grating spatial frequency was 0.125 c/d; inducing grating contrast was 0.4.

Under stabilized viewing conditions canceling contrast is a low-pass function of inducing grating temporal frequency. Grating induction has a temporal cut-off well above 10 Hz. The method of least-squares was used to fit the canceling data to a frequency-domain gamma function: $H(\omega,\alpha,\tau,n) = \alpha((2\pi\omega\tau)2+1)(-n/2)$, where ω is temporal frequency, α is a scaling factor, τ is the time-constant and n is the number of cascaded low-pass filter stages. Optimized parameter values were:

Subject MM (0.5° test field): $\alpha = 0.265$; $\tau = 5.9$ ms; $n = 15$
(1.0° test field): $\alpha = 0.200$; $\tau = 6.4$ ms; $n = 15$

Subject EM-U (0.5° test field): $\alpha = 0.210$; $\tau = 9.9$ ms; $n = 15$
(1.0° test field): $\alpha = 0.153$; $\tau = 11.1$ ms; $n = 15$

The parameters of the frequency-domain gamma functions were used to derive normalized time-domain impulse response functions: $h(t,\tau,n) = (t/\tau)(n-1)\, e(-t/\tau)$, where t is time and τ is the function time-constant. The value of n is the number of cascaded low-pass filter stages.

The time-to-peak of the grating induction process is given by the product of τ and n. These values are 88.5 ms and 96.0 ms (for MM), and 148.5 ms and 166.5 ms (for EM-U), for the 0.5° and 1.0° test field conditions, respectively.

Psychometric functions relating test field appearance (e.g., whether the grating seen in the test field was "in phase" or "out of phase" with the surrounding inducing grating) to "standard" grating contrast were obtained for each stimulus duration. Probit

fits were performed to determine canceling contrast at each stimulus duration. Grating induction magnitude increases with the stimulus duration, reaching asymptotic levels after approximately 400 ms. Mean canceling contrast for subjects MM and BB were fit using a rising exponential function: $f(t,\alpha,\sigma) = \alpha(1-e^{(-\sigma t)})$, where t is stimulus duration, α is the asymptotic level of canceling contrast, and $1/\sigma$ is the time-constant for temporal summation. For the 0.5° test field the optimized parameter values were $\alpha = 0.236$ and $1/\sigma = 83$ ms. Conclusions were that: 1) Scanning eye movements across the test field are not responsible for grating induction; 2) There is good agreement between direct and indirect measures of the temporal properties of grating induction; 3) The frequency response of grating induction exceeds that for classical brightness contrast by a factor of three, and that for afterimages by a factor of 10; 4) Grating induction time constants vary minimally with increasing test field size, suggesting that a fill-in process is not involved in grating induction; and 5) Common neural mechanisms are unlikely to underlie the superficially similar effects of grating induction and classical brightness contrast.

5. Personnel Supported:

Mark E. McCourt, Ph.D. (PI/PD)
Barbara Blakeslee, Ph.D. (Co-I)
Heidi Hoistad, B.S. (Graduate Research Assistant)
Christopher Sackmann (Undergraduate Research Assistant)

6. Publications:

Papers:

McCourt M.E. and Kingdom, F.A.A. (1996) Facilitation of luminance grating detection by induced gratings (Vision Research, in press).

Kingdom, F.A.A., McCourt, M.E. and Blakeslee, B. (1996) In defense of lateral inhibition as the underlying cause of simultaneous brightness contrast. A reply to Spehar, Gilchrist and Arend (Vision Research, in press).

McCourt M.E. (1996) Comparison of spatial frequency response and spatial summation of suprathreshold lateral interactions: Grating induction and contrast-contrast (submitted to Vision Research).

McCourt, M.E. and Sackmann, C. (1996) The differential effects of type 1 and type 2 illusory contours on spatial pattern detection and discrimination: Threshold estimates. (submitted to Vision Research).

Sackmann, C. and McCourt, M.E. (1996) Spatiotemporal tuning of early mechanisms contributing to type II illusory contours: Suprathreshold estimates. (submitted to Vision Research).

Kingdom, F.A.A., Blakeslee, B. and McCourt, M.E. (1996) The effect of perceptual transparency on brightness perception. (submitted to Perception).

McCourt, M.E. and Blakeslee, B. (1996) Lightness, brightness and transparency in the Argyle illusion. (submitted to Perception).

McCourt, M.E. and Olafson, C.L. (1996) Cognitive and perceptual influences on visual line bisection: Psychophysical and chronometric analyses of pseudoneglect. (submitted to Neuropsychologia).

McCourt, M.E., Mark, V.W. Radonovich, K.J., Willison, S. and Freeman, P. (1996) The effects of gender, practice and menstrual phase on the perceived location of the midsagittal plane. (submitted to Neuropsychologia).

McCourt M.E., Blakeslee, B. and Uriegas-Martinez, E. Temporal determinants of grating induction: Modulation transfer function and impulse response measures in stabilized and unstabilized viewing (in preparation).

McCourt, M.E. and Kingdom, F.A.A. Masking and adaptation reveals anisotropic visual filters underlie grating induction (in preparation).

McCourt, M.E. and Blakeslee, B. Subtractive and multiplicative adaptation processes in grating induction (in preparation).

Abstracts:

Blakeslee, B and McCourt, M.E. (1996) Does a Single Mechanism Underlie Simultaneous Brightness Contrast and Grating Induction? Investigative Ophthalmology and Visual Science (Suppl.), 37, S1066.

Sackmann, C. and McCourt, M.E. (1996) the Differential Effects of Type 1 and Type 2 Illusory Contours on Spatial Pattern Detection and Discrimination. Investigative Ophthalmology and Visual Science (Suppl.), 37, S520.

McCourt, M.E., Olafson, C. and Sackmann, C. (1996) Cognitive and Perceptual Influences on Visual Line Bisection in Normal Observers: Psychophysical and Chronometric Analyses of Pseudoneglect. Investigative Ophthalmology and Visual Science (Suppl.), 37, S174.

McCourt, M.E., Martinez-Uriegas, E. and Blakeslee, B. (1995) Temporal Properties of Grating Induction. Investigative Ophthalmology and Visual Science (Suppl.), 36, S469.

McCourt, M.E. and Kingdom, F.A.A. (1994) Facilitation of luminance grating detection by induced gratings. Investigative Ophthalmology and Visual Science (Suppl.),

35, S1901.

7. Interactions/Transitions:

a. Participation/presentations at meetings:

McCourt, M.E., Blakeslee, B. and Kingdom, F.A.A. The Effect of Perceived Transparency on Brightness Judgments. Optical Society of America Annual Meeting, 1997 (submitted).

Sackmann, C. and McCourt, M.E. Suprathreshold Measures of the Mechanisms Mediating Kanizsa-type Illusory Contours. Optical Society of America Annual Meeting, 1997 (submitted).

McCourt, M.E., Olafson, C. and Sackmann, C. Cognitive and Perceptual Influences on Visual Line Bisection in Normal Observers: Psychophysical and Chronometric Analyses of Pseudoneglect. ARVO, 1996.

Blakeslee, B and McCourt, M.E. Does a Single Mechanism Underlie Simultaneous Brightness Contrast and Grating Induction? ARVO, 1996.

Sackmann, C. and McCourt, M.E. The Differential Effects of Type 1 and Type 2 Illusory Contours on Spatial Pattern Detection and Discrimination. ARVO, 1996.

McCourt, M.E., Martinez-Uriegas, E. and Blakeslee, B. Temporal Properties of Grating Induction. ARVO, 1995.

Sackmann, C. and McCourt, M.E. Type 1 and Type 2 illusory contours differentially affect contrast discrimination thresholds for Gabor targets. 1995 North Dakota Science, Engineering and Mathematics Undergraduate Poster Session (ND EPSCoR), North Dakota State University, (July, 1995).

McCourt, M.E. and Kingdom, F.A.A. Facilitation of luminance grating detection by induced gratings. ARVO, 1994.

McCourt, M.E., Mark, V.W., Willison, S., Radonovich, K.J. and Freeman, P. (1996) The Influence of Gender and Menstrual Phase on the Perceived Location of the Midsagittal Plane. Annual Meeting of the Midwest Psychological Association, Chicago, IL (April, 1996).

McCourt, M.E. Cognitive and perceptual influences on line bisection: Psychophysical and chronometric analyses. Presented at Third Annual Symposium on Alzheimer Disease, September, 1995. (invited presentation).

Annual meeting of the Optical Society of America, Dallas, TX, October, 1994,

(attended).

b. Consultative/Advisory: None.

c. Transitions: None.

8. **New Discoveries, inventions or patent disclosures: None.**

9. **Honors/Awards:** None.

COMPARISON OF SPATIAL FREQUENCY RESPONSE AND SPATIAL SUMMATION OF TWO SUPRATHRESHOLD LATERAL INTERACTIONS: GRATING INDUCTION AND CONTRAST-CONTRAST

Mark E. McCourt
Department of Psychology
North Dakota State University
Fargo, ND 58105-5075
U.S.A.

CIG14
submitted 5/17/96
to Vis. Res.

Tel: (701) 231-8625
FAX: (701) 231-8426
e-mail: mccourt@plains.nodak.edu

Key Words: Grating Induction, Brightness Contrast, Brightness Matching, Contrast Matching, Contrast-Contrast, Lateral Inhibition, Contrast Response, Suprathreshold

ABSTRACT

Two suprathreshold lateral spatial interaction effects, grating induction [M.E. McCourt, Vis. Res., 22, 119, 1982] and contrast-contrast [C. Chubb, G. Sperling and J.A. Solomon, Proc. Natl. Acad. Sci., 86, 9631, 1989], were compared regarding their dependence upon inducing grating spatial frequency, "standard" grating contrast, and inducing grating extent. Both effects cause the contrast of "standard" gratings to be matched nonveridically. The magnitudes of each effect were measured in a common unit which indexed the nonveridicality of contrast matches across a large range of "standard" grating contrasts (±0.80). Grating induction possessed a low-pass spatial frequency response whereas that for contrast-contrast was high-pass; the two effects are equipotent at an inducing grating frequency of 1.0 c/d. At their optimal spatial frequencies grating induction magnitude was approximately 140% that of contrast-contrast. At an inducing grating contrast of 0.75, departures from veridical matching varied with "standard" grating contrast such that at low spatial frequencies (0.03125-0.125 c/d) grating induction produced a skewed unimodal pattern of nonveridical matching (peaking at "standard" grating contrasts of 0.60) which smoothly assumed a bimodal shape at intermediate spatial frequencies (0.25-2.0 c/d), peaking at "standard" grating contrasts of -0.20 and +0.60. Above 2.0 c/d grating induction magnitude grew very weak. Contrast-contrast produced a symmetrical pattern of nonveridical contrast matching which was invariant with inducing grating spatial frequency; matching nonveridicality was maximal at "standard" grating contrasts of ±0.60.

Grating induction and contrast-contrast magnitudes decreased as inducing grating height decreased, implying that spatially extended mechanisms underlie both effects. At their optimal spatial frequencies the half-height summation space-constants for the two effects were 6° for grating induction, and 1.2° for contrast-contrast. As inducing grating spatial frequency increased to 4.0 c/d critical summation regions for grating induction decreased, while they increased for contrast-contrast. The integration regions of the two effects varied considerably with the contrast ratio of the inducing and "standard" grating, implying that submechanisms with differing spatial geometries are recruited with changing stimulus contrast.

INTRODUCTION

Grating induction is a suprathreshold lateral spatial interaction effect which causes spatially homogeneous regions of visual space to appear to contain luminance variations which are counterphase versions of the surrounding inducing gratings (McCourt, 1982). Induced gratings produce misperceptions of both the contrast and phase of physical luminance gratings added to them (McCourt & Blakeslee, 1994). Contrast-contrast is a more recently discovered suprathreshold lateral interaction in which the perceived contrast of a "victim" texture (or grating) is reduced when it is situated near a higher contrast surrounding equiluminant inducing texture (Chubb, Sperling & Solomon, 1989; Solomon, Sperling & Chubb, 1993) or grating (Cannon & Fullencamp, 1991, 1993; 1996). One important similarity between the two phenomena is that both almost certainly reflect the operation of various intensity (i.e., luminance and/or contrast) normalization processes which enable "seeing" at suprathreshold intensity levels. Beyond this broad generalization, however, data concerning the quantitative similarities and differences between these two effects, or their relationship to other normalization processes (e.g., light and contrast adaptation) are scant. The present paper describes results from two experiments. Experiment 1 compares grating induction and contrast-contrast with respect to their dependence upon the spatial frequency of the inducing grating in conjunction with the contrast of a series of "standard" victim gratings. Experiment 2 assess areal integration and measures the dependence of each type of effect upon the spatial extent of the inducing grating.

EXPERIMENT 1: EFFECT OF INDUCING GRATING SPATIAL FREQUENCY AND "STANDARD" GRATING CONTRAST

METHODS

Subjects

The author, MEM, and five additional observers, DAB, MAS, SF, SM and TK, participated as subjects. Observers MEM, SF, SM and TK were male; DAB and MAS were female. Subjects possessed normal or corrected-to-normal vision and, except for observer MEM, were naive to the

purposes of the experiment. All were well-practiced as psychophysical observers.

Instrumentation and Calibration

Stimuli were generated and presented by computer (DEC PDP 11/73), and were displayed on an RGB display monitor (Conrac 7211) in yoked-gun (white) mode at a frame-rate of 60 Hz. Images appeared in square aspect ratio at a resolution of 512^2 pixels; pixels possessed 2^8 linear luminance levels. Luminance and contrast calibrations were made using a Spectra Brightness Spotmeter (model UB 1/2°) and/or a photodiode/preamplifier combination, corrected for the human photopic luminosity function (United Detector Technology, photodiode PIN 10AP/UDT101A preamplifier).

Stimuli

To facilitate the comparison of the two suprathreshold effects, stimuli were presented in a common format, consisting of two variations of grating induction type displays which have been described in detail elsewhere (McCourt & Blakeslee, 1994). Figure 1 presents photographs of several displays used in the experiment, and perceptually demonstrates several of the empirical

---

Insert Figure 1 Here

---

results. "Standard" grating stimuli were centered in the upper half of the display and consisted of rectangular strips of vertically oriented sinewave luminance gratings. "Standard" gratings occupied the test field region of grating induction displays (McCourt, 1982), and possessed eleven levels of Michelson contrast: -0.80, -0.60, -0.40, -0.20, 0.0, 0.20, 0.40, 0.50, 0.60, 0.70 and 0.80. Vertically flanking the "standard" gratings were inducing gratings whose contrast was constant at 0.75. In experiments assessing grating induction magnitude the upper and lower inducing gratings were aligned in phase, and the sign associated with "standard" grating contrast indexes the spatial phase of the "standard" grating relative to the inducing grating. Specifically, [-] signifies the two are 180° out-of-phase, and [+] signifies that they are in-phase. In contrast-contrast experiments the upper and lower inducing gratings were offset in phase by 180°, and "standard" gratings were presented in 90° spatial phase to both. Here the sign associated with

"standard" grating contrast refers to either [+] or [-] 90° phase with respect to the upper inducing grating. Inducing and "standard" gratings possessed 10 spatial frequencies, arranged in octave intervals ranging from 0.03125 c/d to 16.0 c/d. Inducing and "standard" grating frequencies were always identical. Depending upon the spatial frequency of the inducing grating (in parentheses), four viewing distances were used: 26.5 cm (0.03125 c/d), 53 cm (0.0625-4.0 c/d), 106 cm (8.0 c/d) and 212 cm (16.0 c/d). At the viewing distance of 53 cm, for example, the entire display subtended 32° in height and width; display height and width scaled with viewing distance. Test field height, however, was constant at 0.5° across all viewing distances. A matching stimulus, consisting of a luminance grating of identical spatial frequency as the inducing and "standard" gratings, appeared in the lower half of the display. Matching gratings, like "standard" gratings, subtended 0.5° in height and varied in width according to viewing distance; they were vertically centered within the lower half of the display.

Procedures

Somewhat different procedures were employed to assess the magnitude of grating induction and contrast-contrast. The magnitude of grating induction was assessed using a matching technique as described previously (McCourt & Blakeslee, 1994). Inducing gratings with identical spatial phase were presented above and below a test field, and a variety of fixed "standard" contrast gratings were added to the test field, either in-phase [+], or 180° out-of-phase [-] with the surrounding inducing gratings. Observers adjusted the contrast (and hence the phase, via contrast reversal) of the matching grating until it appeared to possess a contrast identical to that of the "standard" grating. Grating induction magnitude decreases as the upper and lower inducing gratings become misaligned in phase (Zaidi, 1989; McCourt & Blakeslee, 1994), and grating induction magnitude is zero for upper and lower inducing gratings misaligned by 180°[1]. As illustrated in Fig. 1, the magnitude of contrast-contrast was therefore assessed by

[1] Bright and dark meniscuses can be observed at the borders of the test and inducing fields when the upper and lower inducing gratings are misaligned by 180° spatial phase. However, these brightness variations are probably unrelated to the grating induction effect since they diminish in contrast very rapidly across space, extending to less than half the full test field width, they are demodulated by blurring the test/inducing field border whereas grating induction is not, and they do not complete across the test field to form a coherent plaid grating percept.

shifting the relative phase of the upper and lower inducing gratings by 180° (by + and - 90°, respectively), which eliminates grating induction, and by adding "standard" gratings to the test field in an intermediate (i.e., 0°) spatial phase [2]. The assumption that contrast-contrast magnitude is stable with these changes in inducing grating phase is discussed and evaluated below.

Stimuli were presented on each trial for a duration of 2 sec, during which time subject responses were polled by computer. Stimulus contrast was zeroed between presentations, and mean display luminance was constant at 66 cd/m^2. To begin each adjustment trial matching contrast was randomly assigned a value between 0 and 1.0, and subjects subsequently increased or decreased the contrast of the matching grating by depressing appropriate response buttons. Each button press was echoed by a brief tone pip and resulted in a change of 0.0006 in matching grating contrast. Subjects indicated the completion of each matching setting by depressing a "done" button. All adjustment settings were recorded by computer, which also sequenced and initiated each block of adjustment trials. Five or ten matching settings were obtained from each subject in each experimental condition. Trials assessing grating induction and contrast-contrast were presented in separate blocks, as were trials assessing different levels of inducing grating spatial frequency. The values of "standard" test field contrast were quasi-randomly interleaved within blocks.

Natural eye movements do not produce or otherwise affect the magnitude of grating induction (Foley & McCourt, 1985). Stimuli were viewed binocularly through natural pupils in an otherwise moderately illuminated room, such that the state of light adaptation was held constant.

---

[2] As is apparent in Figs. 1(c) and (f), any reductions in apparent contrast of the "standard" grating due to contrast-contrast are accompanied by a pronounced induced tilt of the "standard" gratings away from vertical. This effect is interesting in its own right, and has been reported previously (Haig, 1989; McCourt, 1991). It does not influence contrast judgements, however, and a detailed treatment of the mechanisms of this illusory orientation shift is beyond the scope of the present paper.

RESULTS AND DISCUSSION

Analysis of Contrast Matching Data

Figure 2 presents examples of contrast matching functions which serve to illustrate the pattern of original data and the method by which the magnitudes of contrast-contrast and grating induction were computed. In Fig. 2(a) the mean of ten matching contrast settings (with 99% confidence intervals) is plotted, for subject DAB, as a function of "standard" grating contrast, for an inducing grating frequency of 0.03125 c/d. Open symbols refer to contrast matches in grating induction conditions (i.e., for phase-aligned inducing gratings), and filled symbols refer to contrast matches made in the contrast-contrast conditions (i.e., with 180° phase-offset inducing gratings).

Insert Figure 2 Here

Both matching and "standard" grating contrasts are signed quantities where, for grating induction, the sign denotes either the perceived spatial phase (for matching grating contrast) or the physical spatial phase (for "standard" grating contrast) of each type of grating with respect to inducing grating spatial phase: [-] signifies that the "standard" or matching gratings are (or are perceived to be) out-of-phase, and [+] signifies that the "standard" or matching gratings are (or are perceived to be) in-phase with the inducing grating. For contrast-contrast conditions the sign associated with "standard" grating contrast again refers to the physical spatial phase of the "standard" grating: it is in either [+]90° or [-]90° phase with respect to the upper inducing grating.

As illustrated in Figs. 2(a, f and g), however, the spatial phase of "standard" gratings is never misperceived in contrast-contrast conditions (filled symbols). Accordingly, the sign associated with "standard" and matching grating contrast is never discrepant; all matching data points lie in either the lower left or upper right quadrants of the graphs. By comparison, in grating induction displays (open symbols) it is not uncommon for induction to cause even relatively high-contrast "standard" gratings (e.g., +0.50) to appear to be (and hence to be matched by) gratings of opposite spatial phase (i.e., negative contrast). Such matches are plotted in the lower right quadrants of these diagrams, e.g., Fig. 2(a).

Veridical contrast matches in Figs. 2(a,f and g) will lie along the dashed diagonal lines. To the extent that contrast-contrast reduces the perceived contrast of the "standard" grating, contrast matching will be nonveridical. Matching in contrast-contrast (phase-offset) conditions is indeed observed to systematically depart from veridicality, such that the absolute value of matching contrast is invariably lower than "standard" contrast. This undermatching is consistent with previous reports, and is the defining characteristic of the contrast-contrast effect (Chubb et. al., 1989; Cannon & Fullencamp, 1991, 1993).

An index of the magnitude of the contrast-contrast effect is obtained from these matching data by numerically integrating the area (either across the entire abscissa, or within selected subregions) between the interpolated matching functions and the diagonal line which denotes veridicality. This area is indicated by vertical hatching in Fig. 2(b), and is replotted in Fig. 2(d) on an ordinate which indexes the difference between "standard" and matching grating contrast. This difference is by definition positive for "standard" contrasts whose absolute value exceeds matching contrast (i.e., for undermatches). Similar plots which illustrate the magnitude of contrast-contrast (phase-offset conditions) as a function of "standard" grating contrast at inducing grating spatial frequencies of 1.0 and 16.0 c/d appear in Figs. 2(h) and (i), respectively. Since phase-offset inducing gratings produce no induction in homogeneous test fields (Zaidi, 1989), matching contrast in the contrast-contrast condition for "standard" gratings of zero contrast is defined as zero.

The extent to which the magnitude of contrast-contrast varies with the relative spatial phase of surrounding textures has not been well quantified. Chubb et. al. (1989), however, observed robust contrast-contrast effects in displays where both inducing and victim (i.e., "standard") textures were two-dimensional bandpass filtered noise patterns, which possess broad phase spectra. Similarly, Solomon et al. (1993) report the occurrence of contrast-contrast effects between texture pairs with broad phase spectra (i.e., dot patterns) designed to selectively stimulate either the on- or off-center systems. Whether or not the contrast-contrast effect is phase-independent, the results of the present experiments themselves reveal that contrast-contrast effects are at least equivalent (for frequencies up to 4.0 c/d) in phase-aligned and

phase-offset displays (e.g., Fig.2g). Based on this latter evidence it is assumed for purposes of analysis that the magnitude of contrast-contrast at all spatial frequencies is equivalent in the phase-aligned and phase-offset inducing grating conditions. The principal implication of this assumption is that an unconfounded assessment of grating induction magnitude must take account of simultaneously occurring contrast-contrast effects. Grating induction magnitude was therefore computed by numerically integrating the area between the matching functions obtained in the phase-aligned (grating-induction) and phase-offset (contrast-contrast) conditions. An example of such an area appears as the vertical hatched region in Fig. 2(c), and is replotted in Fig. 2(e) on a transformed ordinate. Similarly transformed plots of grating induction magnitude at inducing frequencies of 1.0 and 16.0 c/d appear in Figs. 2(j) and (k), respectively. By numerically integrating the areas between the contrast matching functions, a comprehensive assessment of both the overall magnitude and the local structure of both the grating induction and contrast-contrast effects is obtained which allows them to be compared using a common unit: contrast squared [3].

Effect of Inducing Grating Spatial Frequency

The magnitudes of contrast-contrast (filled symbols) and grating induction (open symbols) for the six observers, expressed in units of total integrated contrast area, are plotted as a function of inducing grating spatial frequency in Figure 3. Solid lines smoothly interpolate the aggregate mean values.

Consistent with previous reports (McCourt, 1982, Foley & McCourt, 1985) grating induction is a low-pass effect which, for a test field of 0.5°, is extinguished at inducing grating frequencies above 10 c/d. Contrast-contrast possesses either a highpass or bandpass

---

Insert Figure 3 Here

---

[3] Since the contrast-contrast effect is symmetrical with positive and negative "standard" grating contrast, total integrated contrast area for both grating induction and contrast-contrast (e.g., Fig 3) does not depend on the validity of the assumption that the magnitude of contrast-contrast is equivalent for phase-aligned and phase-offset inducing gratings.

frequency response, and is very weak (indeed, absent for some observers) at inducing grating frequencies below 0.5 c/d. The two effects become equipotent at inducing frequencies near 1.0 c/d. At their optimal spatial frequencies (0.03125 and 4.0 c/d, respectively) mean grating induction magnitude (0.475) exceeds that of contrast-contrast (0.250) by 140% [4].

Fig. 3 also reveals a significant degree of between-subject variability in both suprathreshold effects. Observer MEM, for example, is subject to the weakest overall contrast-contrast effect, and is virtually unaffected by contrast-contrast at spatial frequencies below 1 c/d (square symbols in Fig. 3) [5]. Since each datapoint of Fig. 3 reflects the integrated influence of 50-100 match settings, it is highly unlikely that these large and consistent individual differences are due to random sampling variations. Similar large between-subject variations in both the strength and direction of contrast-contrast have been reported by Cannon & Fullencamp (1991; 1993).

Effect of "Standard" Grating Contrast

Fig. 2 illustrates that for both grating induction (panels e,j,k) and contrast-contrast (panels d,h,i), the degree of nonveridical contrast matching depends strongly upon the level of "standard" grating contrast. To facilitate inspection and cross-comparison of the patterns of nonveridical matching in the two effects, Figure 4 presents mesh plots of mean integrated contrast area (per unit "standard" grating contrast) for both grating induction (panel a), and contrast-contrast (panel b). Effect magnitude is plotted as a function of both "standard" grating contrast, and inducing grating spatial frequency.

Insert Figure 4 Here

---

[4] An absolute magnitude comparison in terms of the mean contrast matching nonveridicality each effect produces is obtained by taking the square-root of the peak values of Fig. 3.

[5] Observers MEM and BB both produced veridical contrast matches in a phase-offset control condition in an earlier experiment (McCourt & Blakeslee, 1994). This result was at that time interpreted to suggest that contrast-contrast did not influence measurements of grating-induction magnitude. While true for some observers, the present data reveal that for others contrast-contrast can and does influence measurements of grating induction magnitude.

Fig. 4(a) shows that for inducing grating frequencies below 0.125 c/d, grating induction produced a skewed unimodal pattern of nonveridical matching, which peaks at "standard" grating contrasts of 0.60, equivalent to a "standard"/inducing grating contrast ratio of 80% (0.60/0.75). This result is consistent with the fact that cancelling contrast is a constant proportion (82%) of inducing grating contrast, and that matching nonveridicality is greatest for "standard" contrasts near the cancelling value (McCourt & Blakeslee, 1994). The skewed unimodal surface gradually flattens with increasing spatial frequency. Interestingly, inducing grating frequencies between 1.0-4.0 c/d appear to produce a shallow bimodal surface with a second maximum for "standard" contrasts of approximately -0.20.

Earlier arguments to the contrary notwithstanding, one wonders if this asymmetry of grating induction magnitude with "standard" grating contrast might be attributable to phase-dependent contrast-contrast effects? Heeger and Robison (1994) used inducing and "standard" textures consisting of 8.0 c/d sinewave grating plaids in which one component was vertically oriented. They found that whereas the strength of contrast-contrast was equivalent for inducing and "standard" plaids whose vertical components were in either 90° or 180° relative spatial phase, it was reduced when they were aligned in 0° phase (i.e., where they appeared continuous). Such a phase dependency of contrast-contrast could produce an asymmetric pattern of nonveridical contrast matching in the grating induction mesh plot of Fig. 4(a), since negative "standard" grating contrasts refer to gratings in 180° phase, whereas positive "standard" grating contrasts are in 0° phase. Two observations cast doubt on this possibility. First, the observed matching asymmetry in the present experiment arises primarily at low inducing grating spatial frequencies (e.g., below approximately 1.0 c/d) where the independently measured contrast-contrast effects become negligible (see Fig. 3). Second, phase-related matching asymmetry is absent in the grating induction data at inducing frequencies above 4.0 c/d, where contrast-contrast effects are greatest (see below).

As expected, contrast-contrast produced a symmetrical pattern of nonveridical matching which was invariant with inducing grating spatial frequency. Interestingly, similar to grating

induction, maximal departures from veridical matching occur for "standard" grating contrasts of ±0.60, again, equivalent to a "standard"/inducing grating contrast ratio of 80%.

EXPERIMENT 2: EFFECT OF INDUCING GRATING HEIGHT

The results of Experiment 1 indicate that grating induction and contrast-contrast are distinct with respect to their overall magnitudes, spatial frequency tuning, and dependence on "standard" pattern contrast. Another significant dimension along which the two effects may differ concerns the area over which their mechanisms sum luminance and/or contrast inputs. Since grating induction is spatially low-pass it might be expected to possess a relatively large integration region. Conversely, the high- or band-pass contrast-contrast effect might be supposed to possess more localized integration regions. To address these questions, the areal integration of both grating induction and contrast-contrast was assessed in a second experiment.

METHODS

Subjects

The author, MEM, and two additional observers, DAB and DLG, participated as subjects. Observers MEM and DLG were male; DAB was female. Subjects possessed normal or corrected-to-normal vision and, except for observer MEM, were naive to the purposes of the experiment. Subjects were well-practiced as psychophysical observers.

Instrumentation and Calibration

As described for Experiment 1.

Stimuli and Procedures

Stimuli and procedures were similar to those of Expt. 1. Contrast matching functions were obtained for each effect (i.e., for both phase-aligned and phase-offset displays) in conjunction with nine inducing grating half-heights, which ranged from 0.0625° to 6.2°. Half-height values refer to the height of the upper or lower half of the inducing grating, which were always equal. "Standard" grating (i.e., test field) height was constant at 0.5°. Matching functions were obtained at four well-separated inducing grating spatial frequencies: 0.0625, 0.25, 1.0 and

4.0 c/d, at the viewing distance of 53 cm. Matching functions obtained in phase-aligned (grating induction) conditions were corrected for the simultaneously occurring effects of contrast-contrast.

RESULTS AND DISCUSSION

Figures 5 and 6 plot relative mean (across the three subjects) matching error (i.e., C_S-C_M) as a function of inducing grating half-height (plotted on a log axis) for grating induction and contrast-contrast, respectively. Panels (a-d) separately plot results obtained at four inducing grating frequencies, shown as parameters. For grating induction (Fig. 5), the nine curves correspond, from bottom to top, to "standard" grating contrasts of -0.80, -0.60, -0.40, -0.20, 0.0, 0.20, 0.40, 0.60 and 0.80. For contrast-contrast (Fig. 6) the four curves correspond to "standard" grating contrasts of ±0.20, ±0.40, ±0.60 and ±0.80. In both Figs. 5 and 6 the functions have been vertically displaced to avoid clutter. The magnitude of both effects increases monotonically with increasing inducing grating half-height at all spatial frequencies. Using a least-squares criterion, nonlinear regression was used to fit the aggregate mean matching errors to rising exponential functions of the form:

Insert Figures 5 and 6 Here

$$E(h) = \alpha^*[1-\exp(-\sigma^*h)] \qquad (1.0)$$

where E is mean matching error (C_S-C_M), h is inducing grating half-height (in degrees), and α and σ are free parameters. Parameter α sets the asymptotic level of the function, and σ^{-1} is the space-constant of summation. The solid curves of Figs. 5 and 6 illustrate the optimized fits of equation (1.0) to the matching data [6].

Figs. 5 and 6 reveal that the degree of spatial summation in both grating induction and contrast-contrast depends jointly upon inducing spatial frequency and "standard" grating contrast. To facilitate the comparison of summation across the two effects, Figures 7 and 8 present mesh

---

[6] The grating induction matching data obtained at "standard" grating contrasts of -0.80 and -0.60 at inducing grating frequencies of 1.0 and 4.0 c/d (i.e., the lowest two data sets plotted in Figs. 5c and d, respectively) could not be satisfactorily fit to equation (1.0) due to the low signal/ noise ratio of these matching data. These means are simply joined by line segments.

plots of the optimized values of the free parameters α (panel a) and σ^{-1} (panel b) for both grating induction and contrast-contrast, as a function of both "standard" grating contrast and inducing grating spatial frequency.

Insert Figures 7 and 8 Here

Asymptotic effect magnitude, α, varies with inducing grating frequency and "standard" grating contrast in a manner similar to that described earlier in the more extensive data set using a the metric of the earlier experimtent (integrated area per unit contrast: Fig. 4a). Grating induction magnitude is greatest at low spatial frequencies, and is asymmetric with "standard" grating contrast, achieving a maximum at a value of approximately 0.60. Contrast-contrast increases in strength with increasing inducing frequency, and is symmetric with respect to "standard" grating contrast, also achieving a maximum at ±0.60 [7]. Confirming earlier measurements (Fig. 4b), maximal grating induction magnitude is approximately twice that of contrast-contrast.

The extent of spatial pooling also varies significantly for both types of lateral interaction as a function of inducing grating frequency and the level of "standard" grating contrast. Summation in grating induction is most extensive at low inducing frequencies, and peaks sharply at "standard" grating contrasts of -0.20, at which summation occurs over a range of ±6.0°. The extent of spatial pooling generally increases with decreasing spatial frequency; this reciprocity is consistent with a multiple-channel model of grating induction (Moulden & Kingdom, 1991; McCourt & Blakeslee, 1993, 1994). Summation for contrast-contrast is greatest at relatively high inducing frequencies (4.0 c/d). It attains a maximum value in conjunction with "standard" grating contrasts of ±0.40 (equivalent to an inducing/target contrast ratio of 53%), at which pooling occurs over a range of ±1.25°.

---

[7] Asymptotic effect magnitudes and space constants for positive and negative values of "standard" grating contrast have been averaged, since contrast-contrast is symmetric with respect to "standard" grating phase.

The contrast-response of individual cortical neurons is both noisy and range-limited (Albrecht & Hamilton, 1982). Encoding the entire range of stimulus contrast while simultaneously preserving high differential sensitivity to contrast variations around the mean level is thus a fundamental challenge for the visual system. Contrast adaptation which shifts the contrast-response function along the contrast axis (gain control) is one potential solution (Ohzawa, Sclar & Freeman, 1982, 1985; Albrecht, Farrar & Hamilton, 1984). Not all neurons exhibit such gain control, however, and even for those which do it is often imperfect. An alternative (or supplementary) scheme is for suprathreshold contrast to be coded by a range-fractionated ensemble of neurons, with each member of the ensemble possessing a steep contrast-response (thus preserving fine contrast discrimination), but possessing response ranges (i.e., thresholds) staggered at partly overlapping intervals along the contrast axis (Albrecht et. al., 1984). The observation that the space-constants for both contrast-contrast and grating induction vary with stimulus contrast level, as indexed by either "standard" grating (C_S) or contrast difference (C_S- C_M), may reflect such a range fractionation solution to intensity coding. In general, non-intensive properties of cortical neurons, e.g., their center frequency, spatial frequency bandwidth and receptive field size, exhibit only modest changes with contrast adaptation (Albrecht et. al., 1984). Indeed, the extent to which a neuron's output is useful in informing subsequent processing sites of the spatial features of the retinal image, it is highly counterproductive for that neuron's spatial selectivity to vary with adaptation state, and several models have been advanced to explain how cortical neurons can preserve response selectivity across a broad range of stimulus contrast (e.g., Albrecht & Geisler, 1994). The systematic variation of spatial summation with "standard" grating contrast level (Figs. 7b and 8b) is therefore most plausibly interpreted as arising due to the successive recruitment of mechanisms of varying size which operate over staggered and restricted ranges of stimulus contrast.

The mean space constants for these two suprathreshold effects, averaged across the three observers and across all levels of "standard" grating contrast, are plotted as a function of inducing grating spatial frequency in Figure 9. At low spatial frequencies grating induction (open symbols) pools over several degrees of space, a range which exceeds that of contrast-contrast

by nearly five octaves. At intermediate spatial frequencies for which effect magnitudes are equivalent (e.g., 1.0-2.0 c/d, see Fig. 3), spatial integration regions are also equivalent. At

---

Insert Figure 9 Here

---

spatial frequencies above 1.0 c/d, contrast-contrast becomes the stronger and more spatially extensive effect [8].

Cannon & Fullencamp (1991) measured contrast-contrast magnitude as a function of inducing pattern extent for inducing frequencies of 2.0, 4.0 and 8.0 c/d. They found that the functions relating contrast suppression to inducing grating extent for the three inducing frequencies superimposed when inducing grating extent was expressed in units of inducing grating cycles, implying that the space constant for contrast-contrast decreased as a function of increasing inducing frequency. While the results of the present experiment demonstrate the opposite, viz., that the spatial integration region for contrast-contrast increases with increasing inducing frequency, the two sets of results are not necessarily discrepant. Space-constants for contrast-contrast were estimated from the matching data for three observers reported by Cannon & Fullencamp (1991; Fig. 2, p. 1989], and reasonable upper and lower bounds for these estimates [9] are indicated as dashed lines in Fig. 9. Taken together the two sets of results

---

[8] The summation space constants derived for both effects using contrast matching error (C_S-C_M) as a metric are not substantively different from those obtained using integrated contrast area per unit contrast, as in Experiment 1.

[9] The target/inducing contrast ratio (0.25/0.50 = 50%) used by Cannon & Fullencamp (1991) is near the peak of the "standard" grating contrast tuning function (0.40/0.75 = 53%) for contrast-contrast space-constant described in Fig. 8(b), so their data are comparable to the present data in that regard. Additional factors, however, make the direct comparison of contrast-contrast space-constants derived from the two studies somewhat problematical. First, in Cannon & Fullencamp's (1991) DISC condition targets were circular patches of sinewave grating within annular inducing fields and effect magnitude was assessed as a function of full disc width/height. Contrast-contrast space-constants estimated from these data should therefore be scaled down by a factor of two to be comparable to the half-height space-constants reported in this paper. A second complication is that annular inducing fields exert contrast-contrast in both vertical and horizontal directions. For inducing fields exerting sub-saturating effect magnitudes the added horizontal suppression of annular inducing fields will produce greater contrast-contrast than will vertical-only flanking inducing fields (indeed, the efficacy of horizontal flanking gratings may exceed that of vertical gratings: Cannon & Fullencamp, 1994). Space-constants derived using

suggest that contrast-contrast mechanisms are largest at inducing frequencies of approximately 2.0 c/d; spatial summation declines for both increasing and decreasing inducing grating frequency.

SUMMARY AND CONCLUSIONS

Both grating induction and contrast-contrast cause the contrast of "standard" gratings to be matched non-veridically. When the magnitudes of each effect are measured in a common unit (contrast^2) which indexes the extent of nonveridicality in contrast matches made across a large range (±80%) of "standard" grating contrasts, grating induction possesses a low-pass spatial frequency response whereas that for contrast-contrast is high-pass. For 0.50° "standard" gratings the two effects are equipotent at inducing grating frequencies between 1.0 and 2.0 c/d. At their optimal spatial frequencies grating induction magnitude exceeded that of contrast-contrast. At the inducing grating contrast of 75%, departures from veridical matching varied with "standard" grating contrast such that at low spatial frequencies (0.03125-0.125 c/d) grating induction produced a skewed unimodal pattern of nonveridical matching (peaking at "standard" grating contrasts of 60%) which smoothly assumed a bimodal shape at intermediate spatial frequencies (0.25-2.0 c/d), peaking at "standard" grating contrasts of -20% and +60%. Above 2.0 c/d grating induction magnitude grew very weak. Contrast-contrast produced a symmetrical pattern of nonveridical contrast matching which was invariant with inducing grating spatial frequency; matching nonveridicality was maximal at "standard" grating contrasts of ±60%.

Both grating induction and contrast-contrast magnitudes decreased as inducing grating height decreased, implying that spatially extended mechanisms underlie both effects. At their

---

annular inducing fields should arguably be scaled up by as much as a factor of two to make them comparable to those derived from the present study. Interestingly, these two factors possess offsetting influences. Finally, the size of the test grating in the Cannon & Fullencamp (1991) study was not constant in angular subtense; instead it's diameter was held constant at 4 inducing grating cycles. The target patch was thus 2° in diameter for inducing gratings of 2.0 c/d, 1° at 4.0 c/d, and 0.5° at 8.0 c/d. Thus, only at 8.0 c/d was "standard" grating size comparable to that used in the present study. Since it is not know how variations in "standard" grating size influence inducing grating spatial summation, an exact comparison of contrast-contrast space constants across the two studies is impossible. The upper and lower dashed lines of Fig. 9 plot the full- and half-height contrast-contrast space-constant values, respectively, estimated from the data of Cannon & Fullencamp (1991). Comparable values are most likely to lie somewhere between these estimates.

optimal spatial frequencies the half-height summation space-constants for the two effects were 6° for grating induction, and 1.2° for contrast-contrast. Thus, grating induction (luminance normalization) mechanisms may sum luminance input from regions as large as 12° (or more, for lower frequencies) of visual angle. Contrast normalization occurs over much more circumscribed regions, about 2.5°. As inducing grating spatial frequency increased to 4.0 c/d critical summation regions for grating induction decreased, while they increased for contrast-contrast. The integration regions of the two effects varied considerably with the contrast ratio of the inducing and "standard" grating, implying that submechanisms with differing spatial selectivities are recruited as stimulus contrast changes.

Acknowledgements: This research was supported by grants from ND-EPSCoR (North Dakota-Experimental Program to Stimulate Competitive Research), the National Eye Institute (EY10133-01), and the Air Force Office of Scientific Research (F49620-94-1-0445). I thank Dr. Barbara Blakeslee for valuable assistance throughout this project. I am indebted to all of the observers for their many hours of patient and careful participation.

REFERENCES

Albrecht, D.G. & Hamilton, D.B. (1982) Striate cortex of monkey and cat: Contrast response function. J. Neurophysiol., 48, 217-237.

Albrecht, D.G., Farrar, S.B. & Hamilton, D.B. (1984) Spatial contrast adaptation characteristics of neurons recorded in the cat's visual cortex. J. Physiol., 347, 713-739.

Albrecht, D.G. & Geisler, W.S. (1994) Visual cortex neurons in monkey and cat: Contrast response nonlinearities and stimulus selectivity. In: Computational Vision Based on Neurobiology, Teri B. Lawton (Ed.), Proc. SPIE 2054, 12-31.

Cannon, M.W. & Fullencamp, S.C. (1991) Spatial interactions in apparent contrast: Inhibitory effects among grating patterns of different spatial frequencies, spatial positions and orientations. Vis. Res., 31, 1985-1998.

Cannon, M.W. & Fullencamp, S.C. (1993) Spatial interactions in apparent contrast: Individual differences in enhancement and suppression effects. Vis. Res., 33, 1685-1696.

Cannon, M.W. & Fullencamp, S.C. (1994) Target apparent contrast in the presence of peripheral flanking stimuli. Invest. Ophthal. Vis. Sci. (Suppl.), 35, 3462.

Cannon, M.W. & Fullencamp, S.C. (1996) A model for inhibitory lateral interaction effects in perceived contrast. Vis. Res., 36, 1115-1125.

Chubb, C., Sperling, G. & Solomon, J.A. (1989) Texture interactions determine perceived contrast. Proc. Nat. Acad. Sci., 86, 9631-9635.

Foley, J.M. & McCourt, M.E. (1985) Visual grating induction. J. Opt. Soc. Am., A, 2, 1220-1230.

Haig, N.D. (1989) A new visual illusion, and its mechanism. Perception, 18, 333-345.

Heeger, D.J. & Robison, R.R. (1994) Is simultaneous contrast divisive? Invest. Ophthal. Vis. Sci. (Suppl.), 35, 3463.

McCourt, M.E. (1982) A spatial frequency dependent grating-induction effect. Vis. Res., 22, 119-134.

McCourt, M.E. (1991) Comparison of brightness and contrast induction. Optics and Photonics News (Suppl.), 2, 89.

McCourt, M.E. and Blakeslee, B. (1993) The effect of edge blur on grating induction magnitude,

Vis. Res., 33, 2499-2507.

McCourt, M.E. and Blakeslee, B. (1994) A contrast matching analysis of grating induction and suprathreshold contrast perception. J. Opt. Soc. Am. A, 11, 14-24.

Moulden, B. & Kingdom, F. (1991) The local border mechanism in grating induction. Vis. Res., 31, 1999-2008.

Ohzawa, I., Sclar, G & Freeman, R.D. (1982) Contrast gain control in the cat visual cortex. Nature, 298, 266-268.

Ohzawa, I., Sclar, G & Freeman, R.D. (1985) Contrast gain control in the cat's visual system. J. Neurophysiol., 54, 651-667.

Solomon, J.A., Sperling, G. & Chubb, C. (1993) The lateral inhibition of perceived contrast is indifferent to on-center/off-center segregation, but is specific to orientation. Vis. Res., 33, 2671-2684.

Zaidi, Q. (1989) Local and distal factors in visual grating induction. Vis. Res., 29, 691-698.

FIGURE CAPTIONS

Figure 1. Photographs of grating induction and contrast-contrast displays which demonstrate the principal methods and findings of these experiments. (a) A grating induction display in which the upper and lower inducing gratings are phase-aligned. Overall display size is 32° by 32°. Inducing grating frequency is 0.03125 c/d, and inducing contrast is 0.75. "Standard" grating contrast (C_S) is 0.0 (e.g., the test field is physically homogeneous). The contrast of the matching grating (C_M), centered in the lower half of the display, is -0.26. It appeared equal in contrast to the test field above to observer DAB (see Figure 2a). "Standard" and matching fields are 0.5° in height. (b) As in (a), except that C_S = -0.40, and C_M = -0.46. These values produced perceptual equivalence for observer DAB. (c) A contrast-contrast display, in which the upper and lower inducing gratings are phase-shifted by 180°; no grating is induced within homogeneous test fields under these conditions. The high contrast gratings which flank the "standard" grating in the upper field cause "standard" gratings to be undermatched by observer DAB: C_S = 0.60, and C_M = 0.47. (d) Same as (a) for a 1.0 c/d inducing grating. At this spatial frequency grating induction in a homogeneous field is very weak, C_M = -0.05. (e) C_S = 0.60; C_M = 0.38. (f) Contrast-contrast condition which illustrates undermatching, C_S = 0.20; C_M = 0.10. Note: reproduction may alter the appearance of these displays.

Figure 2. Examples of contrast matching functions for observer DAB which illustrate the method used to compute contrast-contrast and grating induction magnitude. (a,f,g) Mean contrast matches (n=10, with 99% confidence intervals) to 11 "standard" grating contrasts at inducing grating frequencies of 0.03125, 1.0 and 16.0 c/d, respectively. Open symbols are data from phase-aligned (grating induction) displays and filled symbols are from phase-offset (contrast-contrast) displays. The locus of veridical contrast matching is indicated by the dashed diagonal lines. (b,d) Hatched region, bounded by the interpolated matching function and the diagonal line which denotes veridical matching, is numerically integrated to provide a comprehensive index of the magnitude of contrast-contrast at each inducing grating spatial frequency. This area is replotted in (d) on an ordinate which indexes the difference between "standard" and matching

grating contrast. This difference is by definition positive for "standard" contrasts whose absolute value exceeds matching contrast (i.e., for undermatches). (h,i) Similar plots which illustrate the magnitude of contrast-contrast in phase-offset conditions as a function of "standard" grating contrast at inducing grating spatial frequencies of 1.0 and 16.0 c/d. (c,e) An uncontaminated assessment of grating induction magnitude must take account of simultaneously occurring contrast-contrast effects. Grating induction magnitude was therefore computed at each inducing grating spatial frequency by numerically integrating the area between the matching functions obtained in the phase-aligned and phase-offset conditions. This area is replotted in (e) on a transformed ordinate. (j,k) Similar transformed plots of grating induction magnitude at inducing frequencies of 1.0 and 16.0 c/d.

Figure 3. The magnitudes of contrast-contrast (filled symbols) and grating induction (open symbols) for the six observers, expressed in units of total integrated contrast area, plotted as a function of inducing grating spatial frequency. Solid lines smoothly interpolate the aggregate mean values. Grating induction is a low-pass effect whereas contrast-contrast is highpass or bandpass; the effects are equipotent at 1.0 c/d. There is considerable between-subject variability in both suprathreshold effects. Observers are: DAB (circle), SM (inverted triangle), MEM (square), TK (triangle), MAS (diamond), SF (hexagon).

Figure 4. Mesh plots of mean integrated contrast area (per unit "standard" grating contrast) for both grating induction (a), and contrast-contrast (b). Effect magnitude is plotted as a function of both "standard" grating contrast, and inducing grating spatial frequency. For inducing grating frequencies below 0.125 c/d, grating induction produced a skewed unimodal pattern of nonveridical matching, which peaks at a "standard" grating contrast of 0.60. The skewed unimodal surface gradually flattens with increasing spatial frequency. Inducing grating frequencies between 1.0-4.0 c/d produce a shallow bimodal surface with a second maximum at "standard" contrasts of -0.20. Contrast-contrast produces a symmetrical pattern of nonveridical matching whose general form is largely invariant with inducing grating spatial frequency. Similar to grating induction, maximal departures from veridical matching occur for "standard" grating contrasts of ±0.60.

Figure 5. Relative mean matching error (i.e., C_S-C_M) is plotted as a function of inducing grating half-height for grating induction. Panels (a-d) correspond to results obtained at four inducing grating frequencies, shown as parameters. The nine curves correspond, from bottom to top, to "standard" grating contrasts of -0.80, -0.60, -0.40, -0.20, 0.00, 0.20, 0.40, 0.60 and 0.80. Functions have been vertically displaced by either 0.10 or 0.20 to avoid clutter. With the exception of "standard" contrasts of -0.60 and -0.80 at inducing frequencies of 1.0 and 4.0 c/d (for which grating induction is very weak) the magnitude of grating induction increases monotonically with increasing inducing grating half-height at all spatial frequencies. The solid curves illustrate the optimized fits of a rising exponential function (eq. 1.0) to the matching data.

Figure 6. Relative mean matching error (i.e., C_S-C_M) plotted as a function of inducing grating half-height for contrast-contrast. Panels (a-d) correspond to results obtained at four inducing grating frequencies, shown as parameters. The four curves correspond, from bottom to top, to "standard" grating contrasts of ±0.20, ±0.40, ±0.60 and ±0.80. Functions have been vertically displaced by either 0.10 or 0.20 to avoid clutter. The magnitude of contrast-contrast increases monotonically with increasing inducing grating half-height at all spatial frequencies. The solid curves illustrate the optimized fits of a rising exponential function (eq. 1.0) to the matching data.

Figure 7. Panels (a) and (b) plot the optimized values of the free parameters α and σ^{-1}, respectively, for grating induction as a function of "standard" grating contrast and inducing grating spatial frequency. Asymptotic effect magnitude, α, varies with inducing grating frequency and "standard" grating contrast in manner similar to that described earlier (Fig. 4a). Grating induction magnitude is greatest at low spatial frequencies, and is asymmetric with "standard" grating contrast, achieving maximal at values of approximately 0.60. Spatial pooling also varies significantly with inducing grating frequency and the level of "standard" grating contrast. Summation in grating induction is most extensive at low inducing frequencies, and peaks sharply at "standard" grating contrasts of -0.20, at which summation occurs over a range of ±6.0°. The extent of spatial pooling generally increases with decreasing spatial frequency.

Figure 8. Panels (a) and (b) plot the optimized values of the free parameters α and σ^{-1}, respectively, for contrast-contrast as a function of "standard" grating contrast and inducing grating spatial frequency. Asymptotic effect magnitude, α, varies with inducing grating frequency and "standard" grating contrast in manner similar to that described earlier (Fig. 4b). Contrast-contrast magnitude increases with increasing inducing frequency and is symmetric with respect to "standard" grating contrast; it is maximal at ±0.60. Spatial pooling for contrast-contrast is greatest at relatively high inducing frequencies (4.0 c/d). It attains a maximum value in conjunction with "standard" grating contrasts of ±0.40 (equivalent to an inducing/target contrast ratio of 53%), at which pooling occurs over a range of ±1.25°.

Figure 9. Mean space constants (σ^{-1}) for grating induction (open symbols) and contrast-contrast (filled symbols) are plotted as a function of inducing grating spatial frequency. The strength and size relationships are complimentary. At intermediate spatial frequencies for which effect magnitudes are equivalent (e.g., 1.0-2.0 c/d, see Fig. 3), spatial integration regions are also equivalent. Confidence intervals for space-constants for contrast-contrast estimated from the matching data of Cannon & Fullencamp (1991) are plotted as dashed lines (see text for details). The results suggest that the size of mechanisms underlying contrast-contrast are largest at inducing frequencies of approximately 2.0 c/d, and decrease with changes in inducing frequency in either direction.

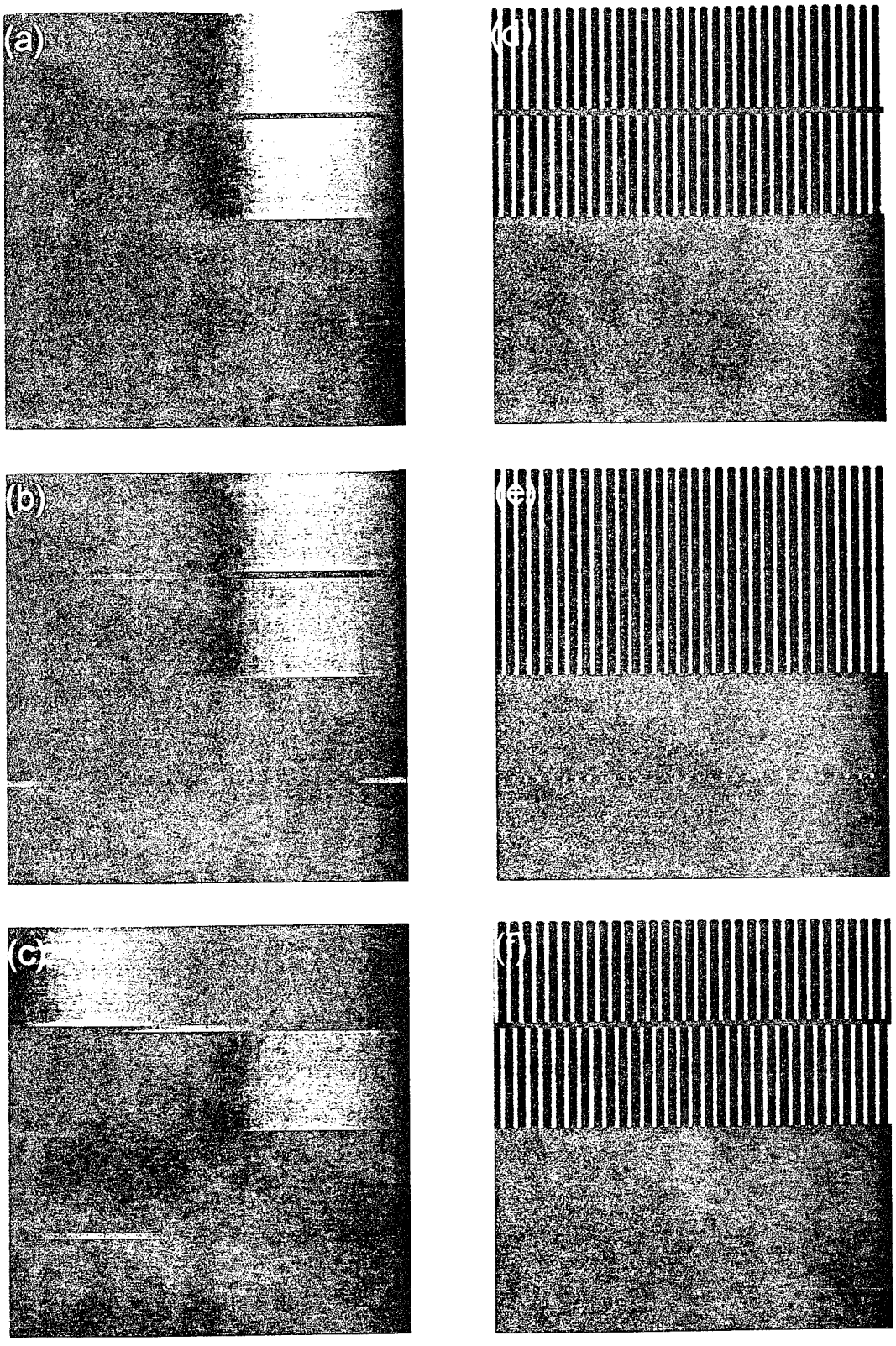

Figure 1

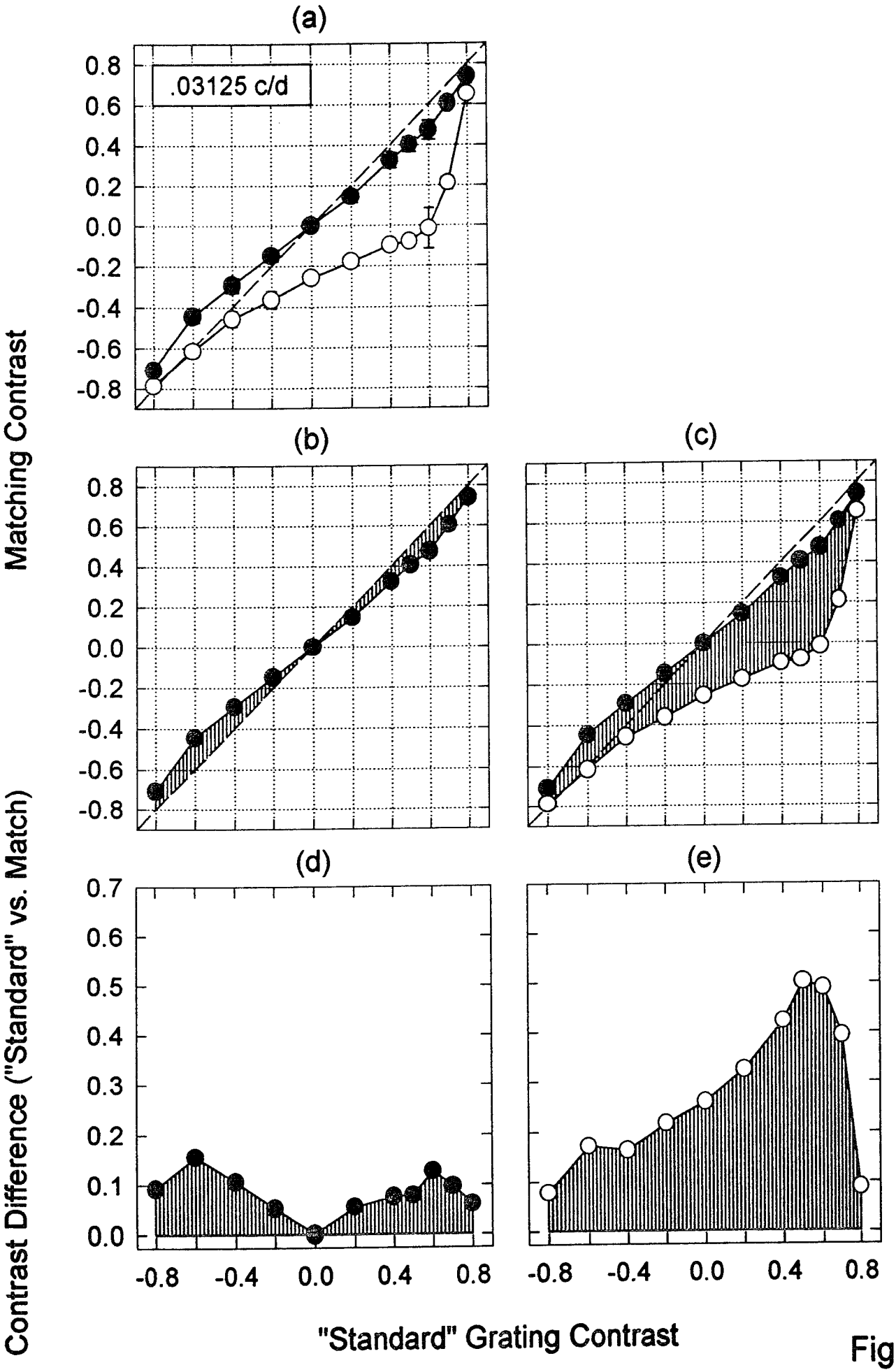
(a)
.03125 c/d
0.8
0.6
0.4
0.2
0.0
-0.2
-0.4
-0.6
-0.8
(b)
(c)
(d)
(e)
0.7
0.5
0.3
0.1
-0.8
-0.4
0.0
0.4
0.8
Matching Contrast
Contrast Difference ("Standard" vs. Match)
"Standard" Grating Contrast

Figure 2

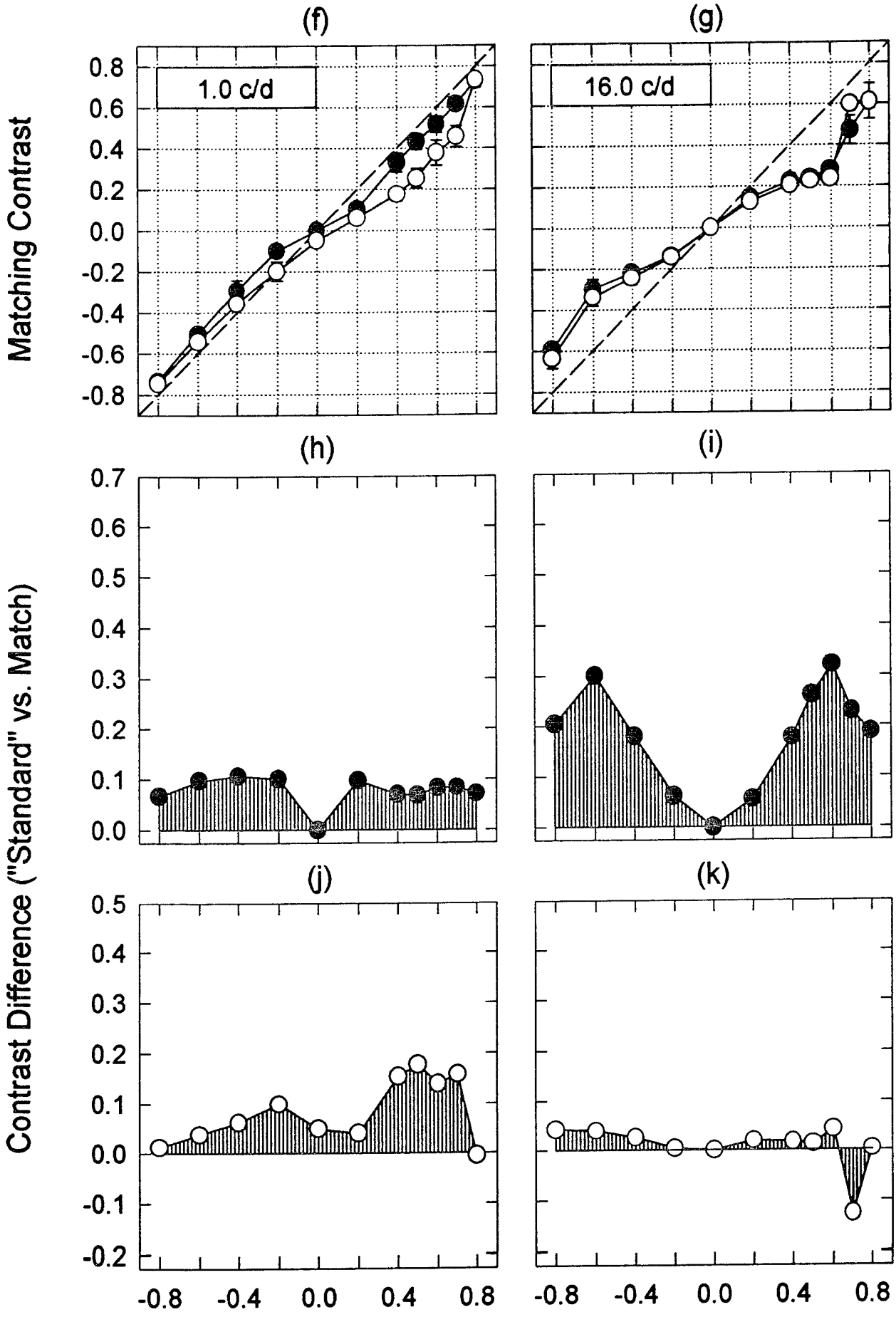

Figure 2 (cont.)

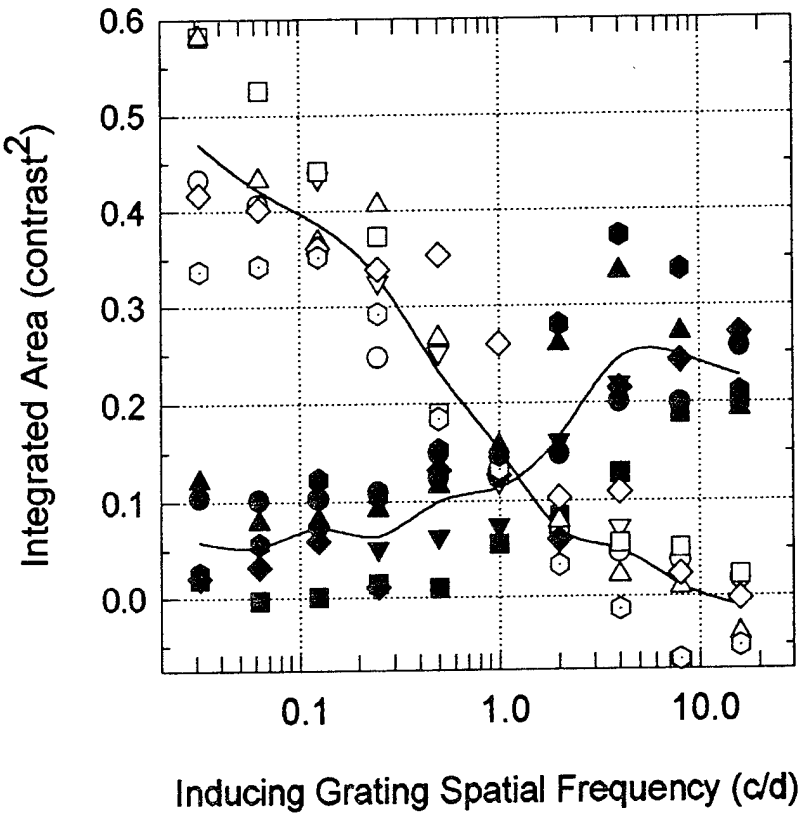
0.6
0.5
0.4
0.3
0.2
0.1
0.0
Integrated Area (contrast^2)
0.1
1.0
10.0
Inducing Grating Spatial Frequency (c/d)

Figure 3

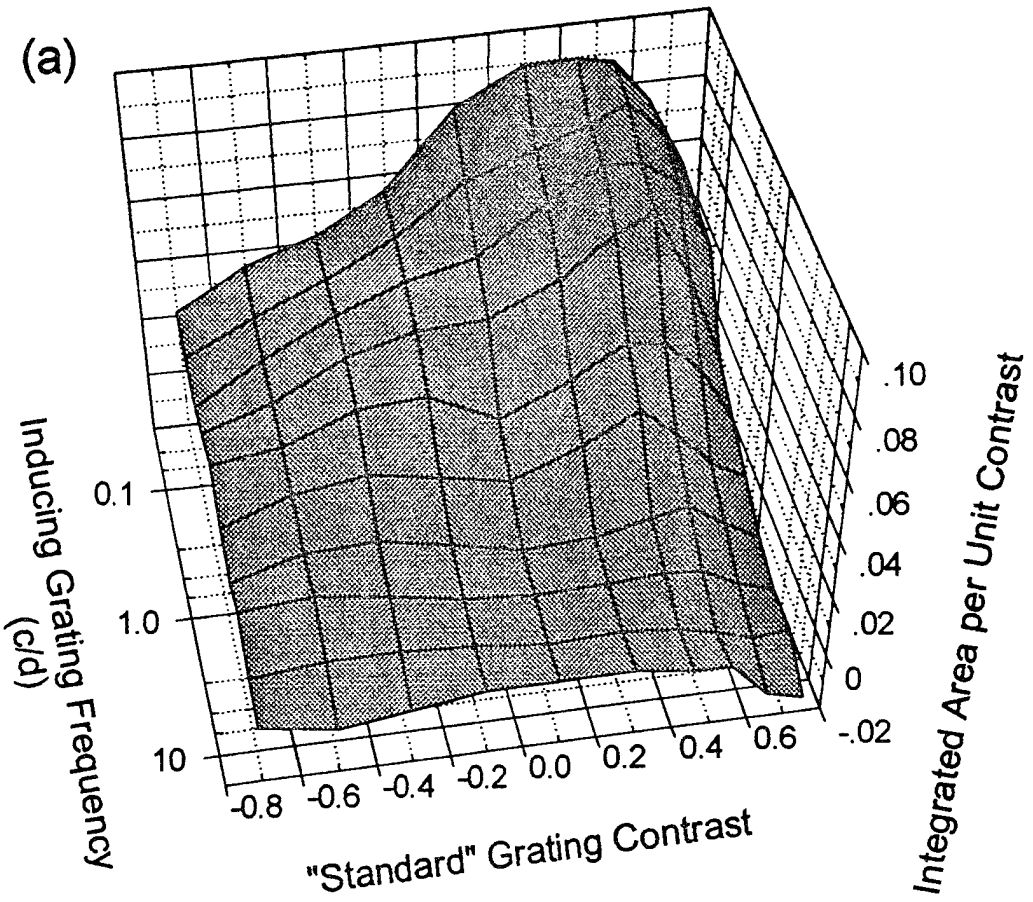
(a)
Inducing Grating Frequency (c/d)
0.1
1.0
10
-0.8
-0.6
-0.4
-0.2
0.0
0.2
0.4
0.6
"Standard" Grating Contrast
.10
.08
.06
.04
.02
0
-.02
Integrated Area per Unit Contrast

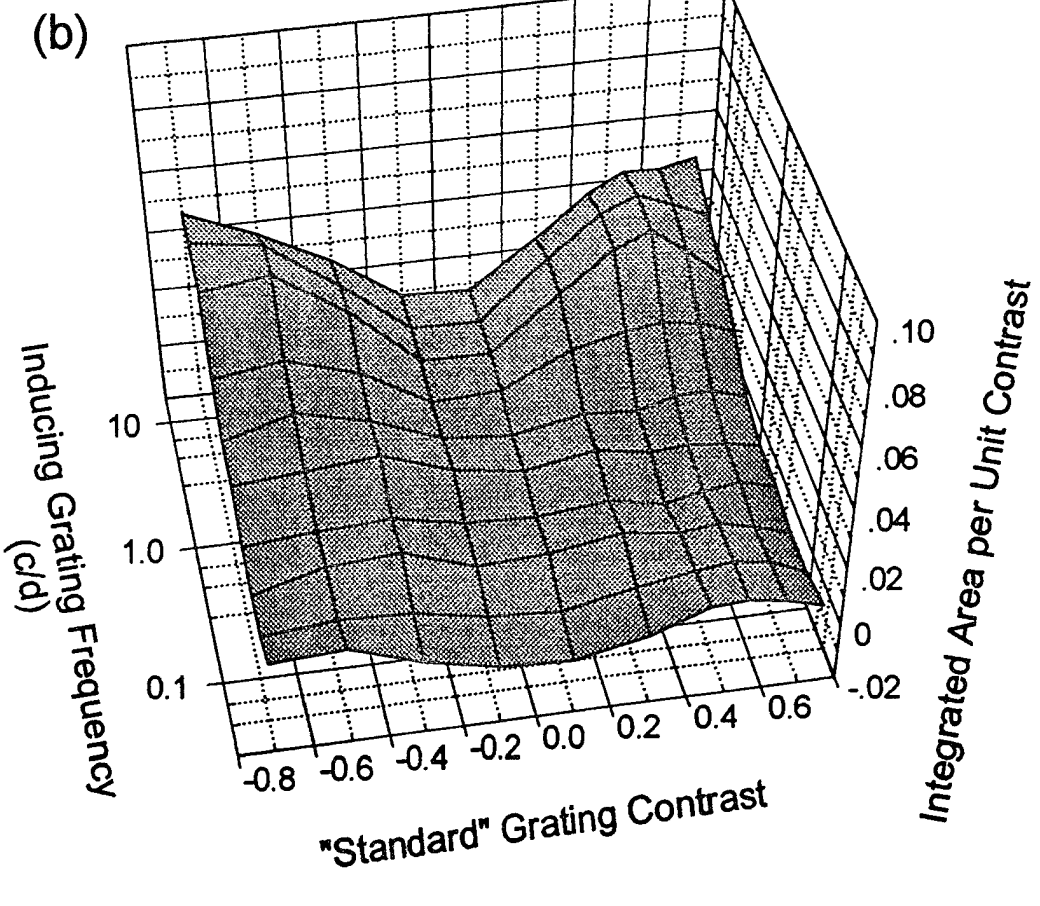
(b)
Inducing Grating Frequency (c/d)
10
1.0
0.1
-0.8
-0.6
-0.4
-0.2
0.0
0.2
0.4
0.6
"Standard" Grating Contrast
.10
.08
.06
.04
.02
0
-.02
Integrated Area per Unit Contrast

Figure 4

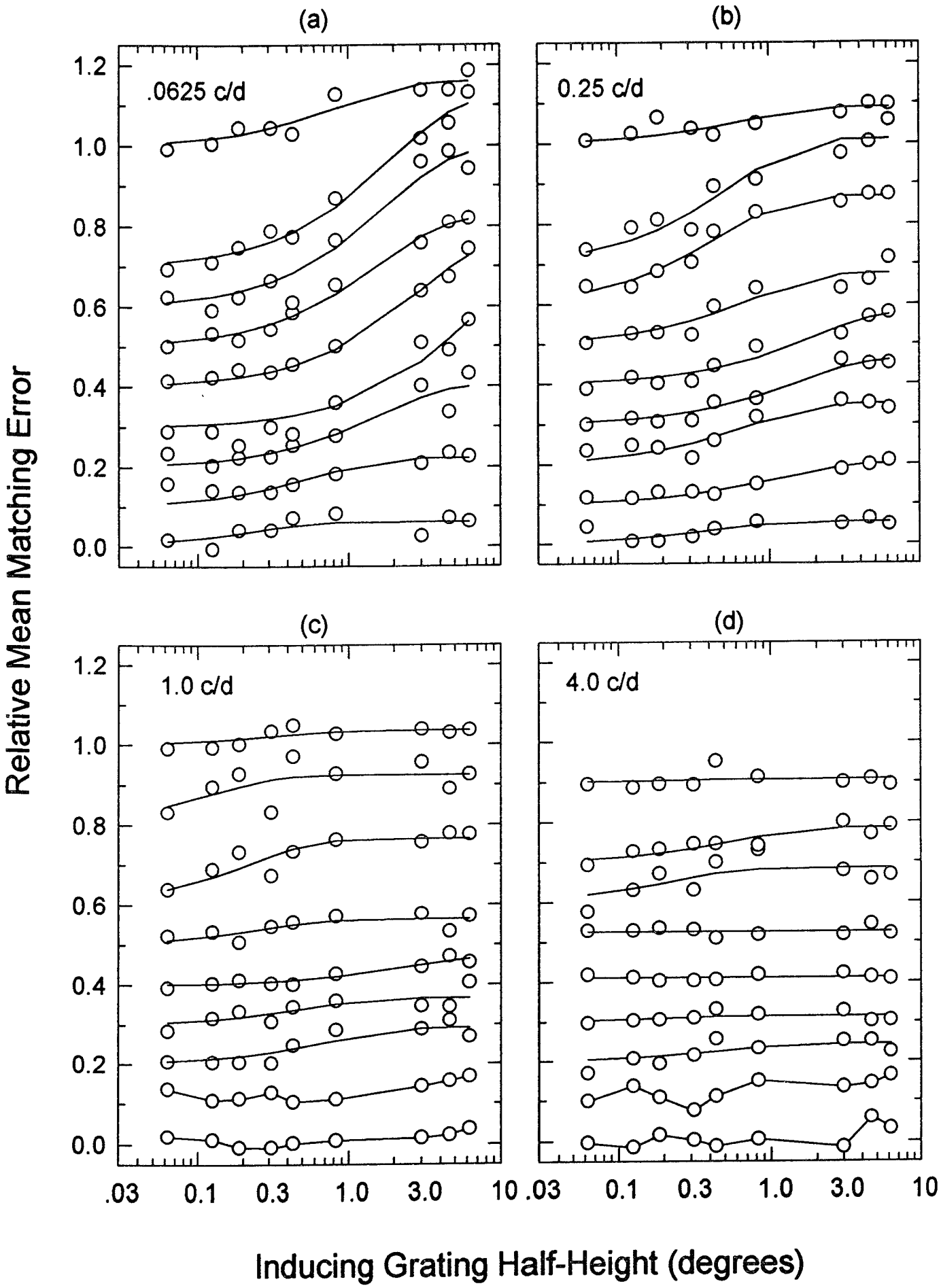
(a)
(b)
(c)
(d)
.0625 c/d
0.25 c/d
1.0 c/d
4.0 c/d
1.2
1.0
0.8
0.6
0.4
0.2
0.0
.03
0.1
0.3
1.0
3.0
10
Relative Mean Matching Error
Inducing Grating Half-Height (degrees)

Figure 5

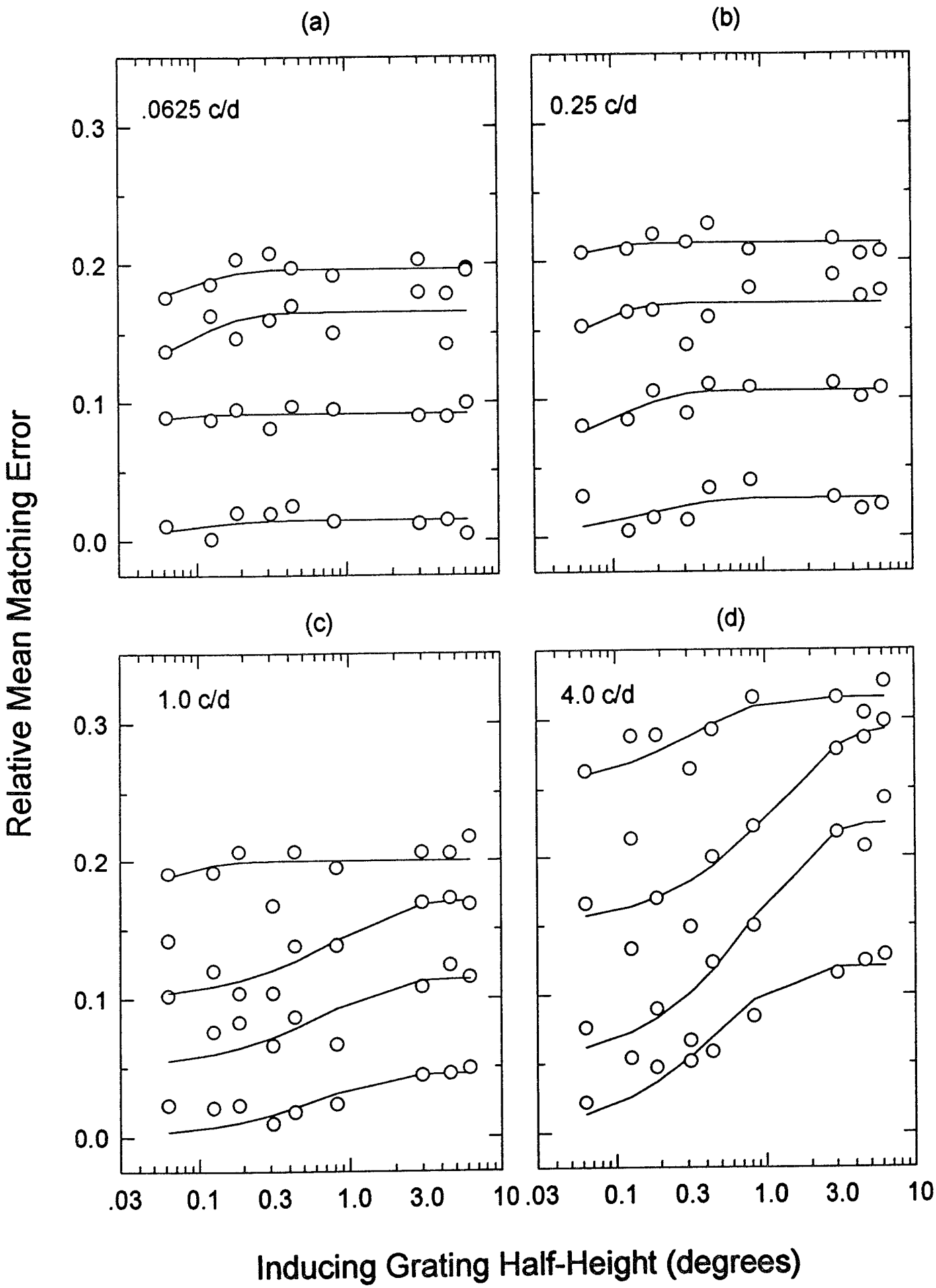
(a)
(b)
(c)
(d)
.0625 c/d
0.25 c/d
1.0 c/d
4.0 c/d
0.0
0.1
0.2
0.3
.03
0.1
0.3
1.0
3.0
10
Relative Mean Matching Error
Inducing Grating Half-Height (degrees)

Figure 6

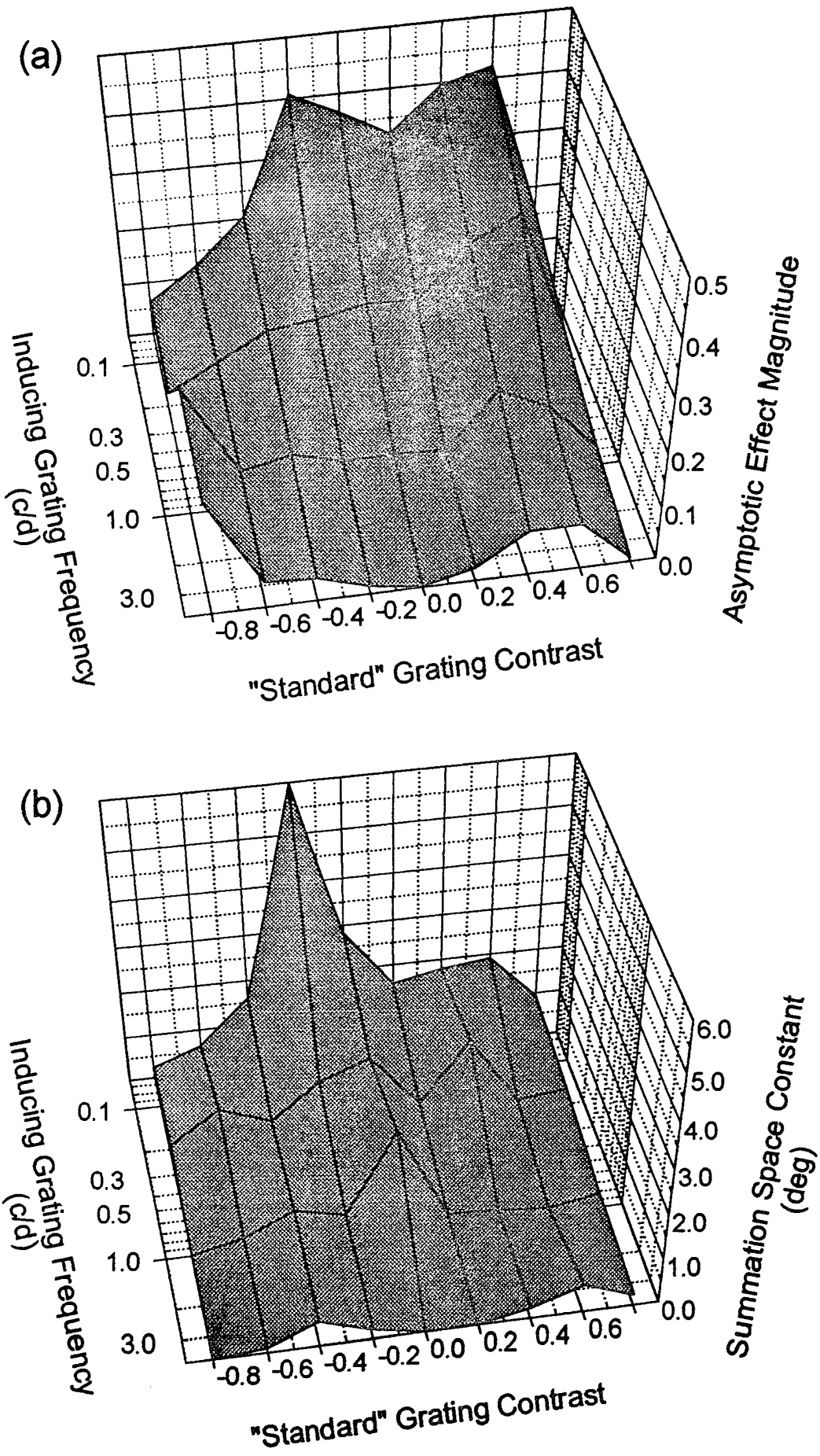
(a)
Inducing Grating Frequency (c/d)
0.1
0.3
0.5
1.0
3.0
-0.8 -0.6 -0.4 -0.2 0.0 0.2 0.4 0.6
"Standard" Grating Contrast
0.0 0.1 0.2 0.3 0.4 0.5
Asymptotic Effect Magnitude
(b)
Inducing Grating Frequency (c/d)
0.1
0.3
0.5
1.0
3.0
-0.8 -0.6 -0.4 -0.2 0.0 0.2 0.4 0.6
"Standard" Grating Contrast
0.0 1.0 2.0 3.0 4.0 5.0 6.0
Summation Space Constant (deg)

Figure 7

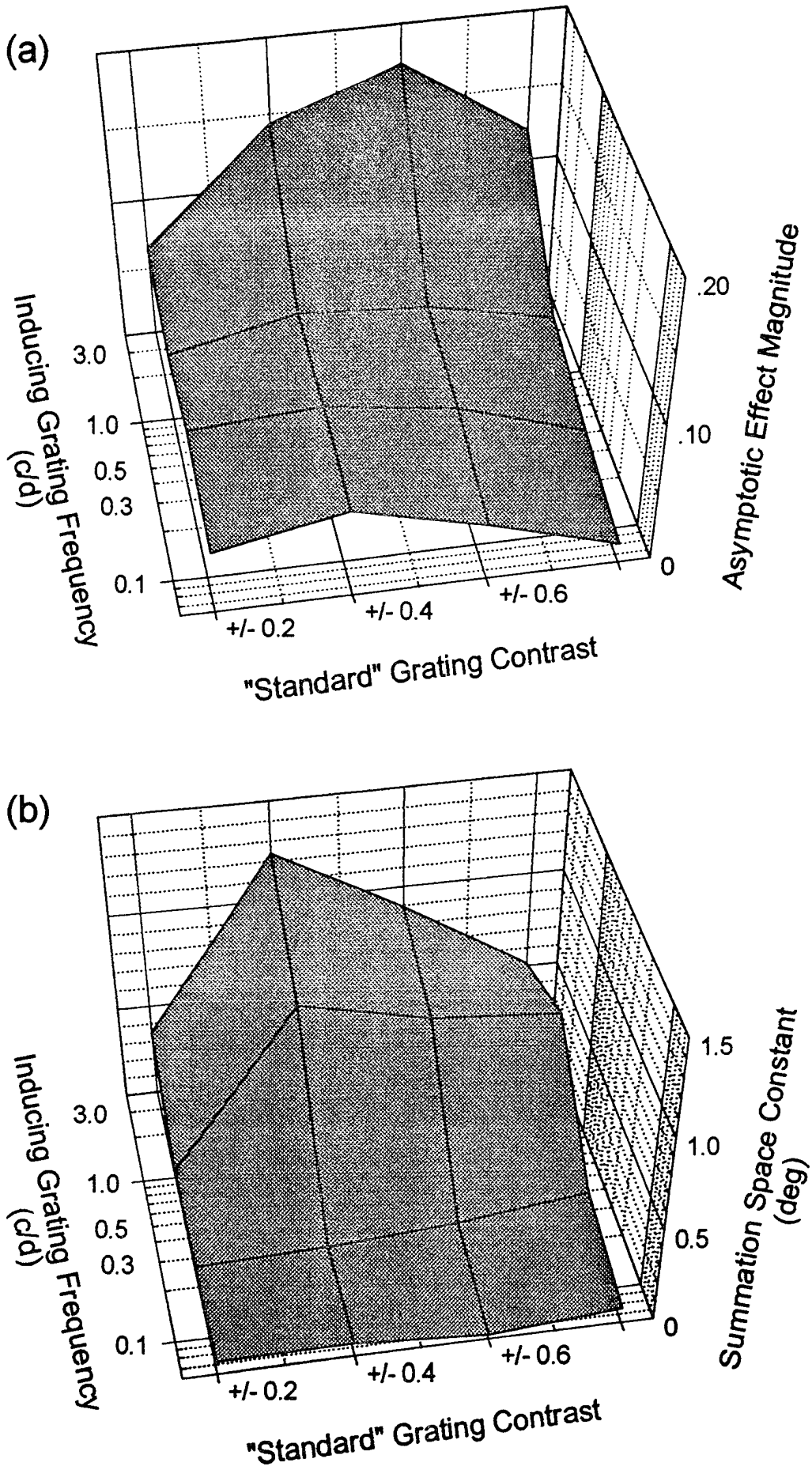
(a)
Inducing Grating Frequency (c/d)
3.0
1.0
0.5
0.3
0.1
+/- 0.2
+/- 0.4
+/- 0.6
"Standard" Grating Contrast
.20
.10
0
Asymptotic Effect Magnitude
(b)
Inducing Grating Frequency (c/d)
3.0
1.0
0.5
0.3
0.1
+/- 0.2
+/- 0.4
+/- 0.6
"Standard" Grating Contrast
1.5
1.0
0.5
0
Summation Space Constant (deg)

Figure 8

Pergamon

0042-6989(95)00279-7

Vision Res., Vol. 20, No. 3, pp. 000–000, 1996
Copyright © 1996 Elsevier Science Ltd
Printed in Great Britain. All rights reserved
0042-6989/96 $15.00 + 0.00

Facilitation of Luminance Grating Detection by Induced ~~Illusory~~ Gratings

delete word "Illusory"

MARK E. MCCOURT*†, FREDRICK A. A. KINGDOM‡

Received 28 November 1994; in revised form 5 September 1995

Please return this as your MARKED PROOF

Grating induction causes a homogeneous test field surrounded by sinewave gratings to possess an induced counterphase grating [McCourt M. E. (1982) Vision Research, 22, 119]. ~~Because~~ there is currently no consensus about the stage of visual processing at which illusory phenomena such as simultaneous brightness contrast are signaled. The masking efficacy of induced gratings ~~was assessed~~ by measuring contrast detection thresholds for targets (sinewave luminance gratings) added in phase to both real and induced gratings which were matched in apparent contrast. At spatial frequencies below ca 0.5 c/deg target detection and discrimination were comparably facilitated by both real and induced low-contrast pedestals (0.5–2%). At higher spatial frequencies (above 1.0 c/deg) facilitation continued to be observed for targets added in-phase to real grating pedestals, but occurred only for targets added out-of-phase with induced pedestal gratings. Higher inducing frequencies by themselves were not responsible for the observed phase shift of facilitation, however, since both real and induced pedestals produced similar target contrast discrimination functions when inducing frequency was varied by manipulating viewing distance (which holds the ~~ratio~~ of inducing grating period and test field height constant). The results imply the existence of at least two types of lateral interactive processes: one producing in-phase facilitation, and a second producing out-of-phase facilitation. The relative contribution of each process depends upon the ~~ratio~~ of inducing grating period and test field height.

Grating induction Brightness contrast Brightness matching Increment threshold Sensitivity

INTRODUCTION

Grating induction (McCourt, 1982) is a brightness illusion in which an illusory (induced) sinewave grating is seen within a physically homogenous test field which cuts through a sinewave inducing grating. Induced gratings are a low-pass function of inducing grating frequency and do not depend on eye movements for their production (Foley & McCourt, 1985; McCourt, Martinez-Uriegas & Blakeslee, 1995). The stage of visual processing at which illusory brightness phenomena such as simultaneous brightness contrast or grating induction arises is unknown, although there is mounting physiological and psychophysical evidence that illusory contours are signaled as early as V1 (Peterhans & Van der Heydt, 1991; Grosof, Shapley & Hawken, 1993; Dresp & Bonnet, 1991, 1993; McCourt & Paulson, 1994). The present experiments were designed to quantify the efficacy of induced gratings as masking stimuli by measuring contrast detection thresholds for sinewave luminance grating targets added in phase to both real and induced gratings which were themselves matched in apparent contrast.

How 'real' are induced (illusory) gratings?

The striking perceptual similarity between induced gratings and the luminance gratings which induce them [see McCourt (1994) for a detailed analysis of the induced grating waveform] raises the question of whether the neural mechanisms which signal phenomena such as induced gratings, illusory contours and the like are the same as those which signal their real counterparts. The identification of a common underlying mechanism would imply that these illusory phenomena are the consequence of operations performed by relatively early visual processes, and are not the result of higher-level interpretive processes. The principal item of evidence consistent with the idea that induced gratings are signaled by luminance grating detectors is that the two types of grating interact strongly. That is, the appearance of an induced grating can be partially or completely canceled by the addition of a real luminance grating of opposite spatial phase. Such a canceling procedure was first used to measure the magnitude of grating induction (McCourt, 1982). Some degree of cancellation would, however, be expected even if induced and real gratings were signaled

*To whom all correspondence should be addressed.
†Department of Psychology, North Dakota State University, Fargo, ND 58105-5075, U.S.A.
‡McGill Vision Research Unit, Department of Ophthalmology, McGill University, [illegible]

here with findings from depth perception, where the various cues to depth such as shading, texture gradient, motion parallax, binocular parallax, etc. are believed to be preliminarily extracted by independent mechanisms. These yet are subsequently combined to produce a fused depth percept in which perceived distance reflects some weighted nonlinear function of the depth signals provided by individual cues (Davis, King, Surdick, Shapiro, Corso, Hodges & Elliott, 1994)

Masking vs facilitation paradigms

An arguably more stringent test of whether two (or more) distinct stimuli share a common low-level processing mechanism is to determine whether the presence of one stimulus facilitates the detection of the other(s). Perhaps the most celebrated example of such facilitation is the 'dipper' portion of the contrast discrimination function, which plots the threshold increment in target grating contrast (ΔC) as a function of the contrast of a pedestal grating (C). Detection threshold is equal to discrimination threshold when pedestal grating contrast is zero. With increasing pedestal grating contrast ΔC decreases to a minimum, which defines the point of maximum facilitation. With increasing pedestal contrast facilitation segues to masking such that discrimination thresholds exceed detection threshold. The dipper portion of the contrast discrimination function has been interpreted to reflect the existence of an accelerating nonlinearity, or a threshold, in contrast transduction within individual spatial channels (Legge & Foley, 1980; Wilson, 1980; Yang & Makous, 1995).* Evidence of such facilitation implies that both target and pedestal stimuli are processed by a common mechanism. Similar facilitation effects have been demonstrated for a variety of stimulus types in addition to gratings, including spots of light presented against various light backgrounds (Barlow, 1972), difference-of-Gaussians patterns (Wilson, 1980), and triphasic stimuli (Burton, 1981).

The present series of experiments sought to determine whether, and under what conditions, an *induced* grating pedestal might facilitate the detection of superposed luminance gratings. At issue here is whether a stimulus which is not itself physically present is nonetheless capable of reducing the detection threshold for a target grating added to it similar spatial phase. Contrast thresholds were also measured in the presence of induced gratings whose perceived contrast might be expected to mask, rather than facilitate, the detection of target gratings. While masking paradigms have been widely employed to measure the spatial and orientation tuning of contrast processing mechanisms (on the assumption that masking occurs maximally when the mask and test are processed by the same mechanism), it is more difficult to support a claim for the common processing of real and illusory gratings based on masking data alone. Masking could, for example, be explained on the basis of the presence of the flanking inducing gratings themselves which might elevate contrast thresholds for target gratings positioned in the test field, independent of any indirect effect via the illusory gratings they induce. On the other hand it is far more difficult to construe a plausible rival explanation for how the detection of target gratings would be *facilitated* by presenting them out-of-phase with the inducing grating, given the more parsimonious prediction that they are facilitated by an in-phase induced grating pedestal. would be

Paradoxical effect of high frequency inducing gratings

Another motivation of the present study follows recent findings on the effects of high frequency inducing gratings on target detection. Using a stimulus configuration similar to those employed in grating induction experiments, Takahashi and Ejima (1985) measured contrast thresholds for a 3 c/deg sinewave target grating patch (2.67 deg wide by 0.67 deg in height) presented either in-phase or out-of-phase with peripheral inducing gratings. For target gratings presented *in-phase* with the peripheral gratings, a dipper-function was observed, such that target grating threshold was reduced when peripheral grating contrasts were below ca 1%, and was elevated at higher contrasts. For target gratings presented *out-of-phase* with the peripheral gratings, however, only a masking effect was found, except perhaps for a small facilitation at the highest contrast (64%). Similar results have been reported by Cannon and Fullencamp (1993) for 8.0 c/deg grating patches (0.5 deg in dia) surrounded by annuli containing gratings of equal spatial frequency and orientation. These results are intriguing in that they suggest that target increment thresholds vary in the opposite direction from that which might be expected if induced gratings (which are out-of-phase with the inducing grating) acted like pedestals to facilitate the detection of superposed like-phase target gratings. It should be noted, however, that inducing gratings above 3.0 c/deg do not produce robust induced gratings except in very narrow (e.g. 0.1 deg) test fields (McCourt, 1982; Foley & McCourt, 1985). The results of Takahashi and Ejima (1985) and Cannon and Fullencamp (1993) nevertheless point out the need to measure target grating contrast thresholds in conjunction with inducing grating spatial frequencies and test field heights for which induced gratings are adequately visible.

Brief reports of the results of these experiments have been given elsewhere (Kingdom & McCourt, 1993; McCourt & Kingdom, 1994).

*Stimulus uncertainty has been proposed as an alternative explanation for the facilitation of target detection when presented on like-phase pedestals (Lasley & Cohn, 1981; Pelli, 1985). Uncertainty does not account, however, for the elevation of target threshold (i.e. the 'bumper' effect) for targets presented out-of-phase with pedestal gratings (Kulikowski, 1976; Bowen & Cotten, 1993; Yang & Makous, 1995), making the concept of an accelerating nonlinearity the generally preferred explanation.

METHODS

Subjects

The authors (MM and FK) served as subjects. Both were experienced psychophysical observers and possessed normal vision.

Stimuli

Stimuli were generated using a VSG2 Digital Signal Generator (Cambridge Research Systems) and were displayed on a Barco CCID RGB monitor operating in yoked-gun (white) mode. Stimulus images were generated using a linearized 12-bit look-up-table constructed by suitable selection from 14-bit digital-to-analogue converters.

The Digital Signal Generator produces waveforms which are modulated at right angles to the direction of the raster. It was necessary therefore that the test field run vertically from the top to the bottom of the screen at right angles to the raster scan.† For consistency with previous descriptions of grating induction displays and for clarity of presentation, examples of the three types of stimulus display used in these experiments appear rotated by 90 deg in Fig. 1.

The display subtended 23 deg in width by 16 deg in height at the standard viewing distance of 74 cm. In the 'induced pedestal' condition [Fig. 1(a)] a sinewave inducing grating occupied the display except for a uniform test field which traversed the inducing grating. In the 'real pedestal' condition [Fig. 1(c)] a sinewave luminance grating served as a pedestal and occupied the region of the test field in Fig. 1(a). The surrounding inducing region was uniform. From the standard viewing distance of 74 cm test field dimensions in both the induced and real pedestal conditions were 23 deg. in width by 1 deg in height. The space-average luminance of the test field was equal to that of the surround at 37 cd/m^2. Inducing and pedestal grating spatial frequencies were always identical at 0.0625, 0.125, 0.25, 0.5, 1.0, and 4.0 c/deg. The target gratings which were added to the induced and real pedestal stimuli are schematically illustrated in Fig. 1(b) and (d). Note that only grating contrast, and not luminance offset, was added. These target gratings were always of the same spatial frequency as the induced or real pedestal gratings. In the induced pedestal condition, as illustrated in Fig. 1(a) and (b), target gratings were always added to the test field 180 deg out-of-phase with the inducing gratings: that is, they were added in-phase with any induced grating that might occupy the test field. In the real pedestal condition, illustrated in Fig. 1(c) and (d), target gratings were always added in-phase with the pedestal grating.

Procedure

Measurement of target grating detection thresholds. Target grating contrast thresholds were measured using a two-interval forced-choice adaptive staircase procedure. On each trial two stimuli were presented and observers selected the temporal interval judged to contain the target grating. Each stimulus consisted of the entire display as illustrated in Fig. 1(a) or (c). Between stimulus presentations the display was a uniform field of equal mean luminance. Thus, in the case of the induced pedestal condition of Fig. 1(a), both intervals contained the inducing grating; the target grating [Fig. 1(b)] was added to the test field in one of the intervals. The uniform field between stimulus presentations was inserted to reduce the effect of long-term adaptation to the inducing grating. Total stimulus duration was 400 msec; display contrast rose and fell under a raised cosine envelope. Onset and offset ramps each lasted 100 msec and stimuli were displayed at full contrast for 200 msec. The staircase procedure employed established the 70.7% correct level (Wetherill & Levitt, 1965). An experimental run was terminated after ten reversals, and thresholds were calculated as the geometric mean of target grating contrast over the last eight reversals.

Measurement of induced grating contrast. In order to meaningfully compare target detection thresholds across the real and induced pedestal conditions, a matching procedure was used to assess induced grating contrast for each inducing grating spatial frequency at each level of inducing grating contrast. Conceptually, each level of inducing grating contrast thus gave rise to an 'equivalent real pedestal contrast'.

The matching procedure established the point of subjective equality determined by method of adjustment under stimulus presentation conditions identical to those employed in the detection threshold experiments (i.e. using exactly the same temporal parameters of stimulus exposure). The inducing [Fig. 1(e)] and pedestal [Fig. 1(f)] stimuli were temporally alternated while the

†We found that there was a small amount of 'bleeding' from the inducing grating into the test field which presumably occurred because the signal defining the inducing grating was incompletely gated at the test field during each raster sweep. Microphotometric measurements with a small (<0.5 cm) aperture established that this bleeding did produce a luminance modulation in the test field whose contrast was ca 5% that of inducing grating. The artifactual grating was in-phase with the inducing grating and its contrast was constant across the test field. This grating was canceled by adding an opposite-phase grating of appropriate contrast into the test field. This canceling grating was subsequently added to all target gratings introduced into the test field. Following the addition of the canceling grating no remaining luminance modulation across the test field could be measured by microphotometer for any spatial frequency or contrast of the inducing grating. As an additional check we measured the detectability of a target grating added into the test field over a range of contrasts between 0.0 and 32% of the inducing grating. The inducing grating was physically occluded by an opaque screen. If the artifact was effectively canceled, as indicated by the microphotoemetric measurements, then the detectability of the target grating should be unaffected by the contrast of the occluded inducing grating. Variations in inducing grating contrast had no effect on target detection thresholds under these conditions. Hence, the effects of inducing grating contrast on target grating detection which we report must possess a perceptual, and not a physical, basis. As a final precaution the results for observer MM were successfully replicated in experiments performed on an independent display system in which the raster sweep was at right angles to the test field.

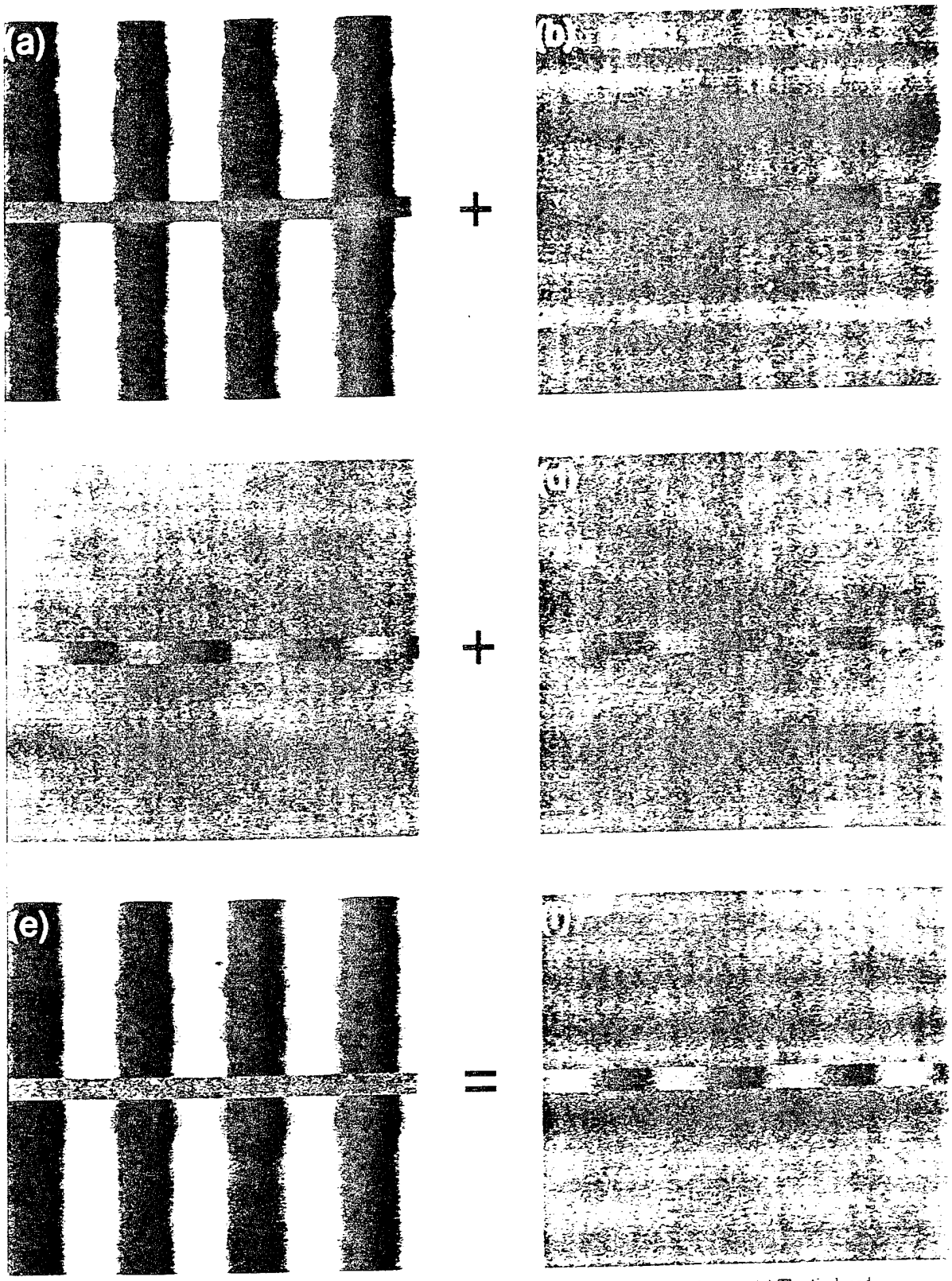

FIGURE 1. Examples of the three types of stimulus displays used in the present experiments. (a) The 'induced pedestal' condition in which a sinewave inducing grating occupied the display except for a uniform test field which traversed the inducing grating. (b) A target luminance grating added in phase synergy to the 'induced pedestal' of (a). (c) The 'real pedestal' condition in which a sinewave luminance grating served as a pedestal and occupied the region of the test field in (a). The surrounding inducing region was uniform. (d) A target luminance grating added in phase synergy to the real pedestal of (c). From the standard viewing distance of 74 cm test field dimensions in both the induced and real pedestal conditions were 23 deg in width by 1 deg in height. Inducing and pedestal grating spatial frequencies were 0.0625, 0.125, 0.25, 0.5, 1.0, and 4.0 c/deg. (e, f) In order to compare the detection thresholds for targets (b and d) across the real and induced pedestal conditions (a and c), a matching procedure was used to assess the perceived contrast of induced pedestals at each inducing grating spatial frequency and level of inducing grating contrast

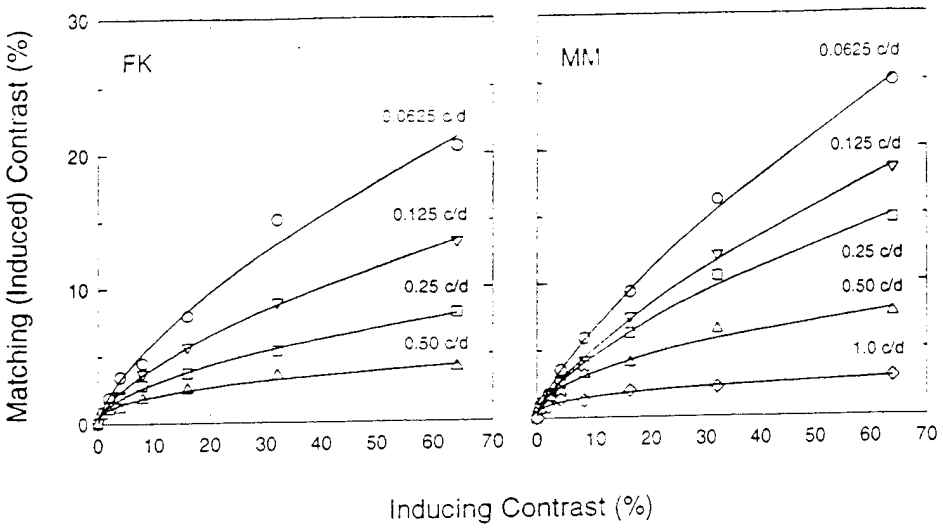

FIGURE 2. The mean percent contrast of real pedestal gratings [Fig. 1(f)] which matched the contrast of induced pedestals of the same spatial frequency [Fig. 1(e)] is plotted as a function of percent inducing grating contrast. Different inducing grating spatial frequencies are shown as parameters. There is no matching function for observer (FK) at 1.0 c/deg because the magnitude of grating induction was too weak at any inducing grating contrast to enable a match to be made. Smooth curves through the data represent the best-fitting power functions as determined by least-squares optimization. The matching functions allowed inducing grating contrast to be converted into 'induced' pedestal contrast.

contrast of the real pedestal was adjusted to match that of the induced grating. No time limit was imposed; when a satisfactory match was obtained the sequence terminated and the observer's adjusted equivalent real pedestal contrast was logged by computer. Five such measurements were made for each condition of the experiment (inducing grating contrasts of 1, 2, 4, 8, 16, 32, and 64% were used), and geometric means were computed. A schematic diagram of the appearance of the matched induced and real pedestal displays at the conclusion of the procedure is shown in Fig. 1(e) and (f), respectively.

RESULTS

Fig. 2 plots the mean contrast of real pedestal gratings [Fig. 1(f)] which matched the contrast of induced gratings of the same spatial frequency [Fig. 1(e)] as a function of inducing grating contrast. Recall that these measurements were made using a homogeneous 1 deg test field, i.e. in the *absence* of any added target grating. Different inducing grating spatial frequencies are shown as parameters. There is no matching function for observer (FK) at 1.0 c/deg because the magnitude of grating induction was simply too weak at any inducing grating contrast to allow matches to be made. Confirming earlier reports (McCourt & Blakeslee, 1993) matching contrast is well described as a power function of inducing grating contrast with an exponent <1. The smooth curves through the data represent the best-fitting power functions (constrained to pass through the origin) as determined by least-squares optimization. The power law relationship between inducing contrast and matching (induced) contrast allowed the analytic conversion of inducing grating contrast into units of 'equivalent real pedestal contrast'. For simplicity we will refer henceforth to 'induced' pedestals.

Fig. 3 plots target grating detection thresholds as a function of real (solid symbols) or induced (open symbols) pedestal contrast. Absolute target grating threshold is indicated by dotted horizontal lines. Contrast discrimination functions for spatial frequencies ranging from 0.0625 to 0.5 c/deg appear in separate panels, as labeled. Again, in the induced pedestal conditions target gratings were added to the test field 180 deg out-of-phase with the inducing grating, and were thus in-phase with the induced gratings. The abscissae of Fig. 3 are plotted in terms of pedestal contrast for the real pedestal condition, and equivalent real pedestal contrast for the induced pedestal condition, the latter having been calculated from the results of the contrast matching functions of Fig. 2.

Fig. 3 reveals a number of important points. First, target grating detection was facilitated by both real and induced grating pedestals. This is revealed by the 'dipper' shape of the discrimination function. Second, the magnitude of facilitation in the induced pedestal condition, and the range of pedestal contrast over which it occurs, diminishes with increasing spatial frequency. Third, the pattern of facilitation and masking is most similar for the induced and real pedestal conditions at 0.0625 and 0.125 c/deg, and progressively diverges at higher spatial frequencies. The increasing compression of the induced pedestal functions (open symbols) along the abscissa as spatial frequency increases is due to the diminishing strength of induction at these higher inducing grating frequencies (see Fig. 2).

What accounts for the observed divergence, with increasing spatial frequency, of contrast discrimination functions measured on real versus induced pedestals? One possibility is that the high levels of inducing grating contrast required to produce the various levels of induced pedestal contrast at high spatial frequencies are exerting lateral masking effects. One way to test this hypothesis would be to produce induced pedestals at high frequen-

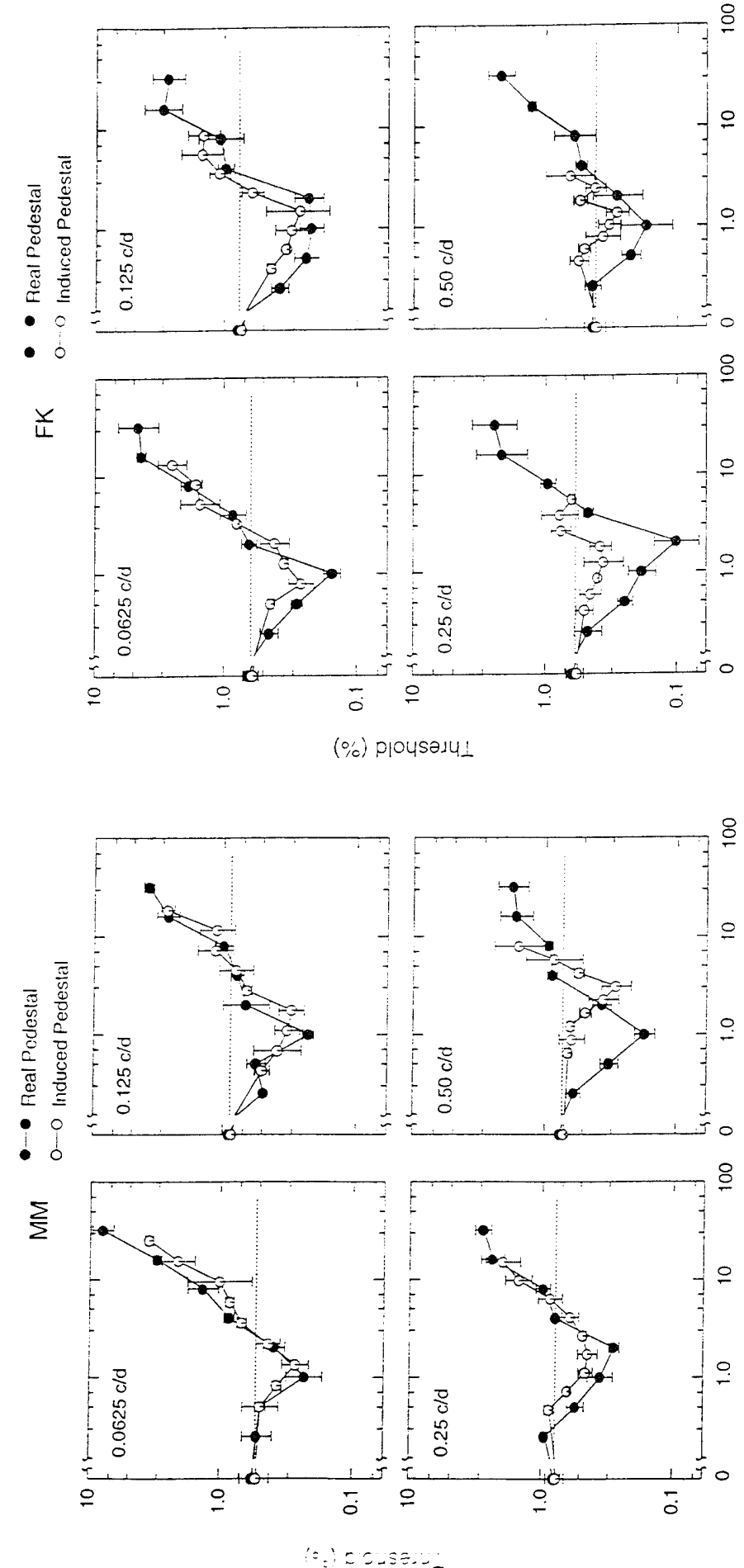

FIGURE 3. Target grating detection thresholds are plotted as a function of real (●) or induced (○) pedestal contrast for observers (MM) and (FK). Absolute target grating threshold is indicated by dotted horizontal lines. Contrast discrimination functions for spatial frequencies 0.0625–0.5 c/deg appear in separate panels, as labeled. Target detection is facilitated by both real and induced grating pedestals, as revealed by the 'dipper' shape of the discrimination function. The magnitude of facilitation by induced pedestals declines with increasing spatial frequency. The overall shapes of the discrimination functions are nearly identical for low frequency induced and real pedestals, but diverges increasing spatial frequency.

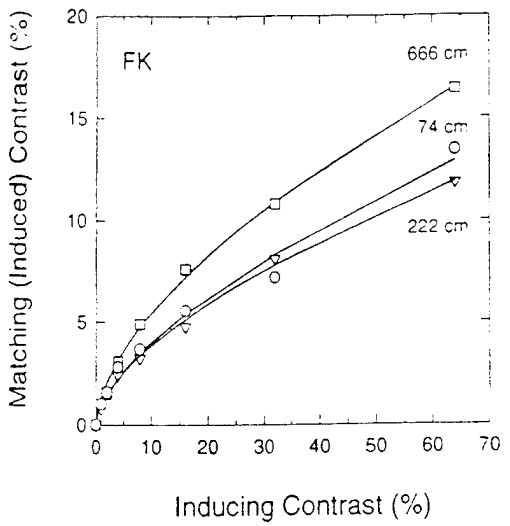

FIGURE 4. Induced pedestal contrast is plotted as a function of 0.125 c/deg inducing grating contrast (1 deg test field height) for observer (FK). Viewing distance is shown as a parameter. Varying viewing distance manipulates inducing grating spatial frequency while preserving a constant ratio of inducing frequency to test field height. Induced pedestal contrast in this 'constant ratio' condition, unlike the 'constant test field height' contrast matching data of Fig. 2, displays no systematic variation with inducing grating frequency.

cies without increasing inducing contrast. This can be accomplished by taking advantage of the fact that grating induction strength is constant for a constant product of inducing grating frequency (ISF) and test field height (TFH). Increasing viewing distance increases inducing grating spatial frequency while proportionally decreasing test field height and thus holding grating induction magnitude (i.e. induced pedestal contrast) constant (Foley & McCourt, 1985). Variations in viewing distance, therefore, can be used to manipulate inducing grating spatial frequency independently from inducing grating and induced pedestal contrast.

A control experiment was run on one observer (FK), whose results are shown in Figs. 4 and 5. Fig. 4 plots matching contrast at three viewing distances, shown as parameters, as a function of inducing contrast for a 0.125 c/deg inducing grating in conjunction with a 1 deg test field. Unlike the contrast matching data of Fig. 2, variations of spatial frequency consequent to changes in viewing distance are here shown to have no systematic effect on grating induction magnitude.

The Fig. 5(a) shows contrast discrimination functions measured on real (●) and induced (○) pedestals measured at the standard viewing distance of 74 cm. These data constitute an exact replication of the 0.125 c/deg condition of Fig. 3 for observer (FK), and are in good agreement. Fig. 5(b) and (c) present contrast discrimination functions measured at viewing distances of 222 and 666 cm, respectively, at which distances stimulus spatial frequencies were 0.375 and 1.125 c/deg. Note that despite the ninefold increase in spatial frequency, contrast discrimination functions on real and induced pedestals nearly superimpose. Compare, for example, the induced pedestal condition of Fig. 5 (c) with those for 0.5 c/deg in Fig. 3.

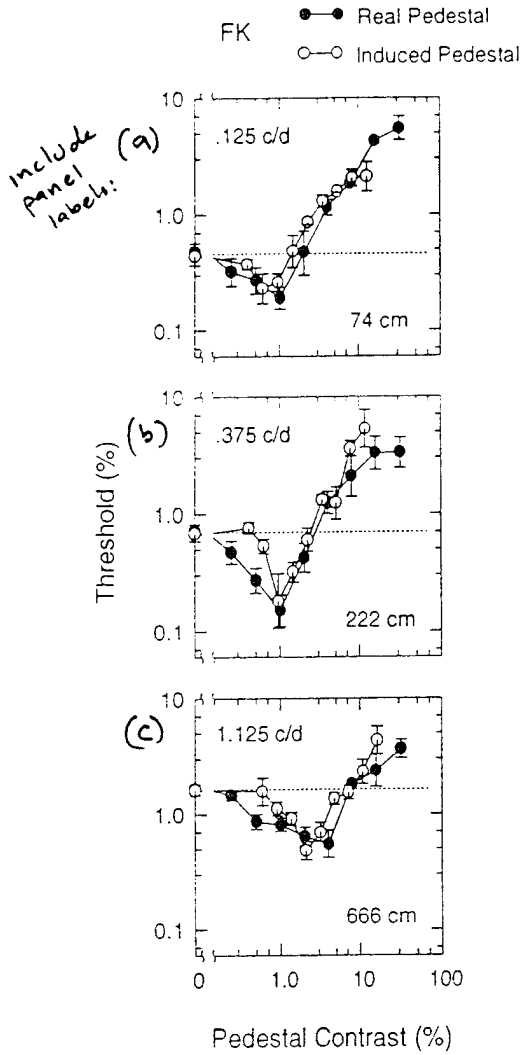

FIGURE 5. Contrast discrimination functions measured on real (●) and induced (○) pedestals measured at three viewing distances, shown as parameters in the three panels. The data in (a) are an exact replication of the 0.125 c/deg condition of Fig. 3 (FK). (b) and(c) are discrimination functions measured at viewing distances of 222 and 666 cm, respectively, at which distances stimulus spatial frequencies were 0.375 and 1.125 c/deg. Despite the ninefold increase in spatial frequency, contrast discrimination functions on real and induced pedestals nearly superimpose.

Finally, as noted earlier, a number of investigators (Takahashi & Ejima, 1985; Cannon & Fullencamp, 1993) have reported that phase-aligned inducing gratings facilitate the detection of high frequency (3.0–8.0 c/deg) target gratings, whereas thresholds are elevated for targets presented in the context of opposite phase inducing gratings. Given the opposite pattern of results (described above) for low frequency inducing gratings, target detection thresholds were also obtained in conjunction with both phase-aligned and opposite phase inducing gratings at spatial frequencies of 1.0 and 4.0 c/deg.

Experimental results from two observers appear in Fig. 6. Unlike Fig. 3, discrimination functions for the real pedestal and inducing grating conditions are plotted in separate panels. Note that results for the inducing grating conditions are plotted in terms of inducing grating

include panel labels

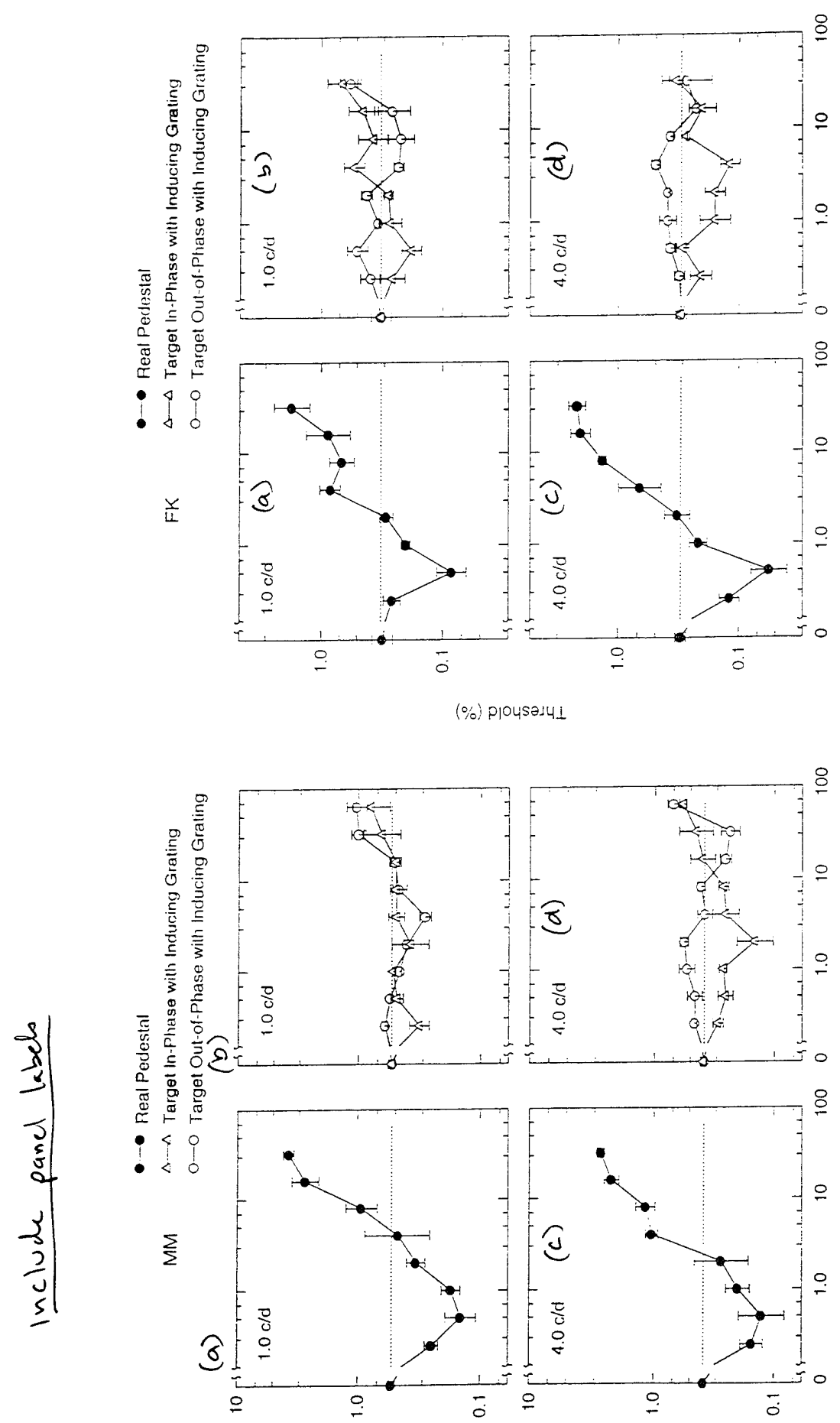

FIGURE 6. Target detection thresholds for both phase-aligned (△) and opposite phase inducing gratings (○,●) at 1.0 and 4.0 c/deg. Discrimination functions for real pedestal and inducing grating contrast conditions are plotted in separate panels. Results for the inducing grating conditions are plotted in terms of inducing grating contrast rather than equivalent real pedestal contrast. In the real pedestal conditions [●, (a) and (c)] the familiar dipper function is observed at both 1.0 c/deg [(a) and(b)] and 4.0 c/deg [(c) and (d)]. For the inducing grating condition [○, △ (b) and (d)] the results are somewhat more complex. For the 1.0 c/deg inducing grating condition [○, △ (b) and (d)] there is no consistent pattern of facilitation or masking across the two observers for target gratings presented either in-phase (△) or out-of-phase (○) with inducing gratings, although there is a hint of in-phase facilitation at the lowest inducing contrasts. A clear pattern emerges at 4.0 c/deg: target gratings presented *in-phase* with inducing gratings are facilitated, whereas they are masked when presented *out-of-phase*, up to inducing contrasts of ca 10%.

contrast rather than equivalent real pedestal contrast. Reasons for this include that:

1. matching results could not be obtained from observer (FK) in the 1.0 c/deg condition, or from either observer in the 4.0 c/deg condition, making conversion into units of equivalent real pedestal contrast impossible; and
2. even for observer (MM) the matching function for the 1.0 c/deg inducing frequency is so compressive (see Fig. 2) that such a transformation would virtually superimpose the data points, thus obscuring any pattern of threshold variation which might exist.

In the real pedestal conditions [●, Fig. 6 (a) and (c)] the familiar dipper function is observed at both 1.0 c/deg [Fig. 6(a) and (b)] and 4.0 c/deg [(c) and (d)]. For the inducing grating condition [○, △ Fig. 6(b) and (d)] the results are somewhat more complex. For the 1.0 c/deg inducing grating condition [○, △ Fig. 6(b) and (d)] there is no consistent pattern of facilitation or masking across the two observers for target gratings presented either in-phase (△) or out-of-phase (○,●) with inducing gratings, although there is a hint of in-phase facilitation at the lowest inducing contrasts. A clear pattern emerges at 4.0 c/deg: target gratings presented *in-phase* with inducing gratings are facilitated, whereas they are masked when presented *out-of-phase*, up to inducing contrasts of ca 10%. This pattern is precisely the opposite of that found for low spatial frequency target/inducing gratings, where robust facilitation is observed for targets presented out-of-phase with inducing gratings at low contrasts. The spatial frequency at which the phase change for facilitation occurs is ca 1.0 c/deg.

DISCUSSION

A brief summary of the results thus far includes that 'induced pedestal' gratings in a 1 deg high test field ('constant height' condition) facilitate the detection of real target gratings added in phase to them, for inducing and target grating spatial frequencies up to ca 0.5 c/deg. The amount of facilitation diminishes as inducing/target grating spatial frequency increases. 'Induced pedestal' gratings facilitate the detection of real gratings across a wide range of inducing/target spatial frequencies (from 0.125 to 1.125 c/deg), when the product of test field height to inducing grating spatial frequency was held constant at 0.125. In this 'constant product' condition the amount of facilitation is largely independent of spatial frequency. For inducing frequencies of 0.0625 and 0.125 c/deg in the constant height condition, and for all three constant product conditions, induced pedestals act nearly identically to their real pedestal counterparts (which were matched in perceived contrast) with regard to their facilitation and masking interactions with added target gratings. As inducing grating spatial frequency increases above 1.0 c/deg, facilitation of target gratings presented out-of-phase with inducing gratings gives way to facilitation of targets presented in-phase with inducing gratings.

Addressing rival hypotheses

Under a wide range of conditions induced gratings were observed to facilitate the detection of real gratings added in-phase to them. Prior to discussing the potential theoretical significance of these findings, however, it is proper to consider whether any other factors besides the existence of an induced pedestal within the test field might be responsible for target grating facilitation. One possibility is that as inducing grating contrast increases from zero, the test field (target) region simply becomes physically demarcated. Such demarcation will reduce positional uncertainty associated with the target and might itself facilitate its detection. Cole, Stromeyer and Kronauer (1990) found that demarcating a region with a black ring did in fact facilitate the detection of targets presented within it. A second possibility is that the inducing grating itself, and not the illusory grating it induces in the test field, might act directly as the pedestal stimulus, as if it simply extended across the test field.

To address both possibilities a control experiment was performed in which detection thresholds were measured for a 0.125 c/deg target grating presented in-phase with inducing gratings (the results of Fig. 3 are for targets presented out-of-phase with inducing gratings). Over the range of inducing grating contrast for which induced pedestals were subthreshold (and for which observers responded as usual by selecting the interval with the higher apparent contrast),* detection thresholds for target gratings presented in-phase with the inducing grating were always elevated relative to a no-pedestal control condition [i.e. displayed the 'bumper' effect described by Kulikowski (1976); Bowen & Cotten (1993); and Yang & Makous (1995)]. Therefore, the phase specificity of the facilitation makes it very unlikely that the reduction of positional uncertainty associated with the physical demarcation of the test region underlies our results. Such phase specificity also rules out the second, inducing grating-as-pedestal hypothesis, at least for frequencies below 1.0 c/deg, since it erroneously predicts that facilitation should occur for targets presented in-phase with inducing gratings.

Common processing of real and induced gratings

It was earlier argued that the strongest test of the hypothesis that induced and real gratings were signaled by a common mechanisms would be to demonstrate that induced gratings facilitate the detection of real gratings. The results of this study therefore confirm this hypothesis and add to the mounting body of evidence which suggests that early, or low-level, visual mechanisms are respon-

*When induced gratings are suprathreshold, target gratings added in-phase with the inducing gratings act as canceling stimuli. This has the paradoxical effect of making the interval containing the target grating appear to possess a lower contrast than the no-target interval.

sible for grating induction. Insofar as real luminance gratings are signaled by activity in linear band-pass filters at an early stage of visual processing, the same can therefore be said of the mechanisms signaling induced gratings, as has been suggested elsewhere (Foley & McCourt, 1985; Moulden & Kingdom, 1991; McCourt & Blakeslee, 1994).

Effect of inducing grating spatial frequency

We now consider why the pattern of target detection diverges for the induced and real pedestal conditions as spatial frequency increases in the 'constant height' condition (Fig. 3), yet not in the 'constant product' condition (Fig. 5). Grating induction magnitude does decrease with increasing spatial frequency in the former, but not the latter, case [see Foley & McCourt (1985)]. The divergence cannot, however, be a trivial consequence of any reduction in induced pedestal contrast in the 'constant height' condition because target thresholds are already plotted in terms of equivalent real pedestal contrast. The only difference is that greater *inducing grating* contrast is required to produce a criterion amount of induction for the 'constant height' versus the 'constant ratio' condition.

A clue to the actual cause of the divergence comes from a consideration of the results with the 1.0 and 4.0 c/deg inducing grating conditions (Fig. 6). Here, the robust facilitation observed for targets presented out-of-phase with inducing gratings observed at low spatial frequencies is replaced at higher frequencies by facilitation for targets presented in-phase with inducing gratings. The results with the 4.0 c/deg inducing gratings confirm previous reports by Takahashi and Ejima (1985) and Cannon and Fullencamp (1993), and imply the existence of at least two distinct mechanisms. One producing facilitation for low-frequency targets presented out-of-phase with inducing gratings, and another facilitating the detection of high-frequency targets presented in-phase with inducing gratings. These mechanisms are presumed to act antagonistically, where their relative activation depends upon factors such as the ratio of inducing grating period and test field height. For a test field height of 1.0 deg the two mechanisms appear roughly equipotent at inducing frequencies of ca 1.0 c/deg. Interestingly, 1.0 c/deg is also the spatial frequency at which the relative magnitudes of grating induction and contrast-contrast (Chubb, Sperling & Solomon, 1989; Cannon & Fullencamp, 1991) become equipotent (McCourt, 1995).

At present we can only speculate as to what these mechanisms might be. One possibility is that at low inducing grating spatial frequencies and/or narrow test field heights, the mechanisms most responsive to target gratings are those whose receptive fields are spatially tuned to the scale of the test field itself rather than to the period of the inducing grating—these could either be concentric center-surround mechanisms whose centers were similar in scale to the test field, or elongated filters (like simple cells) whose spatial half-period and orientation matched that of the test field. Either mechanism will produce a counterphase output in the test field in response to the inducing grating [see Foley & McCourt (1985), Fig. 10, and Moulden & Kingdom (1991), Fig. 2]. At inducing grating spatial frequencies above 1.0 c/deg, however, and particularly in conjunction with large test fields, the mechanisms most sensitive to target gratings may be those actually tuned to the inducing/target grating frequency (i.e. whose centers or half-periods are similar in scale to the inducing grating half-period), and these will respond in-phase with the inducing grating. It is additionally possible that the in-phase facilitation observed at high inducing frequencies is related to the mechanisms responsible for the facilitation and masking interactions of collinear Gabor patches shown recently by Polat and Sagi (1993), although they report that facilitation is phase-indifferent, whereas for our extended gratings it is not. Future experiments measuring the spatial frequency and orientation tuning of the mechanisms producing the facilitation of target gratings by both real and induced pedestals will test this hypothesis.

Suprathreshold brightness and contrast threshold mechanisms

In their classic study Cornsweet and Teller (1965) measured increment thresholds for a small (24 min dia) circular target presented on a wide (8.5 deg dia) background. Whereas the brightness of the background could be substantially altered by variations in the luminance of a surrounding annulus (via simultaneous brightness contrast), induced background brightness variations produced no effect on target thresholds other than that predicted by light scatter from the annulus. On the other hand, changing the luminance of the background itself produced the expected Weber's Law relationship. Other studies employing similar techniques (Van Esen & Novak, 1974; Guth, 1973) or using the fading of stabilized images or Troxler fading to decouple the brightness and luminance of background fields have produced essentially similar results (Burkhardt, 1966; Sparrock, 1969; Buck, Makous & Piantanida, 1983). The weak or nonexistent association between background brightness and target detection has sponsored the view that threshold sensitivity and suprathreshold brightness perception are governed by different mechanisms and are essentially independent.

Similar to simultaneous brightness contrast, induced gratings decouple the luminance and brightness of the test field. In fact, grating induction has been suggested to represent a generalization of simultaneous brightness contrast (McCourt, 1982), such that the latter corresponds to a special case of grating induction in which the inducing grating possesses an effective spatial frequency of 0 c/deg. The current discovery that induced gratings profoundly affect grating detection thresholds and under certain conditions act as nearly perfect spatial metamers of the luminance variations they resemble clearly indicates that sensitivity and brightness are not independent, and calls into question prior conclusions regarding the relationship between simulta-

neous brightness contrast and threshold processes. Interestingly, investigations of other brightness phenomena such as Mach Bands (Fiorentini, 1972), the Ehrenstein figure (Spillmann, Fuld & Neumeyer, 1984; Jory, 1987) and square wave patterns resembling the grating induction display (Jory, 1987) also support the idea that brightness variations can influence detection thresholds. The general similarities between the grating induction and simultaneous brightness contrast phenomena and their distinctly different effects on target sensitivity may make them particularly well-suited to the further investigation of the conditions under which brightness and sensitivity are related.

REFERENCES

Barlow, H. B. (1972). Dark and light adaptation: Psychophysics. In Jameson, D. and Hurvich, L. M. (Eds), *Handbook of sensory physiology Vol. VII/4, Visual psychophysics*. Berlin: Springer-Verlag.

Bowen, R. W. & Cotten, J. K. (1993). The dipper and the bumper: Pattern polarity effects in contrast discrimination. *Investigations Ophthalmic and Visual Science (Suppl.), 34*, 708.

Buck, S. L., Makous, W. & Piantanida, T. (1983). Background visibility and increment thresholds. *Vision Research, 23*, 1107–1113.

Burkhardt, D. A. (1966). Brightness and the increment threshold. *Journal of Optical Society of America, 56*, 979–981.

Burton, G. J. (1981). Contrast discrimination by the human visual system. *Biological Cybernetics, 40*, 27–38.

Cannon, M. W. & Fullencamp, S. C. (1991). Spatial interactions in apparent contrast: Inhibitory effects among grating patterns of different spatial frequencies, spatial positions and orientations. *Vision Research, 31*, 1985–1998.

Cannon, M. W. & Fullencamp, S. C. (1993). Spatial interaction effects at threshold. *Investigations Ophthalmic and Visual Science (Suppl.), 34*, 781.

Chubb, C., Sperling, G. & Solomon, J. A. (1989). Texture interactions determine perceived contrast. *Proceedings of the National Academy of Science, 86*, 9631–9635.

Cole, G. R., Stromeyer III, C. F. & Kronauer, R. E. (1990). Visual interactions with luminance and chromatic stimuli. *Journal of Optical Society of America, A, 7*, 128–140.

Cornsweet, T. N. & Teller, D. Y. (1965). Relation of increment threshold to brightness and luminance. *Journal of Optical Society of America, 55*, 1303–1308.

Davis, E. T., King, R. A., Surdick, R. T., Shapiro, A., Corso, G. M., Hodges, L. F. & Elliott, K. G. (1994). Distance perception of visual objects in a 3D environment. *Optics and Photonics News (Suppl.), 5*, 47.

Dresp, B. & Bonnet, C. (1991). Psychophysical evidence for low-level processing of illusory contours and surfaces in the Kanizsa square. *Vision Research, 31*, 1813–1817.

Dresp, B. & Bonnet, C. (1993). Psychophysical measures of illusory form perception: Further evidence for local mechanisms. *Vision Research, 33*, 759–766

Fiorentini, A. (1972). Mach band phenomena. In Jameson, D. and Hurvich, L. M. (Eds), *Handbook of sensory physiology Vol. VII/4, Visual psychophysics*. Berlin: Springer-Verlag.

Foley, J. M. & McCourt, M. E. (1985). Visual grating induction. *Journal of Optical Society of America, A, 2*, 1220–1230.

Grosof, D. H., Shapley, R. M. & Hawken, M. J. (1993). Macaque V1 neurons can signal 'illusory' contours. *Nature, 365*, 548–549.

Guth, S. L. (1973). On neural inhibition, contrast effects and visual sensitivity. *Vision Research, 13*, 937–957.

Jory, M. K. (1987). Increment thresholds in illusory contour line patterns. In Petry, S. & Meyer, G. E. (Eds), *The perception of* [illegible] New York: Springer-Verlag.

Kingdom, F. A. A. & McCourt, M. E. (1993). Do illusory gratings behave like real ones? *Perception, 22*, A5.

~~Kingdom, F. & Moulden, B. (1988). Border effects on brightness: A review of findings, models and issues. *Spatial Vision, 3*, 225–262.~~

Kulikowski (1976)

Lasley, D. J. & Cohn, T. E. (1981). Why luminance discrimination may be better than detection. *Vision Research, 21*, 273–278.

Legge, G. E. & Foley, J. M. (1980). Contrast masking in human vision. *Journal of Optical Society of America, 70*, 1458–1471.

~~Legge, G. E. & Kersten, D. (1983). Light and dark bars: Contrast discrimination. *Vision Research, 23*, 473–484.~~

McCourt, M. E. (1982). A spatial frequency dependent grating-induction effect. *Vision Research, 22*, 119–134.

~~McCourt, M. E. (1990). Disappearance of grating induction at scotopic luminances. *Vision Research, 30*, 431–437.~~

McCourt, M. E. (1994). Grating induction: A new explanation for stationary visual phantoms. *Vision Research, 34*, 1609–1618.

McCourt, M. E. (1995). Comparison of spatial frequency response and spatial summation of suprathreshold lateral interactions: Grating induction and contrast–contrast. *Vision Research*, (submitted for publication).

McCourt, M. E. & Blakeslee, B. (1993). The effect of edge blur on grating induction magnitude. *Vision Research, 33*, 2499–2508.

McCourt, M. E. & Blakeslee, B. (1994). A contrast matching analysis of grating induction and suprathreshold contrast perception. *Journal of Optical Society of America A, 11*, 14–24.

~~McCourt, M. E. & Foley, J. M. (1985). Spatial frequency interference on grating induction. *Vision Research, 25*, 1507–1518.~~

McCourt, M. E. & Kingdom, F. A. A. (1994). Facilitation of luminance grating detection by induced gratings. *Investigations Ophthalmic and Visual Science (Suppl.), 35*, 1901.

McCourt, M. E., Martinez-Uriegas, E. & Blakeslee, B. (1995). Temporal properties of grating induction. *Investigations Ophthalmic and Visual Science (Suppl.), 36*, S469.

McCourt, M. E. & Paulson (1994).

Moulden, B. & Kingdom, F. (1991). The local border mechanism in grating induction. *Vision Research, 31*, 1999–2008.

Pelli, D. G. (1985). Uncertainty explains many aspects of visual contrast detection and discrimination. *Journal of Optical Society of America, A, 2*, 1508–1531.

Peterhans & Van der Heydt (1991).

Polat, U. & Sagi, D. (1993). Lateral interactions between spatial channels: Suppression and facilitation revealed by lateral masking experiments. *Vision Research, 33*, 993–999.

Sparrock, J. M. B. (1969). Stabilized images: Increment thresholds and subjective brightness. *Journal of Optical Society of America, 59*, 872–874.

Spillmann, L., Fuld, K. & Neumeyer, C. (1984). Brightness matching, brightness cancellation, and increment threshold in the Ehrenstein illusion. *Perception, 13*, 513–520.

Takahashi, S. & Ejima, Y. (1985). Effects on grating detection of vertically displaced peripheral gratings. *Vision Research, 25*, 129–136.

Van Esen, J. S. & Novak, S. (1974). Detection thresholds within a display that manifests contour enhancement and brightness contrast. *Journal of Optical Society of America, 64*, 726–729.

Wetherill, G. B. & Levitt, H. (1965). Sequential estimation of points on a psychometric function. *British Journal Mathematics Statistics Psychology, 18*, 1–10.

Wilson, H. R. (1980). A transducer function for threshold and suprathreshold human vision. *Biological Cybernetics, 38*, 171–178.

Yang, J. & Makous, W. (1995). Modeling pedestal experiments with amplitude instead of contrast. *Vision Research, 35*, 1979–1989.

Acknowledgements—This research was supported by grants (to MM) from the National Eye Institute (EY-1013301), the Air Force Office of Scientific Research (F49620-94-1-0445) and the North Dakota Experimental Program to Stimulate Competitive Research (ND-EPSCoR). FK was supported by a grant from MRC Canada (MT-11554). The authors thank Dr Barbara Blakeslee for comments on the [illegible] and much helpful discussion.

THE DIFFERENTIAL EFFECTS OF TYPE 1 AND TYPE 2 ILLUSORY CONTOURS ON SPATIAL PATTERN DETECTION AND DISCRIMINATION

C. Sackmann[1] and M.E. McCourt[2]
Department of Psychology,
North Dakota State University, Fargo, ND

Supported by grants from ND-EPSCOR[1], NIH (EY1013301)[2] and AFOSR (F49620-94-1-0445)[2].

ABSTRACT

Purpose. Illusory contours (IC's), like luminance-defined contours, possess neurophysiological correlates and interact with physical stimuli. IC's produced by either offset gratings (Type 1 IC's), or by Kanizsa-type inducers (Type 2 IC's), elicit neural responses in primate visual cortical areas V1 and V2, respectively. The effects of Type 1 and Type 2 IC's on contrast discrimination thresholds for Gabor targets were assessed in order to infer the properties of the neural mechanisms which produce these contours in human observers. **Methods.** Type 1 and 2 IC strength was equated for all observers using a matching procedure. Increment thresholds for Gabor targets presented on Type 1 and 2 IC's were measured in four observers as a function of pedestal contrast (0-16%), spatial frequency (1.25-10 cpd, constant octave bandwidth) and orientation (0-90° relative to IC orientation). **Results.** Relative to control conditions which possessed inducers but lacked IC's, Type 1 IC's masked, whereas Type 2 IC's facilitated target detection and discrimination at low (<5%) pedestal contrasts. At higher pedestal contrasts this relationship was reversed. Both Type 1 and Type 2 IC's interacted maximally with targets of approximately 5 c/d which were oriented parallel to the IC's. **Conclusions.** Both Type 1 and Type 2 IC's interacted maximally with Gabor targets whose spatial parameters are those which optimally stimulate primary visual cortical neurons. This finding suggests that Type 1 and Type 2 IC's share a common mechanism of early contrast transduction. Type 1 and 2 IC's equated in strength have opposite effects, however, on the detection and discrimination of Gabor targets. This latter finding suggests a dissimilarity in the pooling mechanisms which underlie the formation of Type 1 and 2 illusory contours.

PURPOSE

Illusory Contours

"Subjective", "illusory" and "anomalous" are just a few terms that are used to describe contours which are visually discernible, yet physically absent from the stimulus itself. Studying illusory contours (IC's) offers insight into both the neural mechanisms of perception and the computational goals of the visual system, since they are formed by synthetic processes occurring within the visual nervous system. The window into the goals and mechanisms of visual processing, as well as compelling perceptual nature of IC's, has sparked research across a wide array of disciplines, including neurophysiologly, computer science and sensory psychology (Purghe & Coren, 1992).

The Varieties of Illusory Contours

IC's may be divided into two broad categories: Type 1 and Type 2. Type 1 IC's arise when a common boundary separates two visually distinct texture regions (see Figure 1). The textures that induce these contours may be gratings, filtered noise, line segments, or a variety of other micropatterns. Type 2 IC's arise when the arrangement of inducing figures (see Figure 2) is such that their cut-out portions are suggested to have been produced by a common occluding foreground object (e.g., an opaque square).

Neurophysiological Studies of Illusory Contours

Type 1 IC's may be generated at an earlier neural locus than Type 2 IC's. Electrophysiological recordings reveal that Type 1 (but not Type 2) IC's elicit neural responses in monkey primary visual cortex (area V1) (Grosof, Shapley & Hawken, 1993), whereas neural responses to Type 2 IC's are not observed until further neural processing has occurred, at visual association cortex (area V2) (von der Heydt, Peterhans & Baumgartner, 1984; 1989; Peterhans & von der Heydt, 1991).

Psychophysical Studies of Illusory Contours

In addition to possessing a phenomenal "realness", IC's also interact with physical stimuli. For example, visual thresholds for detecting small spots of light presented on or near a Type 2 IC are influenced by the presence of the contour (Dresp & Bonnet, 1991; 1993; McCourt & Paulson, 1994).

McCourt and Paulson (1994) found that Type 2 IC's could either facilitate, mask, or not affect the detection of superimposed luminance increments, where the different patterns were observed in different subjects. The variation in outcome was hypothesized to reflect the fact that the salience of IC's varies considerably (by a factor of five) across subjects (Banton & Levi, 1992). It should be noted that the influence of "masking" stimuli on target visibility in known to depend upon masker magnitude. Specifically, as masker magnitude increases target thresholds are first reduced and then elevated, giving rise to a so-called "dipper" in the threshold-versus-contrast (TvC) function (Legge & Foley, 1980). McCourt & Paulson (1994) proposed that IC's might, for a subject who perceives them as low in contrast, act as facilitatory pedestals and reduce target detection threshold. Conversely, for a subject who perceives IC's as higher in contrast, the same IC may act as a masker and elevate target detection threshold. The present experiments were

undertaken to systematically measure the influence of both Type 1 and Type 2 IC's on the detection of a standard visual stimulus (a Gabor wavelet) designed to optimally stimulate visual cortical neurons (Waston, Barlow & Robson, 1983).

GENERAL METHODS

Subjects

Three subjects (MM, CS and WC), two of whom are authors, participated in all of the experiments comprising the study. A fourth subject (AH) participated in Experiment One. All subjects were well-practiced psychophysical observers and possessed normal or corrected-to-normal vision.

Instrumentation

Stimuli were generated using a PC-compatible microcomputer (486/66 MHZ) with a custom-modified TIGA (Texas Instruments Graphics Adapter) graphics controller (Vision Research Graphics, Inc.). Images were presented on a high-resolution display monitor (21" IDEK Iiyama Vision Master, model MF-8221). Display format was 1024 (w) x 768 (h) pixels. Frame refresh rate was 97 Hz (non-interlaced). Viewed from a distance of 60.7 cm the entire display subtended 32° x 32°; individual pixels measured 0.031° x 0.031°. Mean display luminance was 50 cd/m^2. All images possessed 2^8 simultaneously presentable linearized intensity levels selected from a palette of approximately 2^{15}.

Stimuli

Type 1 Illusory Contours

Experimental Condition: Type 1 illusory contours (IC's) were produced using two vertically offset, horizontally oriented sinewave gratings. Grating spatial frequency was 3 cycles per degree (cpd). Grating contrast was 4.15% (see below for a description of the procedure used to establish this contrast value). The grating patches measured 6.9° (w) x 10.35° (h). The abutting inducing gratings were vertically offset by 180° spatial phase, resulting in the formation of an IC. All display regions unoccupied by inducing gratings were set to the mean display. Figure 1(a) presents an illustration of the Type 1 IC stimulus.

Control Condition: The control condition consisted of abutting Type 1 IC inducing gratings with zero vertical spatial phase offset. Figure 1(b) presents an illustration of the Type 1 IC control configuration.

Type 2 Illusory Contours

Experimental Condition: Type 2 IC's were produced using four inducing elements consisting of circular sinewave gratings of 3 cpd (radial) spatial frequency; inducer diameter was 6.9°. Right-angle wedges were removed from the inducing elements resulting in the classic "pacman" inducer (Kanizsa, 1976). The "mouths" of the pacmen were arranged to give the impression that the corners of four circular inducers were occluded by an opaque square. The corner-to-corner dimensions of the occluding square measured 10.35°. Illusory contours were thus 3.45° in length, as

measured between the outer edges of the inducers, resulting in a support ratio of 0.667. The inducer spatial frequency and support ratio were selected to maximize the perceived clarity and contrast of the IC (Banton & Levi, 1992; Lesher & Mingolla, 1993). All display regions that were not occupied by the circular inducing elements were set to the mean display luminance. The use of luminance-balanced circular sinewave inducers allowed the effect of illusory contours *per se* to be studied in the absence of any brightness contrast between the interior of the illusory square and the background which solid inducers produce. Figure 2(a) presents an illustration of the Type 2 IC experimental stimulus.

Control Condition: In the control condition the two right-hand inducing elements were rotated through 180°, such that the wedges pointed outward. This arrangement eliminated the impression of occlusion and destroyed the illusory contour while controlling for the presence and proximity of the inducing elements. Figure 2(b) presents an illustration of the control Type 2 IC control configuration.

Luminance-Defined Contours

The luminance-defined contour (LDC) was produced using a two-dimensionally Gaussian-damped 0.05 cpd square-wave. The patch measured 6.9° (w) x 10.35° (h) with the luminance step occurring at the centroid of the Gaussian. Edge contrast was 1.6% (see below for a description of the procedure used to establish this contrast value) with σ_x=2° and σ_y=5°.
All display regions unoccupied by the patch were set to the mean display luminance. Figures 3(a) and (b) present illustrations of the luminance-defined contour stimulus with Gabor targets in either complimentary or opposite spatial phase to the edge, respectively.

Target Stimuli

The target stimulus was a sine (odd-symmetric), vertically-oriented Gabor wavelet. This stimulus was a product of a one-dimensional sinewave grating and a two-dimensional Gaussian function. The luminance distribution (L) of this stimulus is a function of five parameters:

$$L(x,y,\mu_{xy},\sigma_x,\sigma_y,\omega_x,C)=C[0.5\sin(\omega_x x)+1]\ \exp[-(x-\mu_{xy})^2/\sigma^2_x]\ \exp[-(y-\mu_{xy})^2/\sigma^2_y]$$

where μ_{xy} specifies the centroid of the distribution, ω_x determines the vertical spatial frequency and C defines the contrast of the sinusoidal grating, which can range from 0 to 1.0. Parameters σ_x and σ_y are space-constants which set the spatial dispersion of the Gabor target in the x and y dimensions, respectively. The Gabor target was selected because it has been shown to be the stimulus which is detected by the human visual system with the greatest statistical efficiency (Watson, Barlow & Robson, 1983). Figure 4 provides images of the target stimuli used in these experiments.

Pedestal Stimuli

The spatial parameters of the pedestal stimuli were identical to those of the target stimuli; only the contrast (C) of the pedestal was varied.

Procedure

All experiments (except where noted) utilized an adaptive two temporal interval forced-choice procedure (QUEST, Watson & Pelli, 1983), to obtain target contrast discrimination thresholds. Runs were terminated after 30 trials. No feedback with respect to response was given. A minimum of 5 thresholds (mean=6) were obtained for each level of the manipulated variable in all experiments.

Inducing Stimuli

All inducing stimuli which gave rise to either real or illusory contours, were presented such that the contours appeared in the same relative position. The Type 2 IC was used as a reference for the location to present Type 1 and real contours as well as determining there contour length which was kept constant at a support ratio of 0.667 as determined by the Type 2 IC. Presentation of control and experimental stimuli consisted of two independent temporal intervals with duration's of 2 sec. In each temporal interval the contrast of the inducing stimuli was linearly ramped on and off, with a ramp duration lasting 100 msec. Each interval was preceded by a brief cueing tone: 1000 Hz for the first interval and 2000 Hz for the second interval. The inter-stimulus interval was 500 msec and the inter-trial interval was approximately 1 sec.

Target Stimuli

The target stimulus randomly appeared in one of the two cued temporal intervals; pedestal stimuli were present in both temporal intervals. Target and pedestal contrast were modulated by a Gaussian temporal envelope with a time-constant (σ_t) of 100 msec and a peak of (μ_t) of 154.6 msec in each 2 sec interval. Except were noted, all targets were vertically oriented and centered on the IC's. When presented on Type 1 IC's, targets were vertically centered on a location corresponding to a zero-crossing for both inducing gratings.

Equating Contour Strength

A one-down one-up two-alternative forced-choice adaptive staircase procedure was used to establish subjective equality between the clarity and contrast of Type 1 and Type 2 IC's, as well as for luminance-defined contours. This procedure was adopted to help ensure that valid comparisons could be made concerning the differential effects which Type1, Type 2 and luminance-defined contours have on Gabor target thresholds. Type 1 and luminance-defined contours were pair-wise matched with the Type 2 contour. Each contour was presented for 2 sec in separate temporal intervals. Subjects indicated the temporal interval containing the contour possessing the greatest clarity or strength by depressing the appropriate response button. The contrast of Type 1 IC's and luminance-defined contours was adjusted contingent upon the response. Each staircase terminated after eight reversals in the direction of the contrast change, and the mean contrast was then computed. Each subject completed a minimum of five staircases.

Type 2 illusory contour strength equaled Type 1 IC strength when Type 1

inducing grating contrast was 4.34% (CS), 3.96% (AH) or 7.87% (MM). Due to the close similarity of individual equivalent contrast values, Type 1 inducing grating contrast was set to the mean value (4.15%) for all observers in subsequent experiments. Type 2 illusory contour strength was equated with that of the luminance-defined contour when the latter possessed a contrast of 1.66% (CS) or 1.54% (MM). Due to the close similarity of individual equivalent contrast values, the luminance-defined contour contrast was set to the mean value (1.60%) for all observers in subsequent experiments.

Experiment 1: Increment Threshold Functions

Rationale

The effect which superimposed "masking" stimuli have on target visibility depends upon masker magnitude, such that as masker magnitude increases, thresholds are initially reduced and subsequently elevated, giving rise to the so-called "pedestal effect" (Legge & Foley, 1980). McCourt & Paulson (1994) proposed that IC's might facilitate the detection of luminance increments and decrements by acting as low contrast pedestals. If this hypothesis is correct, then increment threshold functions for targets positioned on illusory contours should simply be shifted laterally along the pedestal contrast axis by an amount equal to the intrinsic pedestal contrast value of the IC.

Methods

Gabor targets thresholds were determined in conjunction with six pedestal contrasts (0, 0.01, 0.02, 0.04, 0.08 and 0.16). Pedestal contrast was incremented in ascending order to minimize any contrast adaptation effects. Thresholds were also measured for targets presented on homogeneous backgrounds of equal mean luminance, absent any inducing stimuli.

Results

Figure 5 plots mean target threshold (across all four subjects) versus contrast functions, ±1 standard error (TvC functions). Upper and lower panels refer to Type 1 and Type 2 IC's, respectively. Left- and right-hand panels illustrate TvC functions in the experimental and control conditions, respectively. Dashed lines in these panels indicate mean TvC functions for targets obtained in the absence of the IC inducing stimuli. The ratio of target contrast thresholds in the control and experimental conditions are plotted as a function of pedestal contrast in the rightmost panels. At pedestal contrasts below approximately 4%, Type 1 IC's significantly elevate target thresholds while Type 2 IC's exert a facilitory effect. With increasing pedestal contrast the masking effect of Type 1 IC's and the facilitation effect of Type 2 IC's diminishes.

Experiment 2: Effect of Target Orientation

Rationale

One proposition is that IC's arise from activity in spatially localized neural

pools, which is pooled by spatially extensive "collector" units at a subsequent stage of processing. Feedback from the "collector" units recruits, in turn, activity in those spatially localized neurons whose receptive fields are positioned within the homogeneous region along the length of the IC (Grossberg & Mingolla, 1985). If this model, or one like it, is correct, then it is of interest to determine how specific such feedback is with respect to the fundamental response selectivities of the recipient neurons, such as orientation, spatial frequency, and positional specificity. In order to answer this question, Gabor target thresholds were measured on both Type 1 and 2 IC's as a function of target orientation.

Methods

How specific is collector unit feedback with respect to recipient unit orientation tuning? To answer this question thresholds were measured on Type 1 and 2 IC's for targets at ten different orientations (1°, 2°, 4°, 8°, 16°, 32°, 45°, 64° and 90° relative to IC orientation). Pedestal contrast was zero.

Results

Figure 6 plots mean target thresholds (across three observers) as a function of target orientation (± 1 standard error). Upper and lower panels refer to Type 1 and Type 2 IC's, respectively. Left- and right-hand panels plot data from the experimental and control conditions, respectively. Dashed lines in these panels indicate mean target thresholds obtained in the absence of IC inducing stimuli. The ratio of target contrast thresholds in the control and experimental conditions are plotted as a function of target orientation in the rightmost panels. Type 1 IC's exert a masking effect on target threshold across a wide range of orientations, with the greatest masking effect occurring at the 0° (collinear) orientation, and a steadily decreasing effect as target orientation approaches orthogonality (90°). Type 2 IC's exert a facilitory effect, but also influence target detection across a narrower range of orientations. Unlike Type 1 IC's, however, the facilitory effect of Type 2 IC's may be bimodal, with a narrow peak of facilitation near 0° (collinear), and a broader peak near 60°.

Experiment 3: Effect of Target Position from Illusory Contour

Rationale

How specific is collector unit feedback with respect to recipient unit spatial position? To answer this question thresholds were measured on Type 1 and 2 IC's for vertically oriented (i.e, optimal) targets located at various positions from both Type 1 and 2 IC's.

Methods

Targets were randomly presented in experimental and control conditions at eight locations (+1, -1, -3, -6, -12, -24, and -48 pixels from the IC). See Figure 7 for a pictorial illustration of the sampled positions. For Type 1 IC's positive values denote positions to the left of the illusory contour, while negative values denote rightward shifted positions. For Type 2 IC's positive values denote positions exterior to the

illusory square, while negative values denote interior positions. Pedestal contrast was zero.

Results

Figure 8 shows the mean thresholds (across four observers) as a function of target position (± 1 standard error). Upper and lower panels refer to Type 1 and Type 2 IC's, respectively. Left- and right-hand panels plot data from the experimental and control conditions, respectively. Dashed lines in these panels indicate mean target thresholds obtained in the absence of any IC inducing stimuli. The ratio of target contrast thresholds in the control and experimental conditions are plotted as a function of target position in the rightmost panels. Consistent with previous results, Type 1 IC's exert a masking effect on target threshold at all spatial positions out to approximately 12 pixels (0.37°, equivalent to approximately 2 wavelengths of the Gabor target), with the greatest masking occurring for targets directly on the IC. Type 2 IC's exert a facilitation effect with an oscillatory spatial profile, with a prominent notch for targets positioned nearest the IC (locations 0 and -1).

Experiment 4: Effect of Target Spatial Frequency

Rationale

How specific is collector unit feedback with respect to recipient unit spatial frequency? To answer this question thresholds were measured on Type 1 and 2 IC's for vertically oriented targets located directly on IC's. Target spatial frequency was varied; pedestal contrast was zero.

Methods

Targets were randomly presented in experimental and control conditions at five spatial frequencies (1.25, 2.5, 5.0, 7.5, and 10 cpd). Gabor target bandwidth was held constant (in octaves); the Gaussian space constant was changed in accord with spatial frequency to encompass a fixed number of cycles. Pedestal contrast was zero.

Results

Figure 9 shows the mean thresholds (across four observers) as a function of target spatial frequency (± 1 standard error). Upper and lower panels refer to Type 1 and Type 2 IC's, respectively. Left- and right-hand panels plot data from the experimental and control conditions, respectively. Dashed lines in these panels indicate mean target thresholds obtained in the absence of IC inducing stimuli. The ratio of target contrast thresholds in the control and experimental conditions are plotted as a function of target spatial frequency in the rightmost panels. Both Type1 and Type 2 IC's exert the greatest effects on target detection thresholds for targets whose spatial frequency is 5.0 cpd. The masking effect of Type 1 IC's is somewhat broader with respect to spatial frequency than is the facilitation effect of Type 2 IC's.

Experiment 5: Effect of Target Aspect Ratio

Rationale

Are the effects which IC's are observed to exert on target contrast detection and discrimination mediated by at the processing site at which feedback from higher-order "collector" units converges, or at the level of the "collector" units themselves? If the former hypothesis is correct, then the interaction of targets and IC's should be maximal when targets are matched to the receptive field properties of the recipient units. On the other hand, if latter hypothesis is correct, then the interactions should be maximal when the stimulus characteristics of the target are matched to the receptive field characteristics of the "collector" units. One characteristic of the hypothetical "collector" units is that they have elongated receptive fields relative to the low-level units they are proposed to provide feedback upon. To address this question thresholds were measured on Type 1 and 2 IC's for vertically oriented, 5.0 cpd (i.e, optimal) targets located directly on IC's. Target aspect ratio was varied; pedestal contrast was zero.

Methods

Targets were randomly presented in experimental and control conditions at multiple aspect ratios by varying the vertical space constant of the Gaussian envelope. For Type 1 IC's height:width aspect ratios of the target were: 1:1 (σ_x=0.15°, σ_y=0.15°), 5:1 (σ_y=0.75°, σ_x=0.15°), and 13.3:1 (σ_y=2.0°, σ_x=0.15°). For Type 2 IC's target aspect ratios were: 1:1 (σ_x=0.15°, σ_y=0.15°) and 5:1, (σ_y=0.75°, σ_x=0.15°). For Type 2 IC's targets with aspect ratios larger than 5:1 encroached on the inducing stimuli, and were therefore excluded. See Fig. 4 for images of these Gabor targets. Pedestal contrast was zero.

Results

Figure 10 shows the mean thresholds (across four observers) as a function of target aspect ratio (± 1 standard error). Upper and lower panels refer to Type 1 and Type 2 IC's, respectively. Left- and right-hand panels plot data from the experimental and control conditions, respectively. The ratio of target contrast thresholds in the control and experimental conditions are plotted as a function of target aspect ratio in the rightmost panels. Target contrast detection thresholds did not vary with target aspect ratio for either Type1 or Type 2 IC's.

Experiment 6: Effects of Target and Inducer Polarity

Rationale

In some respects IC's are line-like, whereas in other respects they are edge-like. If the feedback from "collector" units is predominately onto lower-level mechanisms with even-symmetric receptive field (line-like) structure, then thresholds for Gabor targets positioned on the IC would not be expected to vary as a function of contrast polarity. On the other hand, if such feedback is predominately onto mechanisms possessing odd-symmetric (edge-like) receptive field structure, then an

interaction with Gabor target polarity is predicted. Gabor target polarity was varied in combination with variations in IC inducer polarity, in order to explore this issue.

Methods

Gabor targets in either sine or anti-sine spatial phase were randomly presented in either control or experimental IC conditions, and on a luminance-defined edge. Type 1 IC's were as shown in Fig. 1. Type 2 IC inducers were either luminance-balanced (circular sinewaves: see Fig. 2), which do not induce a brightness change within the illusory square figure, or consisted of solid black (0 cd/m^2) or white (200 cd/m^2) inducers (see Figure 11 for reproductions of the latter stimulus conditions). Background luminance was 100 cd/m^2.

Results

Figure 12 plots mean target thresholds (across four observers) as a function of target contrast polarity (± 1 standard error). Upper and lower panels refer to Type 1 and Type 2 IC's, respectively. Left- and right-hand panels plot data from the experimental and control conditions, respectively. The ratio of target contrast thresholds in the control and experimental conditions are plotted as a function of target aspect ratio in the rightmost panels. Target thresholds in the absence of inducers is shown by the dashed lines.

Luminance-Defined Edges

Gabor target thresholds on luminance defined edges are polarity-sensitive (triangular symbols): threshold is significantly lower for targets in complimentary (anti-sine) spatial phase (see Fig. 3a).

Type 1 IC's

The masking effect of Type 1 IC's is independent of target contrast polarity.

Luminance-Balanced (Circular Sinewave) Inducers

The facilitating effect of Type 2 IC's in which there is no brightness induction is independent of target contrast polarity.

Brightness-Inducing Configurations

Even in the presence of brightness changes within the illusory figure, target thresholds are independent of contrast polarity.

CONCLUSIONS

- Type 1 IC's mask whereas Type 2 IC's facilitate Gabor target contrast detection and discrimination. The two types of IC are likely to arise from different neural mechanisms. Either effect diminishes with increasing pedestal contrast.

- IC's do not act as simple pedestals; they vertically displace Gabor target TvC functions, implying an effect mediated by divisive inhibition.

- Type 1 IC's mask Gabor targets most effectively at zero displacement; Type 2 IC's facilitate most effectively at small lateral displacements. Type 1 IC's exert effects over much larger distances than do Type 2 IC's, whose effect is oscillatory with distance.

- Type 1 and 2 IC's interact most strongly with Gabor targets of 5 cpd.

- The effects of IC's is independent of Gabor target aspect ratio.

- Luminance-defined contours exert polarity-dependent effects on Gabor target threshold. Target threshold is independent of contrast polarity for both Type 1 and Type 2 IC's, even those which give rise to brightness changes within the illusory square figure.

LITERATURE CITED

Banton, T. & Levi, D.M. (1992) The perceived strength of illusory contours. *Perception and Psychophysics, 52*, 676-684.

Dresp, B. & Bonnet, C. (1991) Psychophysical evidence for low-level processing of illusory contours and surfaces in the Kanizsa square. *Vision Research, 31*, 1813-1817.

Dresp, B. & Bonnet, C. (1993) Psychophysical measures of illusory form perception: Further evidence for local mechanisms. *Vision Research, 33*, 759-766.

Grosof, D. H., Shapley, R. M. & Hawken, M. J. (1993) Macaque V1 neurons can signal `illusory' contours. *Nature, 365*, 548-549.

Grossberg, S. & Mingolla, E. (1985) Neural dynamics of form perception: Boundary completion, illusory figures, and neon color spreading. *Psychological Review, 92*, 173-211.

Kanizsa, G. (1976) Subjective contours. *Scientific American, 234*, 48-52.

Legge, G.E. & Foley, J.M. (1980) Contrast masking in human vision. *Journal of the Optical Society of America, 70*, 1458-1471.

Lesher, G.W. & Mingolla, E. (1993) The role of edges and line-ends in illusory contour formation. *Vision Research, 33*, 2253-2270.

McCourt, M. E. & Paulson, K. (1993) The influence of illusory contours on the detection of luminance increments and decrements. *Vision Research, 34,* 2469-2475.

Peterhans, E. & Von der Heydt, R. (1991) Subjective contours: Bridging the gap between psychophysics and physiology. *Trends In Neuroscience, 14,* 112-119.

Purghe, F. & Coren, C. (1992) Subjective contours 1900-1990: Research trends and bibliography. *Perception & Psychophysics, 51*, 291-304.

Von der Heydt, R., Peterhans, E. & Baumgartner, G. (1984) Illusory contours and cortical neuron responses. *Science, 224,* 1260-1262.

Von der Heydt, R., Peterhans, E. & Baumgartner, G. (1989) Mechanisms of contour perception in monkey visual cortex. II. Contours bridging gaps. *The Journal of Neuroscience, 9,* 1749-1763.

Watson, A.B. & Pelli, D. G. (1983) QUEST: A Bayesian adaptive psychometric method. *Perception and Psychophysics, 33,* 113-120.

Watson, A.B., Barlow, HB. & Robson, JG (1983) What does the eye see best? *Nature, 302*, 399-422.

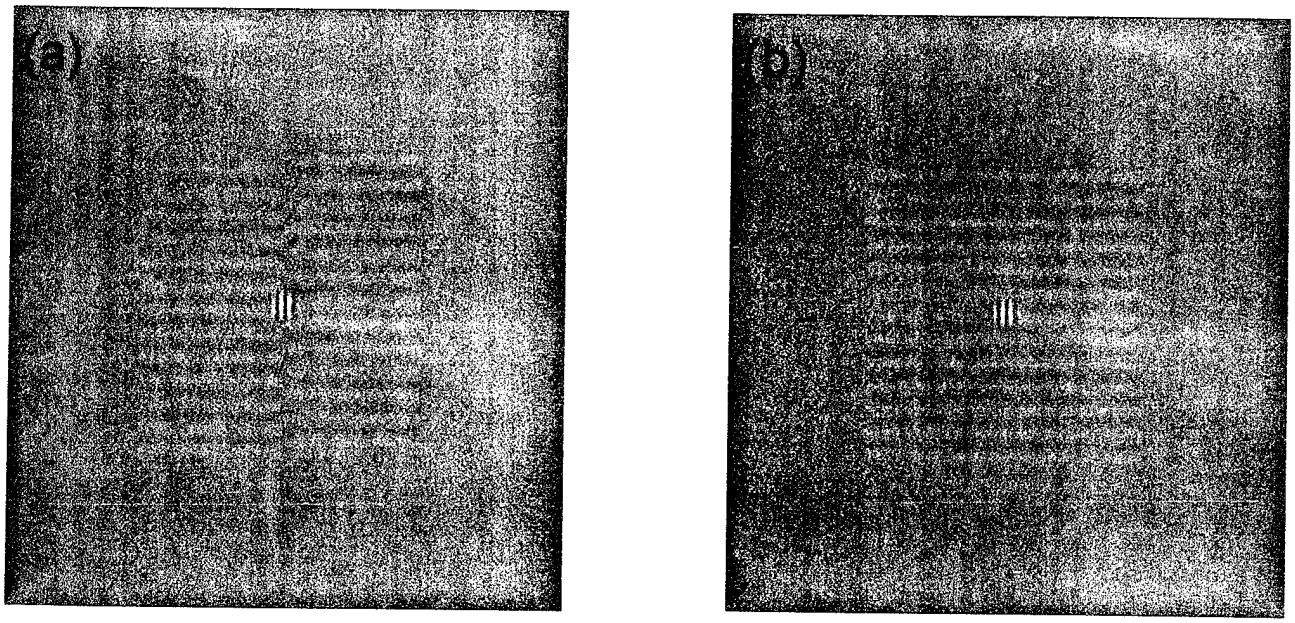

Figure 1

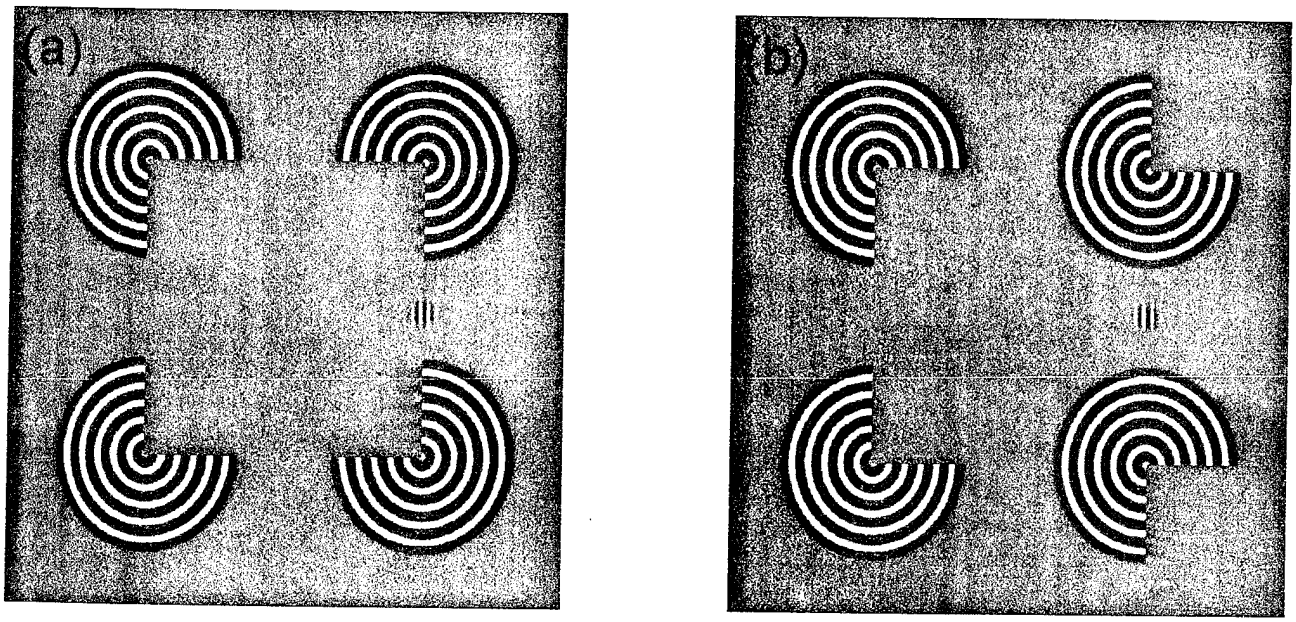

Figure 2

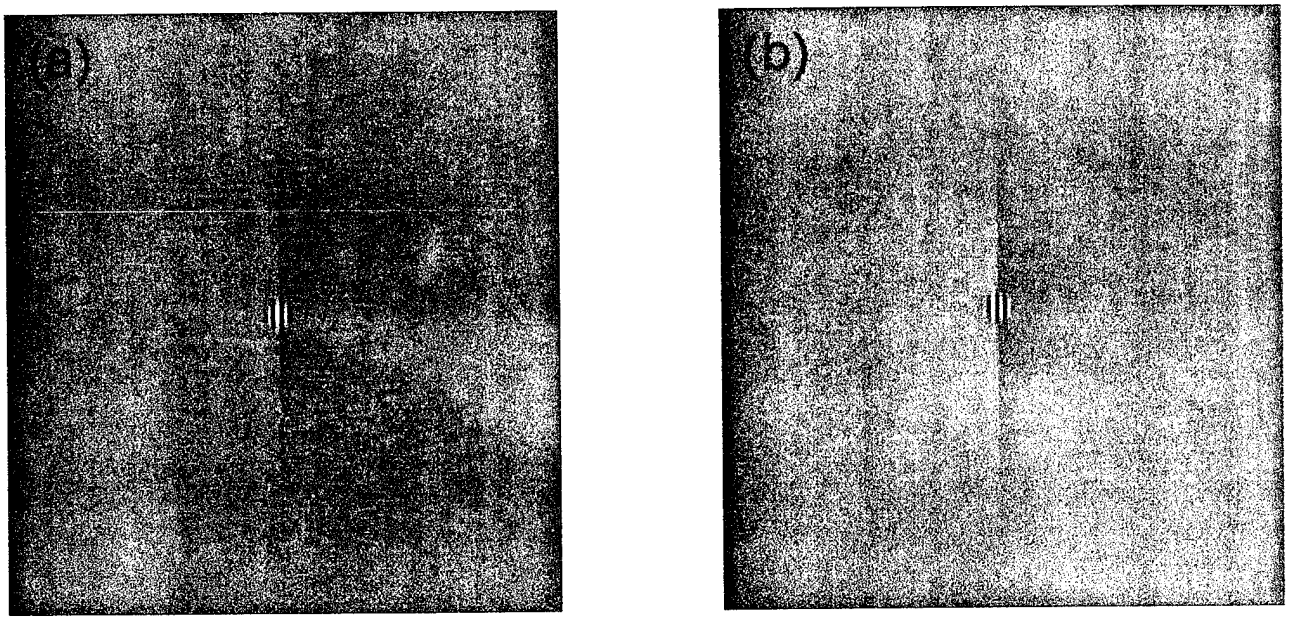

Figure 3

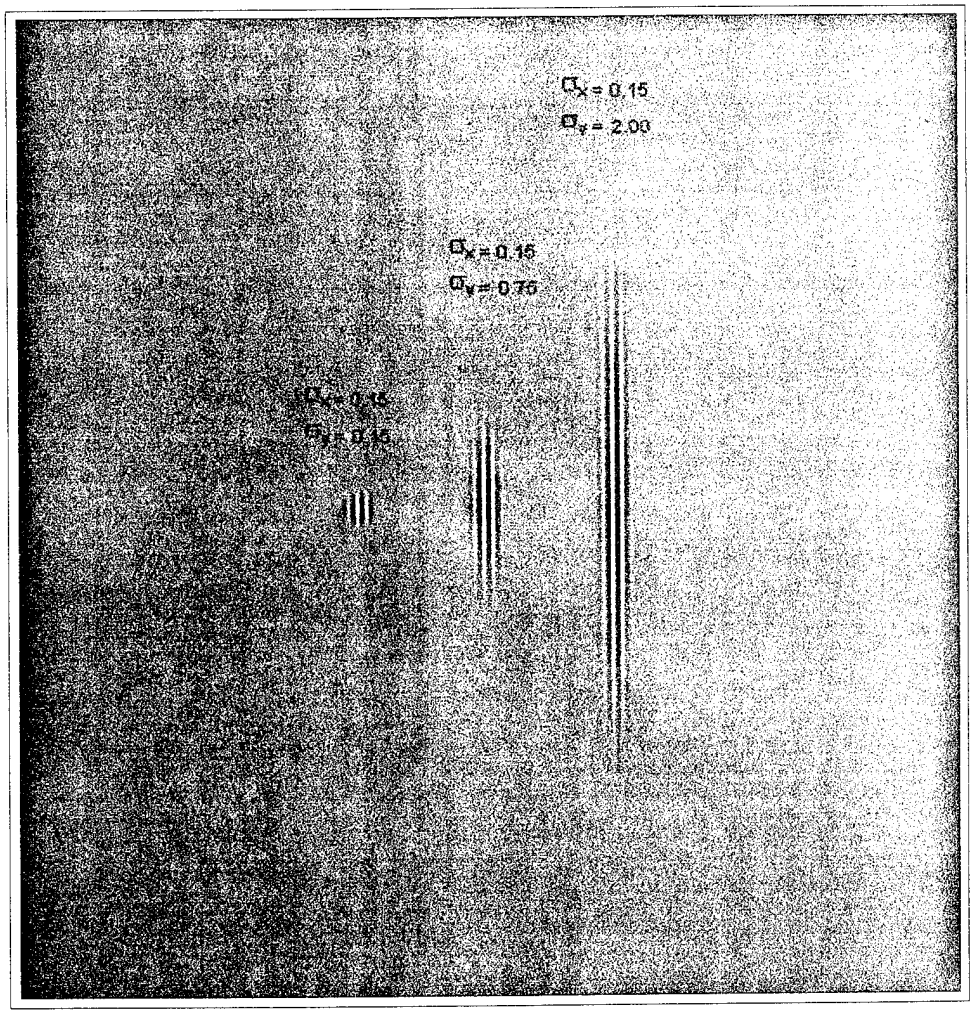

Figure 4

Increment Threshold Functions

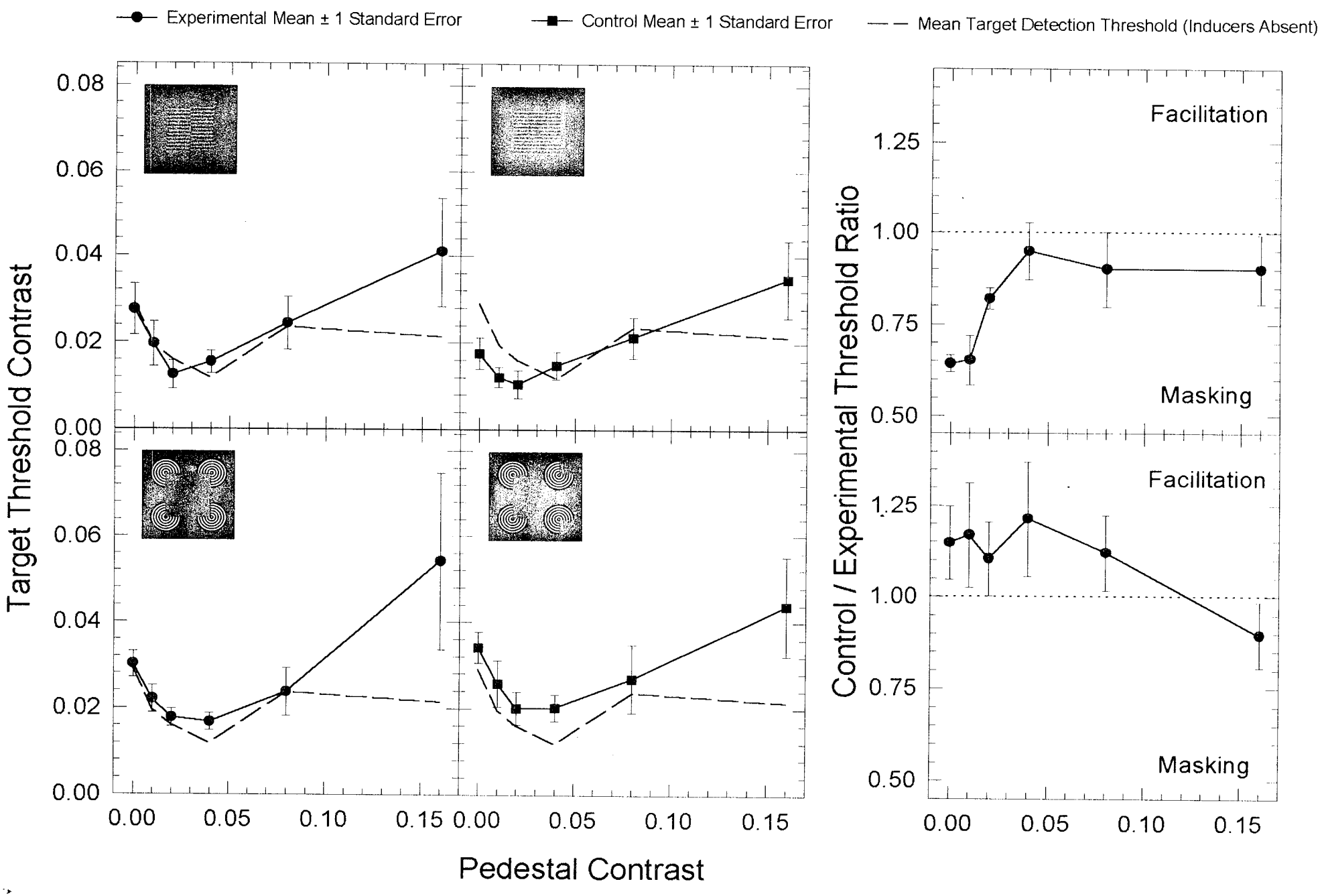

Figure 5

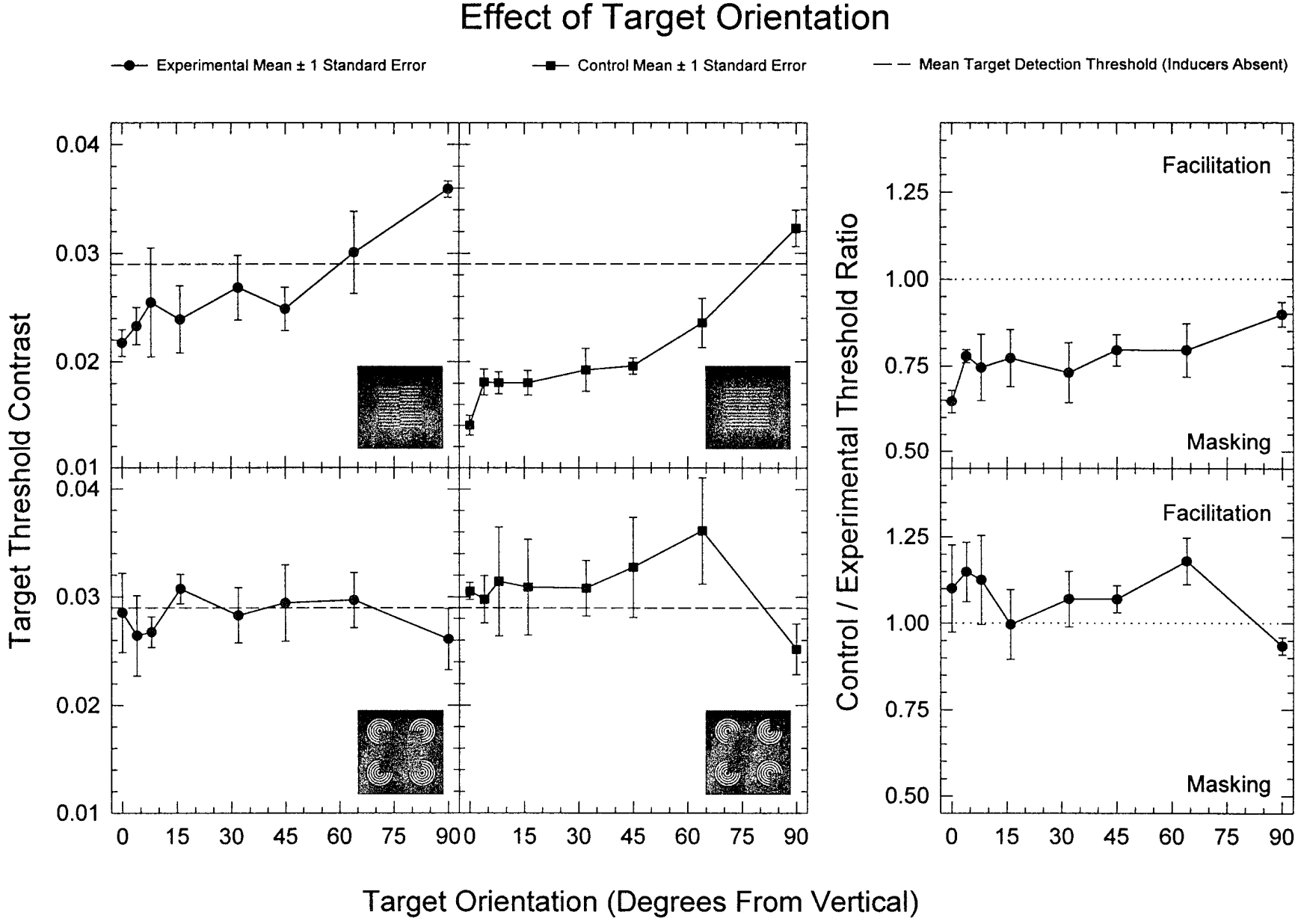
Effect of Target Orientation
Experimental Mean ± 1 Standard Error
Control Mean ± 1 Standard Error
Mean Target Detection Threshold (Inducers Absent)
Target Threshold Contrast
0.04
0.03
0.02
0.01
0 15 30 45 60 75 90
Control / Experimental Threshold Ratio
1.25
1.00
0.75
0.50
Facilitation
Masking
Target Orientation (Degrees From Vertical)

Figure 6

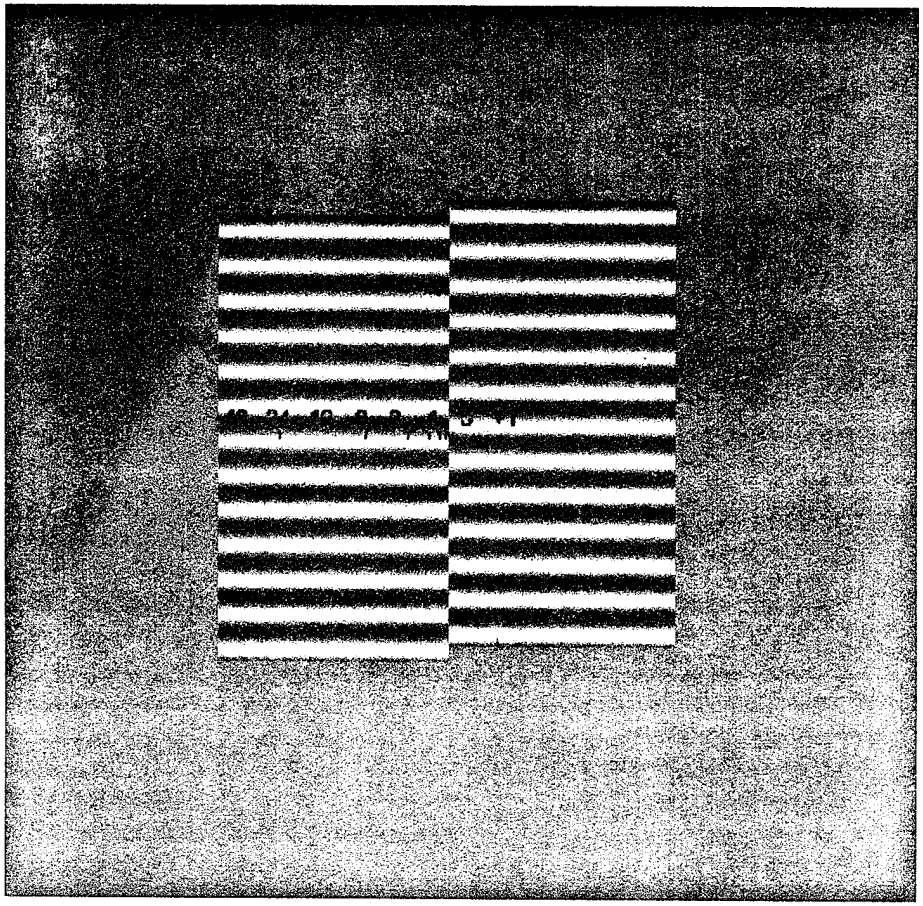

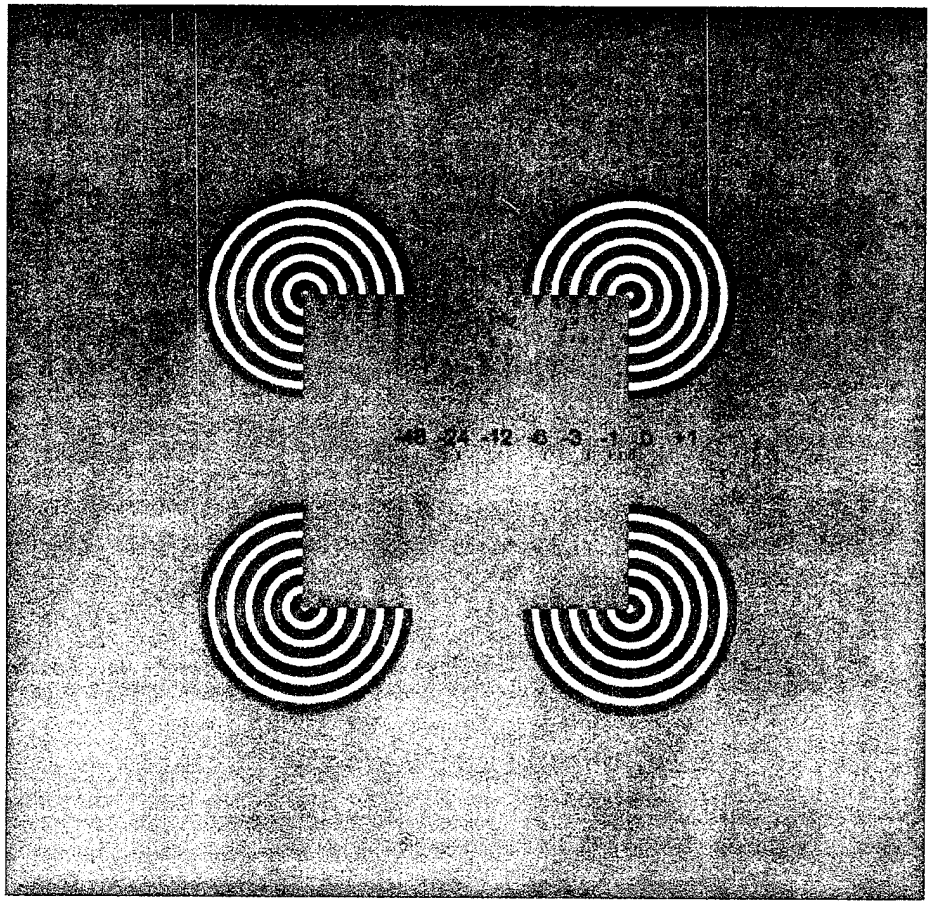

Figure 7

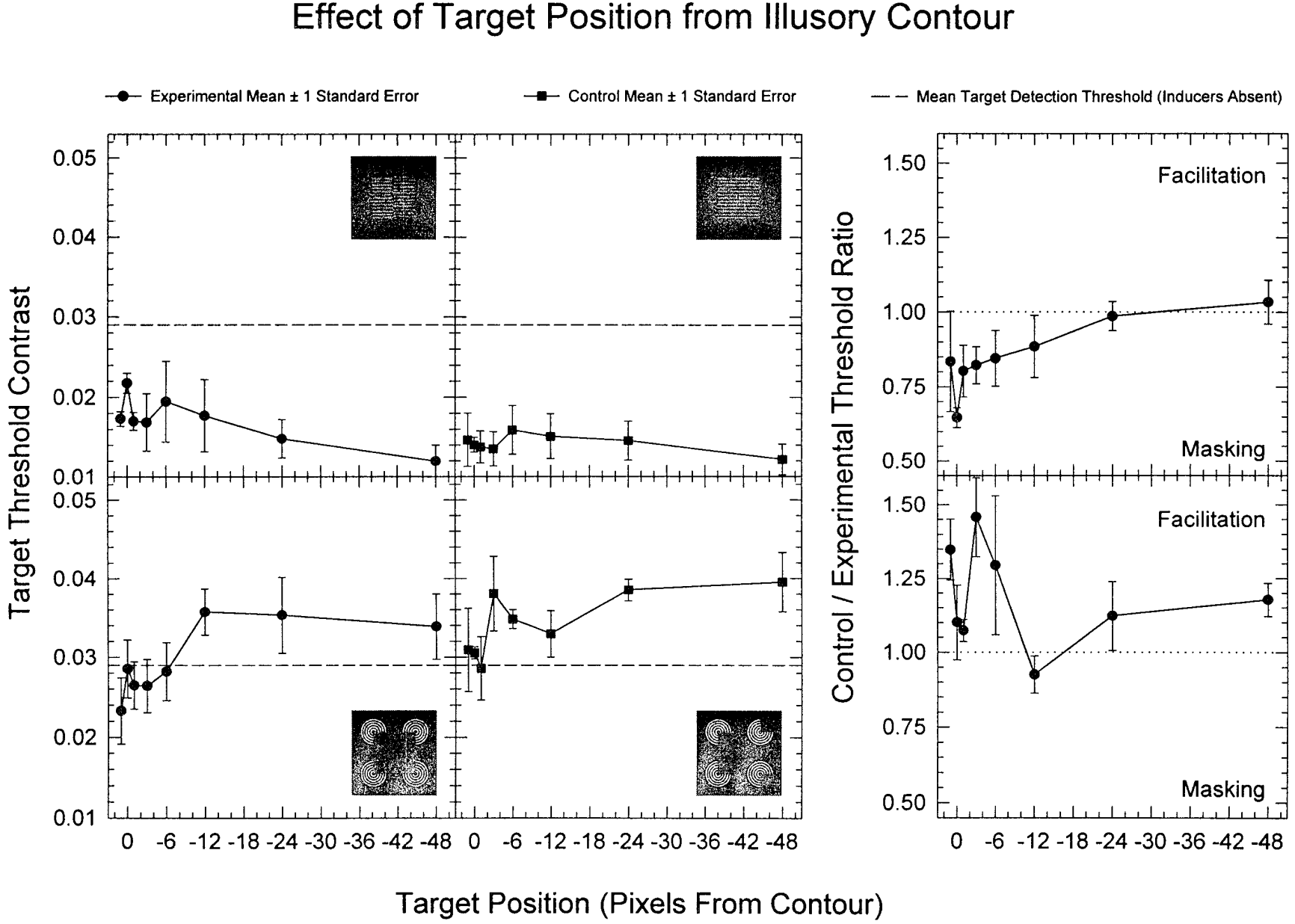
Effect of Target Position from Illusory Contour
Experimental Mean ± 1 Standard Error
Control Mean ± 1 Standard Error
Mean Target Detection Threshold (Inducers Absent)
Target Threshold Contrast
0.05
0.04
0.03
0.02
0.01
0 -6 -12 -18 -24 -30 -36 -42 -48
Control / Experimental Threshold Ratio
1.50
1.25
1.00
0.75
0.50
Facilitation
Masking
Target Position (Pixels From Contour)

Figure 8

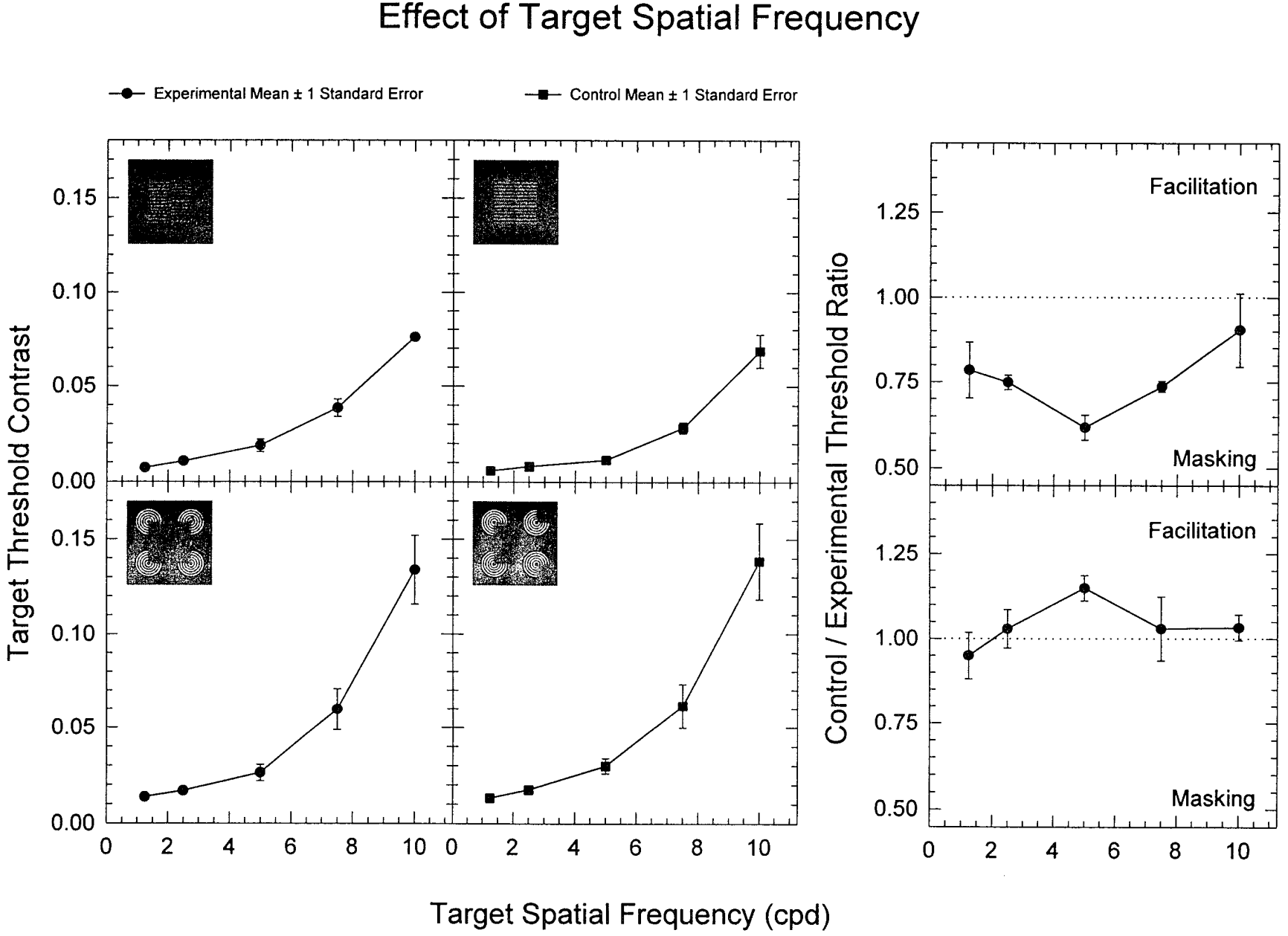
Effect of Target Spatial Frequency
Experimental Mean ± 1 Standard Error
Control Mean ± 1 Standard Error
Target Threshold Contrast
0.15
0.10
0.05
0.00
0 2 4 6 8 10
Target Spatial Frequency (cpd)
Control / Experimental Threshold Ratio
1.25
1.00
0.75
0.50
Facilitation
Masking
Facilitation
Masking

Figure 9

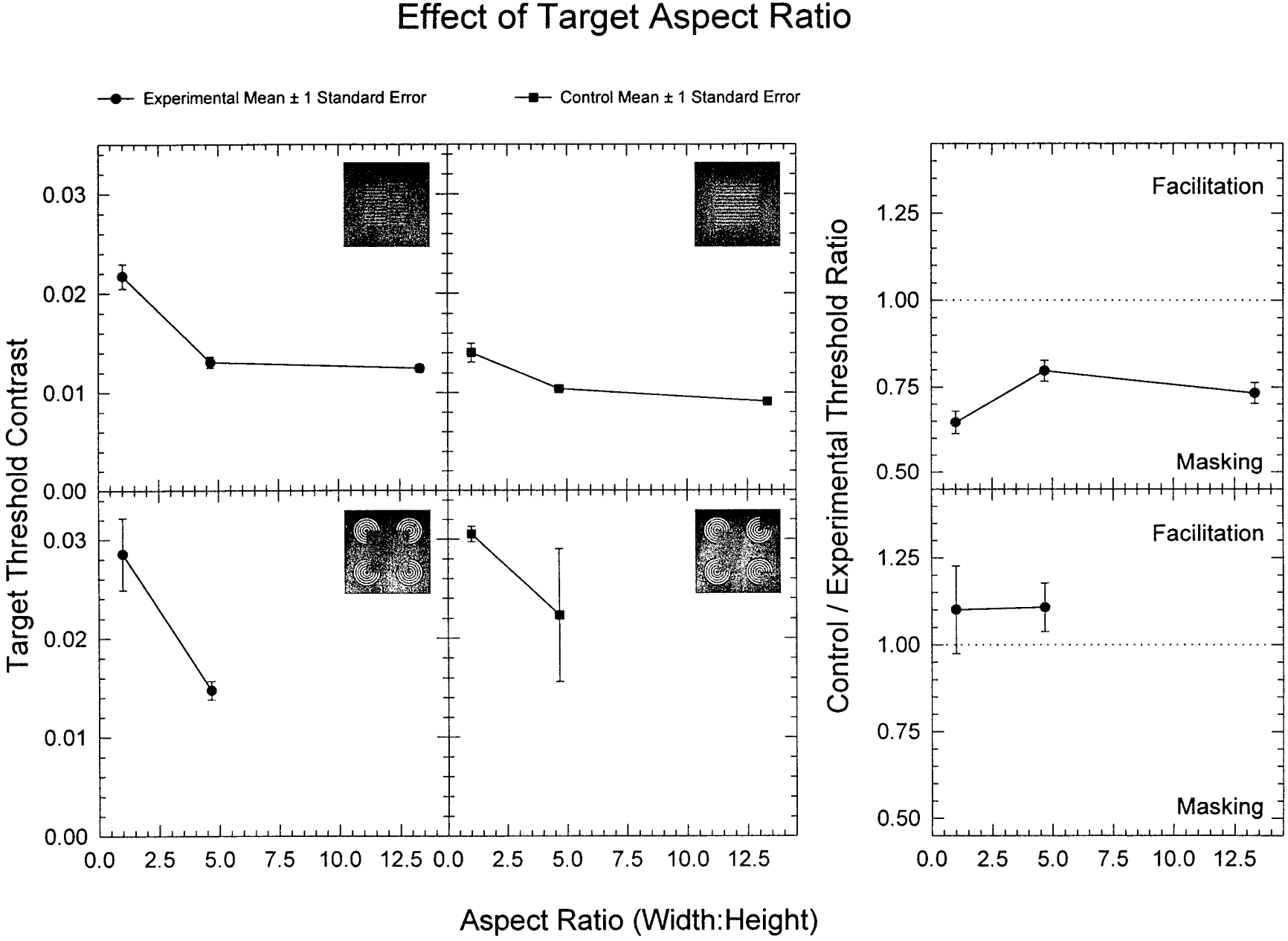
Effect of Target Aspect Ratio
Experimental Mean ± 1 Standard Error
Control Mean ± 1 Standard Error
Target Threshold Contrast
0.03
0.02
0.01
0.00
0.0
2.5
5.0
7.5
10.0
12.5
Aspect Ratio (Width:Height)
Control / Experimental Threshold Ratio
1.25
1.00
0.75
0.50
Facilitation
Masking

Figure 10

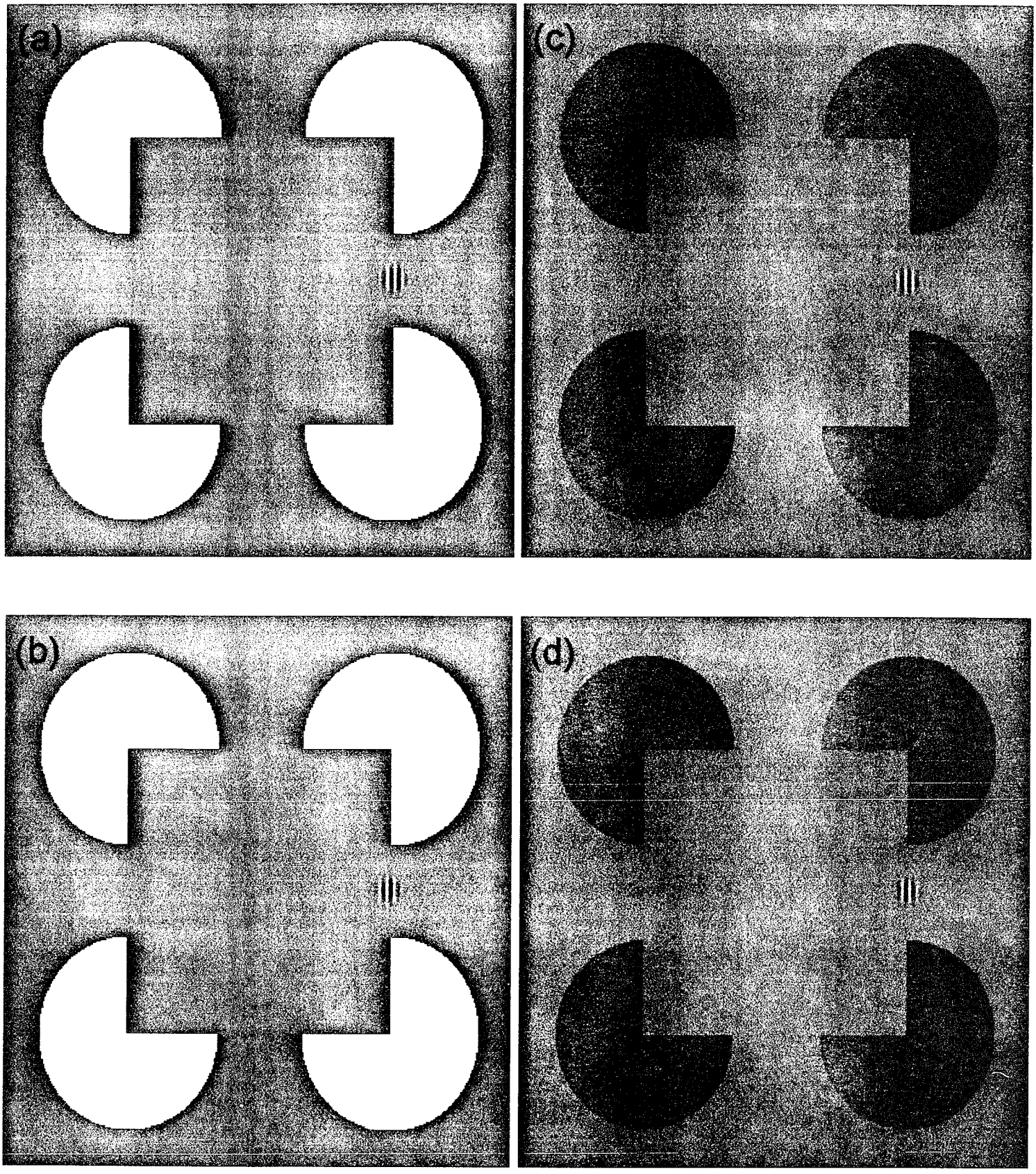

Figure 11

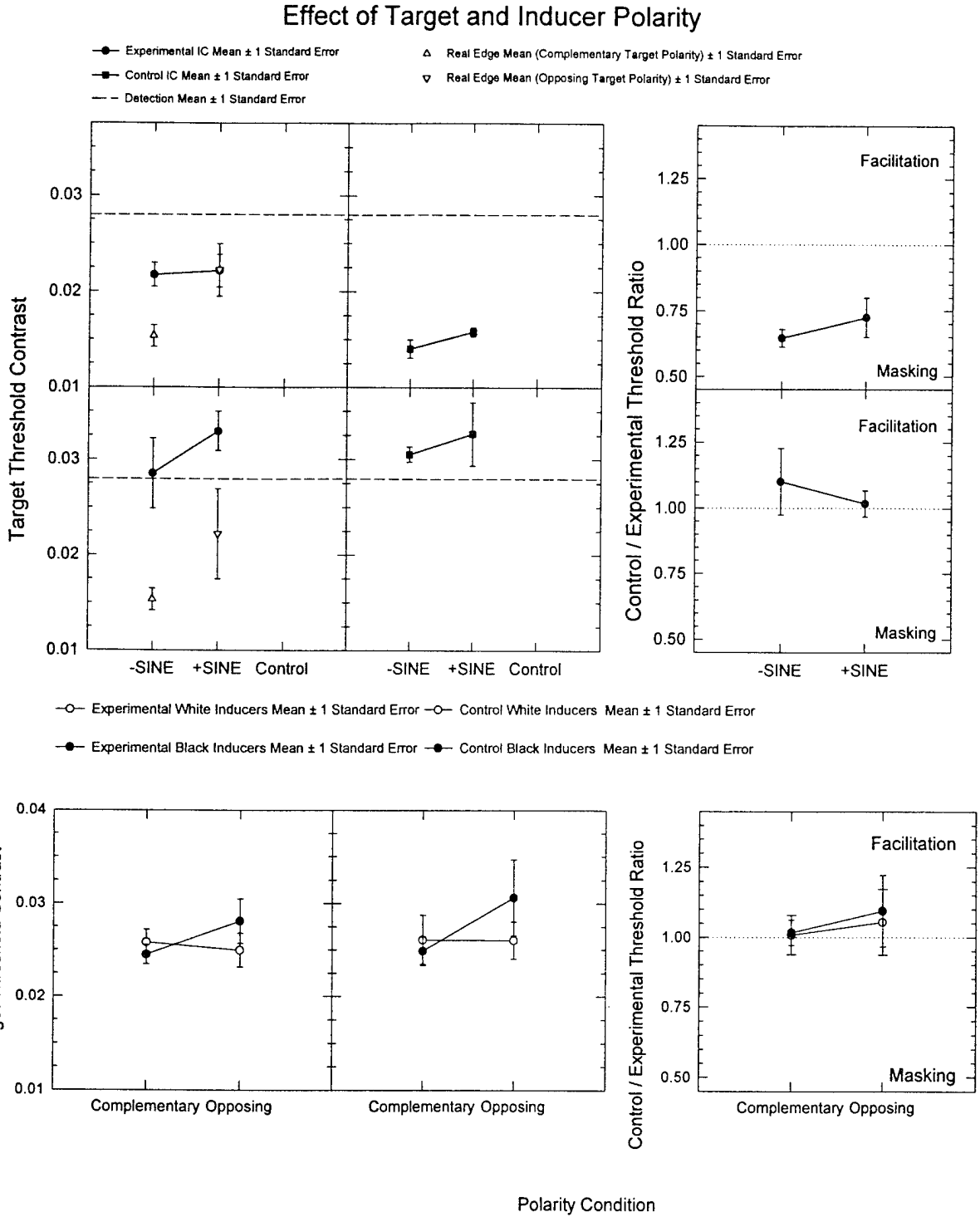
Effect of Target and Inducer Polarity
Experimental IC Mean ± 1 Standard Error
Control IC Mean ± 1 Standard Error
Detection Mean ± 1 Standard Error
Real Edge Mean (Complementary Target Polarity) ± 1 Standard Error
Real Edge Mean (Opposing Target Polarity) ± 1 Standard Error
Target Threshold Contrast
0.03
0.02
0.01
0.03
0.02
0.01
-SINE
+SINE
Control
-SINE
+SINE
Control
Control / Experimental Threshold Ratio
Facilitation
1.25
1.00
0.75
0.50
Masking
Facilitation
1.25
1.00
0.75
0.50
Masking
-SINE
+SINE
Experimental White Inducers Mean ± 1 Standard Error
Control White Inducers Mean ± 1 Standard Error
Experimental Black Inducers Mean ± 1 Standard Error
Control Black Inducers Mean ± 1 Standard Error
Target Threshold Contrast
0.04
0.03
0.02
0.01
Complementary
Opposing
Complementary
Opposing
Control / Experimental Threshold Ratio
Facilitation
1.25
1.00
0.75
0.50
Masking
Complementary
Opposing
Polarity Condition

Figure 12

THE EFFECT OF PERCEPTUAL TRANSPARENCY ON BRIGHTNESS JUDGMENTS

by

Frederick A. A. Kingdom[1], Barbara Blakeslee[2] and Mark E. McCourt[2]

[1] McGill Vision Research Unit
687 Pine Av. W. Rm. H4-14
Montreal, Quebec, H3A 1A1
Canada
[Email: fred@jiffy.vision.mcgill.ca]

[2] Department of Psychology
North Dakota State University
Fargo, ND, 58105-5075
USA

[1] Author to whom all correspondence should be sent

ABSTRACT

Subjects matched the brightness of test patches located within a larger surround, where the surround was made to appear either different in reflectance from neighbouring regions, or of the same reflectance but viewed beneath a transparent film. In both conditions the luminance and spatial extent of the immediate surround was equivalent, thus controlling for the effects of surround luminance. Perceived transparency had a significant effect on brightness. Test patch brightness was significantly elevated when the perception of transparency was supported by stereo depth cues. The effect was, however, mediated by the virtual transmittance of the transparent overlay, increasing in magnitude with decreasing transmittance. Further, the effect of transparency on brightness was greatest for test patch luminances near to those of their immediate backgrounds. The implications of these results for the understanding of configurational effects on brightness is discussed.

INTRODUCTION

Since the time of Helmholtz the influence of coloured* surrounds on the perceived colour of test patches (i.e., 'induced' colour) has been rightly considered critical to our understanding of brightness (perceived luminance), lightness (perceived reflectance) and chromatic processing. In an early and prescient discussion of the issue, William James in the Principles of Psychology described two views on induced colour, the first championed by Helmholtz, the latter by Hering (James, 1890). Helmholtz argued that induced colour was a "deception of judgement", according to which observers judged the colour of the test region as if it were illuminated by light with the same colour composition as the surround. Thus, in the classic simultaneous brightness contrast display, in which a grey patch on a light background looks darker than on a black background, the visual system assumes the patch on the white surround to be the more highly illuminated. Given that the luminances of the two patches are nevertheless the same, the visual system infers on the basis of this assumption that the patch on the white background has to be of lower reflectance, and that is how it is perceived. Hering, on the other hand, advanced a different view; he argued for a low-level physiological explanation for induced colour in terms of lateral interactions at the retinal level. James summarized these two opposing views in the following way (p. 19, vol 2): "Helmholtz maintains that the neural process and the corresponding sensation also remains unchanged, but are differently interpreted; Hering, that the neural process and the sensation are themselves changed, and that the 'interpretation' is the direct conscious correlate of the altered retinal conditions. According to the one, contrast is psychological in its origin; according to the other, it is purely physiological".

The Helmholtz/Hering debate predates and is in many ways cognate to recent controversy concerning the cause(s) of induced brightness phenomena. The extent to which induced brightness phenomena reflect primarily early-stage filtering operations, as opposed to higher-level inferential mechanisms, is still contested (e.g. Spehar, Gilchrist and Arend, 1995; Gilchrist, 1996a,b; Kingdom, McCourt & Blakeslee, 1996). By inferential mechanisms we refer to those mechanisms which attribute categorical properties to the intensive and chromatic properties of surfaces. These mechanisms are involved in the description of a 3-D world of reflecting objects and surfaces illuminated by various light sources. Inferential mechanisms are clearly essential to lightness perception, since the visual system must be able to distinguish luminance discontinuities arising due to changes in reflectance from those that arise due to changes in illumination. That the visual system can accomplish this under many circumstances with apparent ease is evidenced by the simple observation that one can tell the lightness of a surface to be uniform even when partially covered by shadow, or by a transparent overlay, as illustrated in Figure 1. The involvement of inferential processes in lightness perception is, moreover, well documented in the psychophysical literature (Gilchrist, 1977; Schirillo, Reeves and Arend, 1990; Knill and Kersten, 1991; Agostini and Proffitt, 1993; Arend and Spehar, 1993a; Schirillo and Shevell, 1993;

Buckley, Frisby and Freeman, 1994; Catalliotti and Gilchrist, 1995).

Figure 1 about here

Figure 1 also demonstrates the distinction the visual system is capable of making between lightness and brightness. On the one hand the regions behind and outside of the apparently transparent overlay appear to be made from the same piece of material, i.e. possess the same lightness. On the other hand the same regions appear markedly different in brightness. That the visual system can distinguish brightness from lightness under a range of circumstances is now well documented (Arend and Goldstein, 1990; Schirillo et. al., 1990; Sewall and Wooten, 1991; Arend and Spehar, 1993a,b). The influence of inferential processes in brightness, as opposed to lightness, perception is, however, less clearly established. The computational necessity of inferential processes is arguably limited to lightness perception, since brightness, as perceived luminance, is directly given. There is thus no a priori reason to expect an influence of inference on brightness. There are, nevertheless, a number of studies which have found evidence for just such an influence. Changes in perceived brightness that have been attributed to inferential processes have been demonstrated for perceived stereo-depth (Spehar, Gilchrist and Arend, 1995; Schirillo and Shevell, 1993); perceived pictorial depth or shape (Adelson, 1993; Wishart, Frisby and Buckley, 1996; Knill and Kersten, 1991); subject instruction in ambiguous displays (Arend and Spehar, 1993b); and perceived transparency (Adelson, 1993). Although the effect of transparency on brightness reported by Adelson (1993) is one of the most compelling demonstrations, there is a problem in that the transparency manipulation introduced local surround luminance differences which might account for at least some of the brightness effect.

In this communication we examine to what extent the brightness of a test patch is influenced by perceived transparency. Brightness was measured for test patches whose retinally adjacent surrounds were made to appear either as transparent overlays on a wider background that included the test patch, or as regions differing in reflectance from a wider surround. Example stimuli are shown in Figure 3. The luminance arrangement of the surround was nearly identical across all conditions to control for any effects of local surround luminance. Subjects were explicitly instructed to make brightness, and not lightness judgements. The results of the study show that under some conditions brightness can be significantly altered by the perceived configuration of the surround. Whereas in general the effects are quite modest, they can under optimal conditions increase brightness matches by 50%.

METHODS

Subjects

Five subjects participated: MM, JG, FK, BB, and HH. MM, FK and BB were the authors. JG and HH were undergraduate and graduate student volunteers, respectively, who were naive about the purpose of the experiment. All subjects were well-practiced psychophysical observers, were stereo-normal, and possessed normal or corrected-to-normal vision.

Stimulus Generation

Stimuli were generated using a PC-compatible microcomputer (486/66 MHZ) with a custom-modified TIGA (Texas Instruments Graphics Adapter) graphics controller (Vision Research Graphics, Inc.). Images were presented on a high-resolution display monitor (21" IDEK Iiyama Vision Master, model MF-8221). Display format was 1024 (w) x 768 (h) pixels. Frame refresh rate was 97 Hz (non-interlaced). Viewed from a distance of 60.7 cm the entire display subtended 32o(w) x 24.2o(h); individual pixels measured 0.031o x 0.031o. Mean display luminance was 50 cd/m2. All images could possess 2^8 simultaneously presentable linearized intensity levels selected from a palette of approximately 2^15. Stereo projection was achieved by a pair of pi-cell liquid crystal shutters (Tektronix, Inc.) synchronized to the monitor frame rate, such that alternate frames were presented to the two eyes. In their open state, transmittance through the shutter glasses was 35%. Thus, viewed through the shutter glasses the mean and the maximum display luminances were 17.5 and 35 cd/m2, respectively.

Stimuli

The basic stimulus configuration is illustrated in Fig. 2, which indicates the arrangement of the test patch, test inner surround, test outer surround, and matching patch common to all conditions. Figs. 3(a) and (b) present facsimiles of stimuli used in the experiments, but without the matching patch. The four transparency conditions are:

Figures 2 and 3 about here

---

transparency-with-stereo-depth-cues (Fig. 3a, upper panels); transparency-without-stereo-depth-cues (Fig. 3a, lower panels); no-transparency-without-stereo-depth-cues (Fig. 3b, upper panels); and no-transparency-with-stereo-depth-cues (Fig. 3b, lower panels). When fused using convergence, the stimulus in the upper panels of Fig. 3(a) appears to consist of two surfaces, a horizontally oriented light-grey rectangle containing a coplanar test patch, and a vertically-oriented transparent rectangle floating in front. Pictorial depth cues in the stimulus in the lower panels of Fig. 3(b) also

suggest the existence of a transparent overlay, but this stimulus lacks the stereoscopic depth cues of Fig. 3(a). Pictorial depth cues in the stimulus in the upper panels of Fig. 3(b) suggest that the horizontal light-grey rectangle partially occludes the dark-grey rectangle, which thus appears to lie in a recessed depth plane. In the lower panels of Fig. 3(b) the addition of stereo depth enhances the impression of occlusion. Note that in all four transparency conditions, the pattern of surround luminance is identical extending to a distance of 6.7 deg. from the center of the test patch. In the stereo-depth conditions, the disparity of the transparent overlay was 0.3125 deg. (10 pixels), and that of the occluded rectangle was -0.3125 deg.

Three stimulus luminance parameters were varied in the experiment: test patch luminance and the luminances composing the vertical rectangle (the inner surround and upper and lower flanks of the outer surround). All other parameters were held constant. For ease of exposition luminances are given in terms of the percent maximum of the full display luminance. Background luminance was fixed at 50% max. and the luminance of the right and left flanks of the outer surround was fixed at 80% max. (see Figure 2). Five luminances of the square inner surround were employed: 8%, 27%, 54%, 72%, and 80% max. These were paired with five luminances of the top and bottom outer surround flanks (5%, 17.5%, 33%, 45% and 50%), such that in two configurations they were consistent with the interpretation of the stimulus as a vertical transparent rectangle overlying a horizontal rectangle which included the test patch. The transmittance values of the transparent vertical rectangle were 10%, 33%, 66%, 90% and 100% (i.e. no transparent overlay). Test patch luminances spanning most of the range from 0% to 100% max. were examined.

Procedure

The method of adjustment was employed to determine the luminance at which the brightness of the matching patch was the same as that of the test patch. On each stimulus presentation the subject adjusted, by button press, the luminance of the matching patch (which was situated on the 50% max. background) until it appeared equal in brightness to that of the test patch. When subjects were satisfied with their matches another button press registered the response, and the next stimulus was presented. In each experimental session all test patch luminances and surround luminances were presented for each transparency condition. These were presented in random order. Each subject completed either three or six sessions, from which the means and standard errors of the matches were computed.

RESULTS

Figures 4(a-e) illustrate the pattern of match values, with each figure giving the complete data set for one subject. Fig. 4(f) plots mean luminance matches collapsed across all subjects. In each graph mean matching luminance is plotted as a function of test patch luminance for each of the four transparency conditions: transparency-with-

stereo-depth-cues, no-transparency-with-stereo-depth-cues, transparency-without-stereo-depth-cues, and no-transparency-without-stereo-depth-cues. The vertical dotted line on each panel indicates the luminance of the test patch surround, and thus also represents the line dividing decrements (to the left) from increments (to the right). The number on each panel gives the transmittance of the two simulated transparency conditions. Thus, the further leftward the vertical dotted lines (and the lower the associated transmittance values) the darker the test patches' inner surround. The fixed diagonal dashed lines (long dashes) represent the prediction for perfect luminance matching, while the variable-in-slope dashed lines (short-dashes) illustrate the predictions for perfect ratio matching. In other words, these lines index the match luminance necessary to make the ratio of matching luminance to its immediate surround luminance (50% max) equal to the ratio of test patch luminance to its immediate surround.

Figure 4 about here

Consider first the condition in each figure labelled 100%. This is the condition in which only the horizontal rectangular surround was present (80% max.), i.e. without the added transparent overlay or its no-transparency comparisons. Subject matches lay somewhere between luminance matching (long-dashed line) and ratio matching (short-dashed line). This is typical behaviour for brightness matching in side-by-side displays (Whittle, 1994). Subjects also show the "crispening effect" recently investigated by Whittle (1993), in which brightness changes most rapidly when test patch luminance is close to the luminance of its immediate surround.

Note that while the surround luminance of the matching patch was constant, that of the test patch varied with local background luminance. Inspection of the results in the figures labelled 90%-10%, reveals that matching luminance increases as the luminance of the inner surround decreases. This is indicated by the increase in slope of the matching functions as the dotted vertical line (inner surround luminance) moves leftwards, or the transmittance value decreases. It is clear, in addition, that while brightness matches in all cases still fall somewhere between luminance matching and ratio matching, decrement matches are in general much closer to the ratio matching prediction than are increment matches, which lie closer to the luminance matching prediction (Arend and Spehar, 1993a).

More germane to this study, however, are the relative changes in test patch brightness which occur as a function of the four transparency configurations within each local background luminance condition. Table 1 shows the results of an independent-groups analysis of variance conducted on the matching data of each observer at each transmittance level. In the 10% transmittance condition all subjects

---

Table 1 about here

---

showed a significant main effect of transparency condition, an obvious and highly significant main effect of test patch luminance and (for all but subject HH) a significant transparency condition by test patch luminance interaction. The source of the interaction, as revealed by an analysis of simple main effects, is the absence of a significant effect of transparency condition at one or more of the lowest test patch luminances, whereas transparency condition is highly significant at higher test patch luminance values. The effect of transparency condition was also significant (for all but subject BB) at the 33% and 66% transmittance levels. For subjects who expressed a significant interaction, the source was the same as in the 10% condition. Only for subject MM was there a significant effect of transparency condition at the 90% transmittance level.

Figure 5 plots mean luminance matches (normalized to mean match value in the transparency-with-stereo-depth-cues conditions) in the four transparency conditions collapsed across subjects and test patch luminances. Transmittance level is shown as a parameter in four separate panels. Displayed in this way it is clear that the effect of transparency is consistently greatest in the transparency-with-stereo-depth-cues condition and that this effect decreases with increasing transmittance. One-way repeated-measures ANOVAs performed on the mean luminance matches collapsed across subjects and test patch luminances indicated a significant ($p<.05$) effect of transparency condition at all transmittance levels. Post-hoc comparisons of the mean luminance matches in the 10%, 33%, 66% and 90% transmittance levels revealed that mean matching luminance in the transparency-with-stereo-depth-cues condition was significantly higher than in all other conditions. In addition, for the 10% transmittance condition, mean luminance matches in the transparency-without-stereo-depth-cues condition were significantly greater than in the no-transparency-with-stereo-depth-cues condition. No other pairwise comparisons were significant.

Figure 5 about here

A comparison of the magnitude of the transparency-with-stereo-depth-cues effect as compared to the magnitude of simple brightness induction was obtained by calculating, across all five subjects, the percent change in brightness matches between the transparency-with-stereo-depth-cues condition and the average of the other three conditions. Percent brightness change is plotted as a function of the ratio of test patch luminance to inner surround luminance in Fig. 6. Two features of these data are notable. First, across all levels of transmittance, the largest brightness enhancements occur for test patches whose luminances are very near to that of the inner background

luminance (that is, for ratios of test patch to inner background luminance near 1.0). Second, brightness enhancement increases with decreasing transmittance where, at maximum in the 10% transmittance condition, test patch brightness is enhanced by slightly more that 50%.

Figure 6 about here

DISCUSSION

The purpose of this study was to determine whether, and to what degree, perceived transparency affected the judgement of brightness. We measured the brightness of a test patch as a function of test patch luminance, surround luminance, and transparency configuration. The stimulus was designed such that it could be interpreted as 1) a transparent overlay of a given transmittance on top of a horizontal rectangular surround which included the test patch, or as 2) a square inner surround surface of a given reflectance with outer surround flanks of differing reflectance. Only when the stimulus suggested the presence of a transparent overlay which (except in the 10% transmittance condition) appeared in a nearer stereo-depth plane from the test patch and its surround, did transparency exert a significant effect on the brightness of the test patch. The largest effect occurred in the 10% transmittance condition, at a ratio of test patch to background luminance of approximately 1.0. Here brightness judgements were on average about 50% greater than the average for the other configurations. While our results show a very restricted transparency-with-stereo-depth effect it is nevertheless significant, and we must consider how it might have arisen.

Transparency-with-stereo-depth affected brightness such that subjects perceived the test patch to be brighter than it would otherwise have appeared. This is consistent with the perception of the brightness of the test patch being determined by what the brightness of the patch would be if the transparency were not present. It is as if subjects discounted, in part, the transparency when computing brightness. A possible explanation as to why this effect manifested itself predominantly in the stereo-depth conditions is that only under these circumstances is there an unambiguous and compelling impression of transparency. The ordinal pattern of mean brightness matches (Fig. 5) appears to support this interpretation, since brightness matches are consistently highest in conditions containing both stereo and pictorial (e.g., x-junctions) cues to transparency, are next highest in conditions containing only pictorial depth cues, and are actually lowest in conditions where both stereo and pictorial depth cues serve to falsify the perceptual hypothesis of transparency. According to this view one might also expect a brightness effect, even in the absence of stereo-depth cues, by using a more complex background such as a Mondrian. The additional information provided by a complex background, such as more numerous x-junctions and luminance

ratios consistent with physical transparency, might render transparency a more parsimonious (and hence more compelling) interpretation, thus leading to a brightness effect. This is consistent with Gestalt theories where percepts are posited to be organized according to various principles such as "goodness" or "simplicity" (Knill, Kersten and Mamassian, 1996).

Two noteworthy results are that the effect of transparency on brightness decreased with increasing transmittance, and that it is maximal for test field to background luminance ratios near unity. This ratio corresponds to the region where brightness changes most rapidly with changes in test field luminance, resulting in the "crispening effect" (Whittle, 1994). This is also the region where luminance discrimination thresholds are smallest (Whittle, 1993). Thus, if the effect of transparency on brightness were small, its expression might be expected to be maximal where the sensitivity of the brightness system is highest.

How do our results compare with other studies which have measured brightness under different configurations? Arguably the closest study to our own is that of Adelson (1993). He created a stimulus, the Argyle illusion, in which a transparent overlay consisting of a series of stripes of high and low transmittance appeared superimposed on columns of light-grey diamond-shaped patches. Despite all the diamonds being equal in luminance, subjects reported that the column of diamonds seen beneath the higher transmittance (light) transparency appeared darker than those beneath the lower transmittance filter. Our results differ from Adelson's in that, with the exception of the lowest transmittance condition, we found significant effects of perceived transparency on brightness only when the transparency interpretation was supported by stereo depth cues. Their are two possible explanations for this apparent discrepancy. The first refers back to the possibility mentioned earlier, viz., that a compelling or "simplifying" percept of transparency might be achieved even without stereo depth cues for sufficiently complex stimuli. The pattern of luminances comprising the Argyle illusion is certainly far more complex than the stimulus used in the present study, and so stereo depth may not be necessary. A second possibility stems from the fact that the manipulation Adelson used to disrupt the impression of transparency in his control condition also changed the configuration of local luminance surrounding the diamonds, making it problematical whether the brightness effect in his stimulus arises due to transparency, to the change in local luminance, or to some combination of these factors.

A number of prior studies have been explicitly concerned with the effects of depth on brightness. Schirillo et. al. (1990), in a replication of an earlier experiment by Gilchrist (1977), reported that brightness (but not lightness) was unaffected when the test region appeared to be moved into a differently illuminated depth plane from that of its retinally-adjacent surround. This negative result was later challenged by Schirillo and Shevell (1993), who found a small effect (15%) on the brightness of a test patch in a similar experiment to that of Schirillo et. al. (1990), but one using Mondrian stimuli.

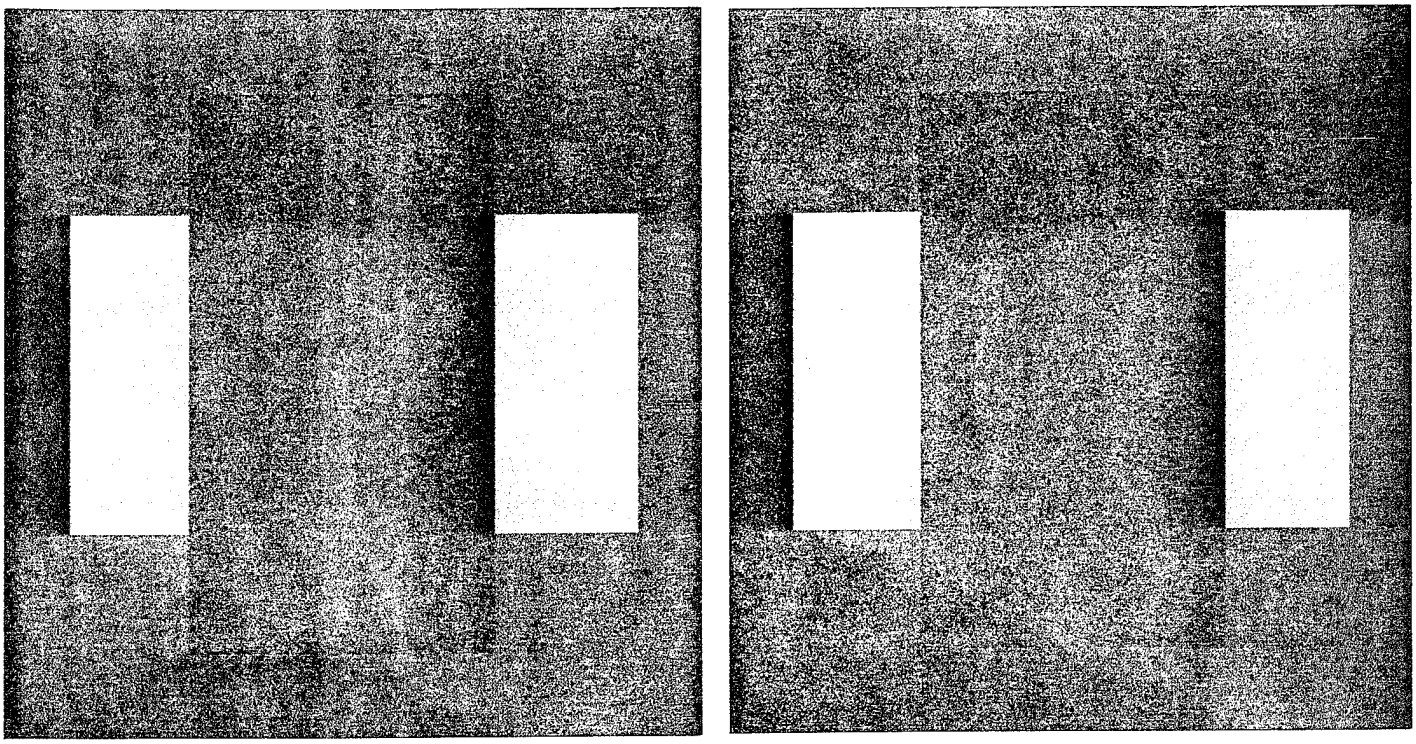

Transparency-with-Stereo-Depth-Cues

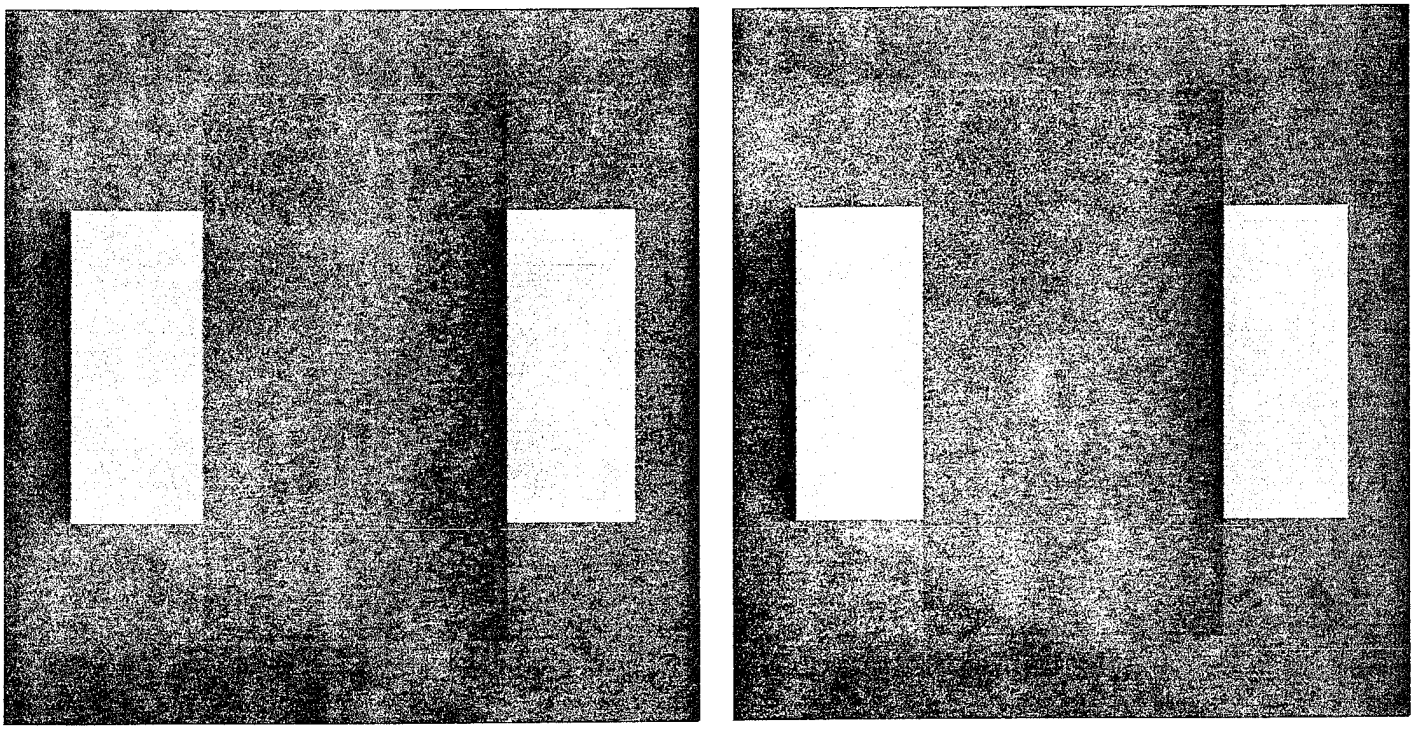

Transparency-without-Stereo-Depth-Cues

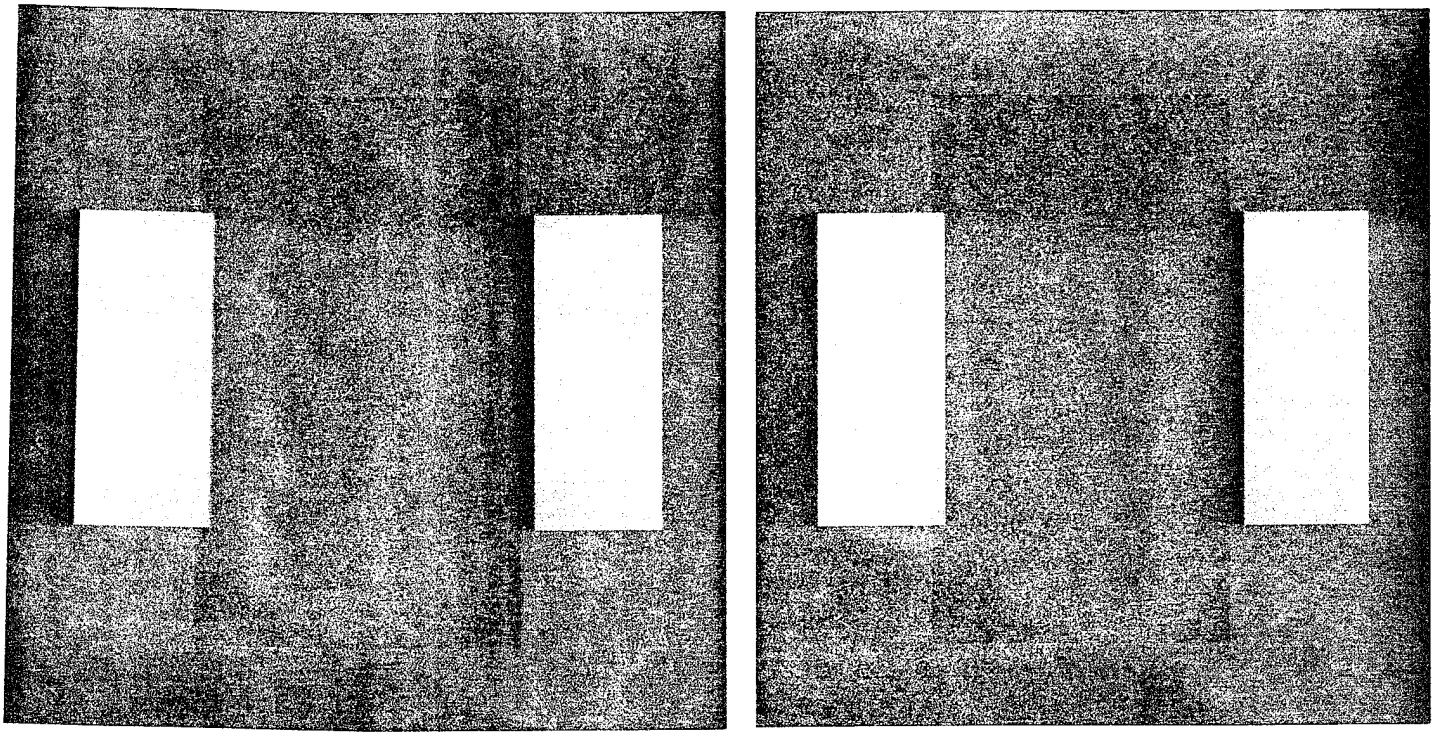

No-Transparency-without-Stereo-Depth-Cues

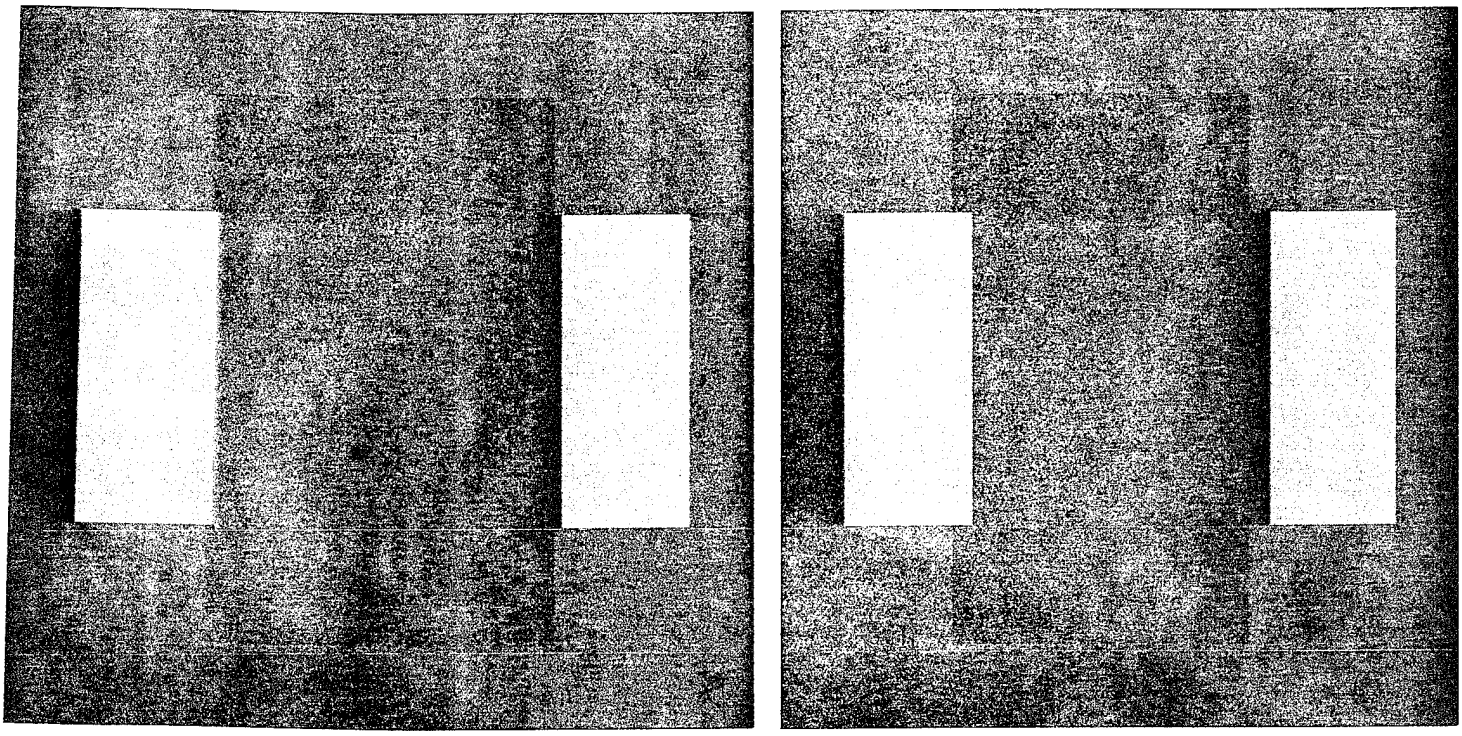

No-Transparency-with-Stereo-Depth-Cues

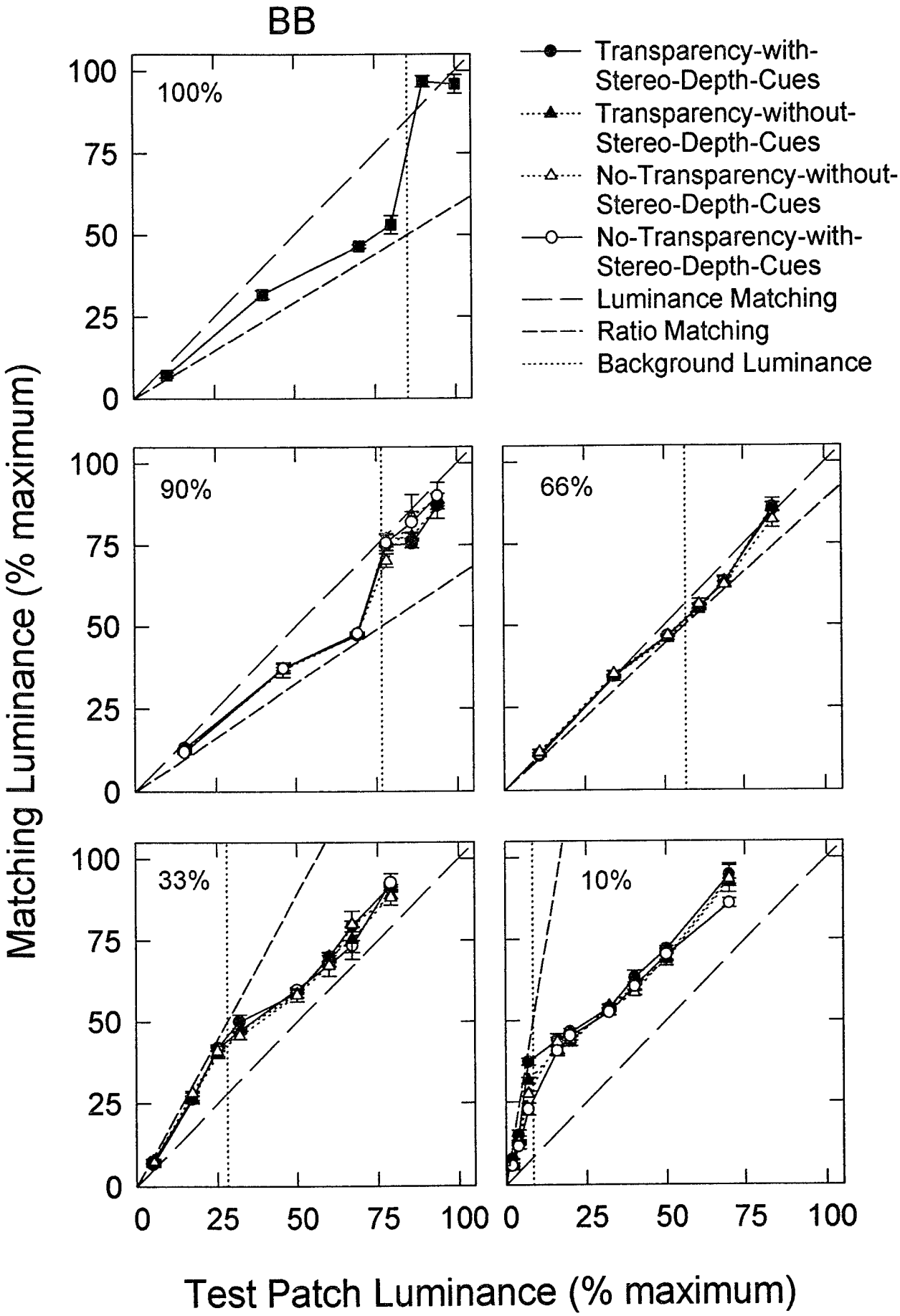
BB
Transparency-with-Stereo-Depth-Cues
Transparency-without-Stereo-Depth-Cues
No-Transparency-without-Stereo-Depth-Cues
No-Transparency-with-Stereo-Depth-Cues
Luminance Matching
Ratio Matching
Background Luminance
100%
90%
66%
33%
10%
Matching Luminance (% maximum)
Test Patch Luminance (% maximum)
0
25
50
75
100

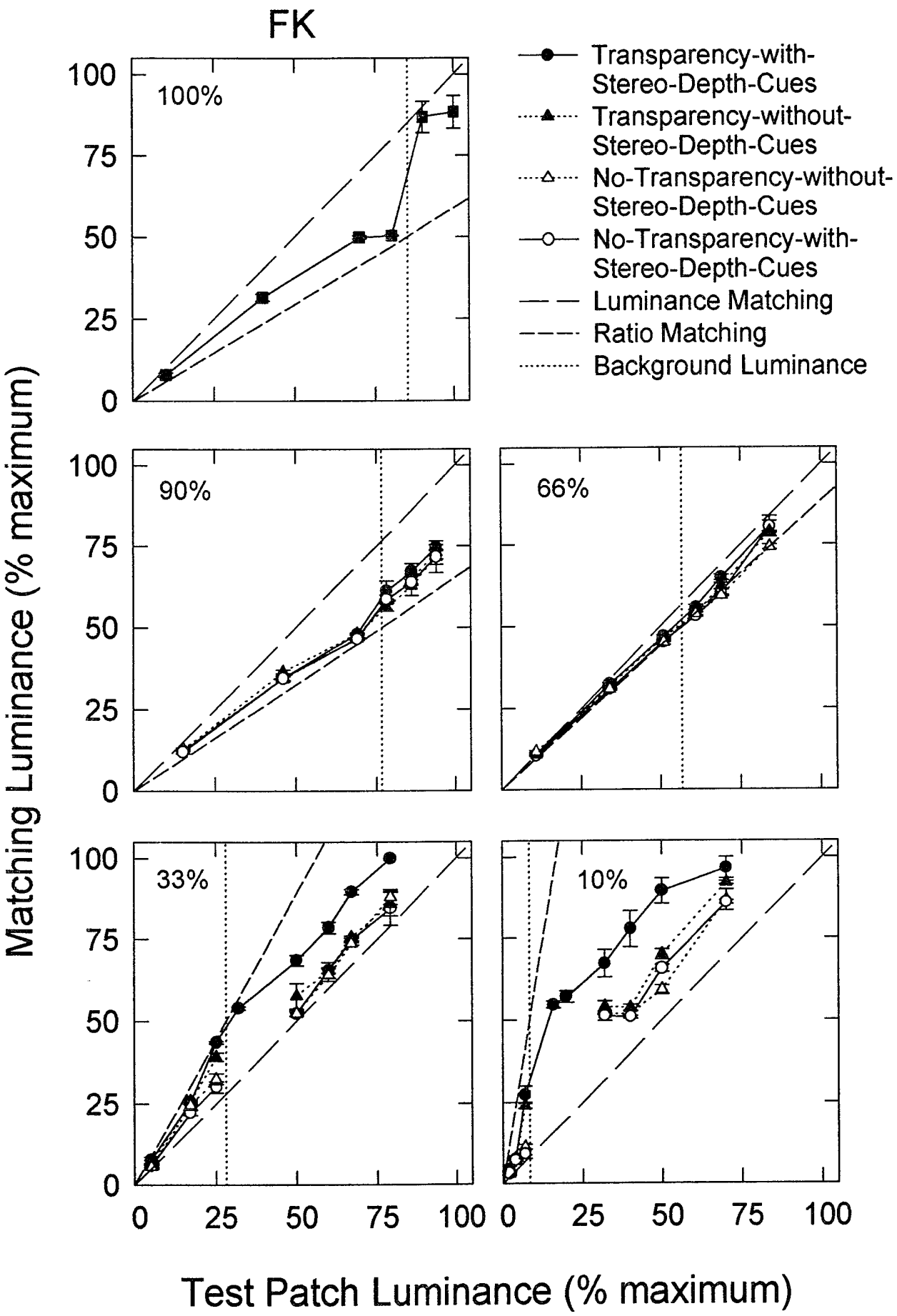
FK
Transparency-with-Stereo-Depth-Cues
Transparency-without-Stereo-Depth-Cues
No-Transparency-without-Stereo-Depth-Cues
No-Transparency-with-Stereo-Depth-Cues
Luminance Matching
Ratio Matching
Background Luminance
100%
90%
66%
33%
10%
Matching Luminance (% maximum)
Test Patch Luminance (% maximum)
0
25
50
75
100

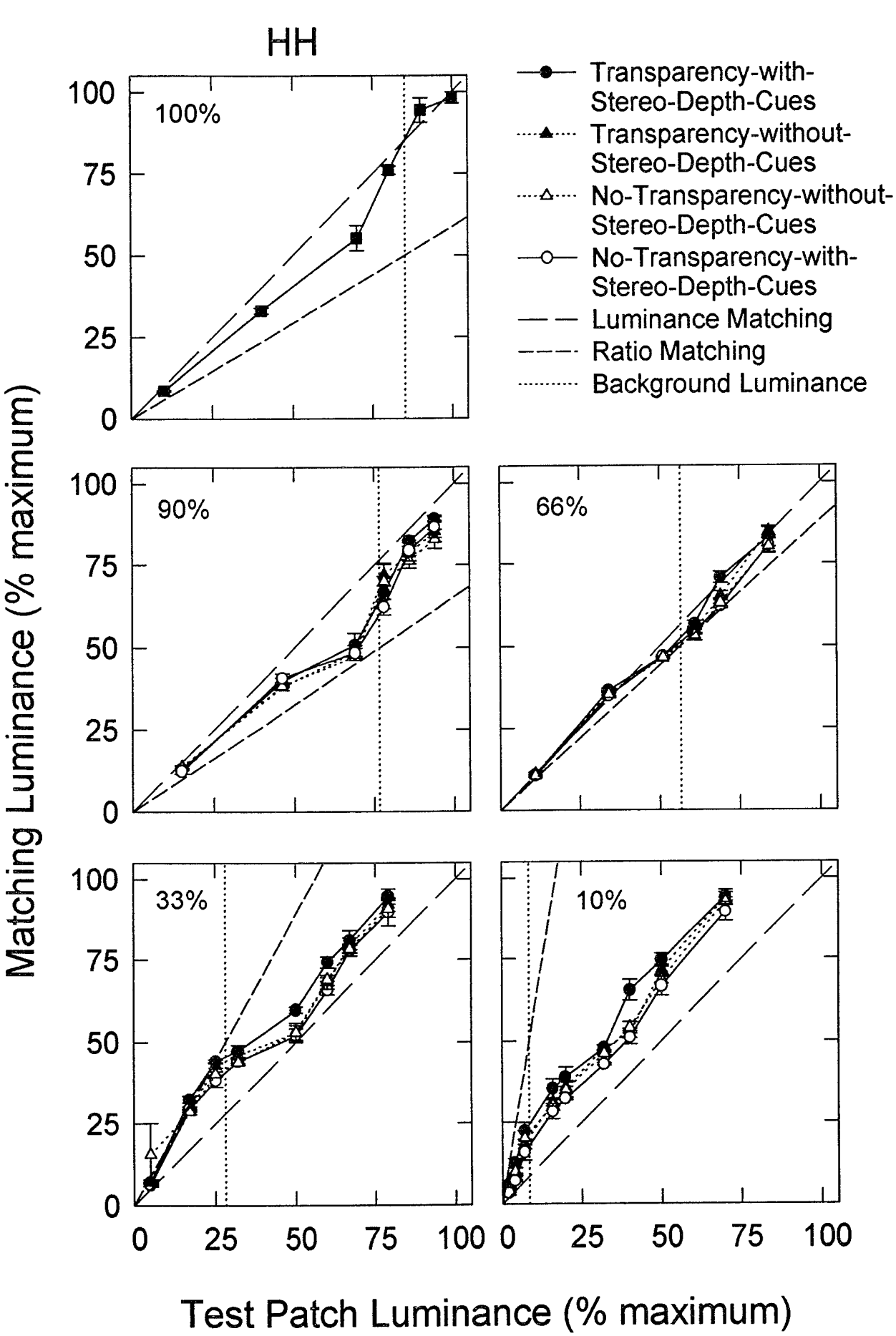
HH
Transparency-with-Stereo-Depth-Cues
Transparency-without-Stereo-Depth-Cues
No-Transparency-without-Stereo-Depth-Cues
No-Transparency-with-Stereo-Depth-Cues
Luminance Matching
Ratio Matching
Background Luminance
100%
90%
66%
33%
10%
Matching Luminance (% maximum)
Test Patch Luminance (% maximum)
0
25
50
75
100

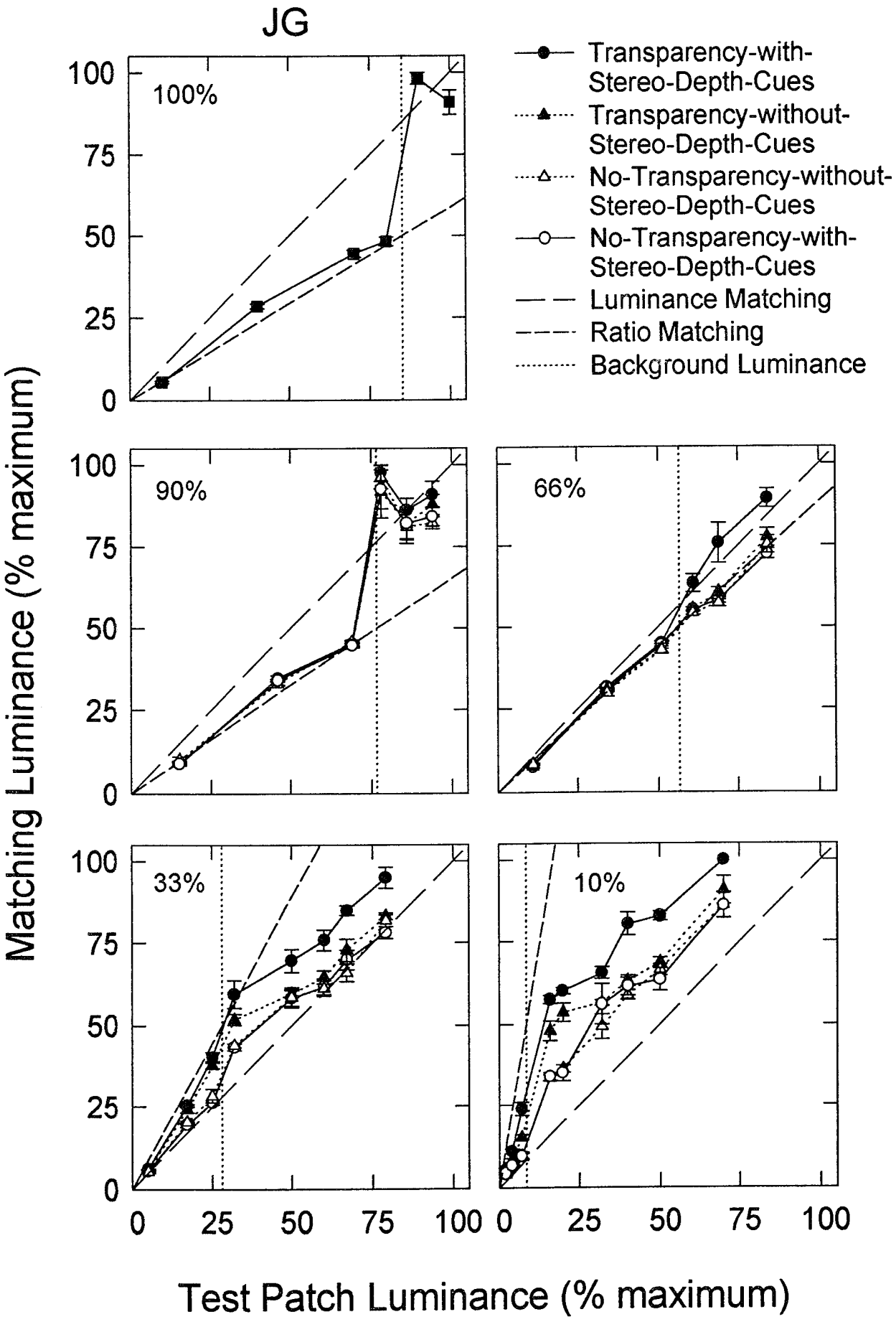
JG
Transparency-with-Stereo-Depth-Cues
Transparency-without-Stereo-Depth-Cues
No-Transparency-without-Stereo-Depth-Cues
No-Transparency-with-Stereo-Depth-Cues
Luminance Matching
Ratio Matching
Background Luminance
100%
90%
66%
33%
10%
Matching Luminance (% maximum)
Test Patch Luminance (% maximum)
0
25
50
75
100

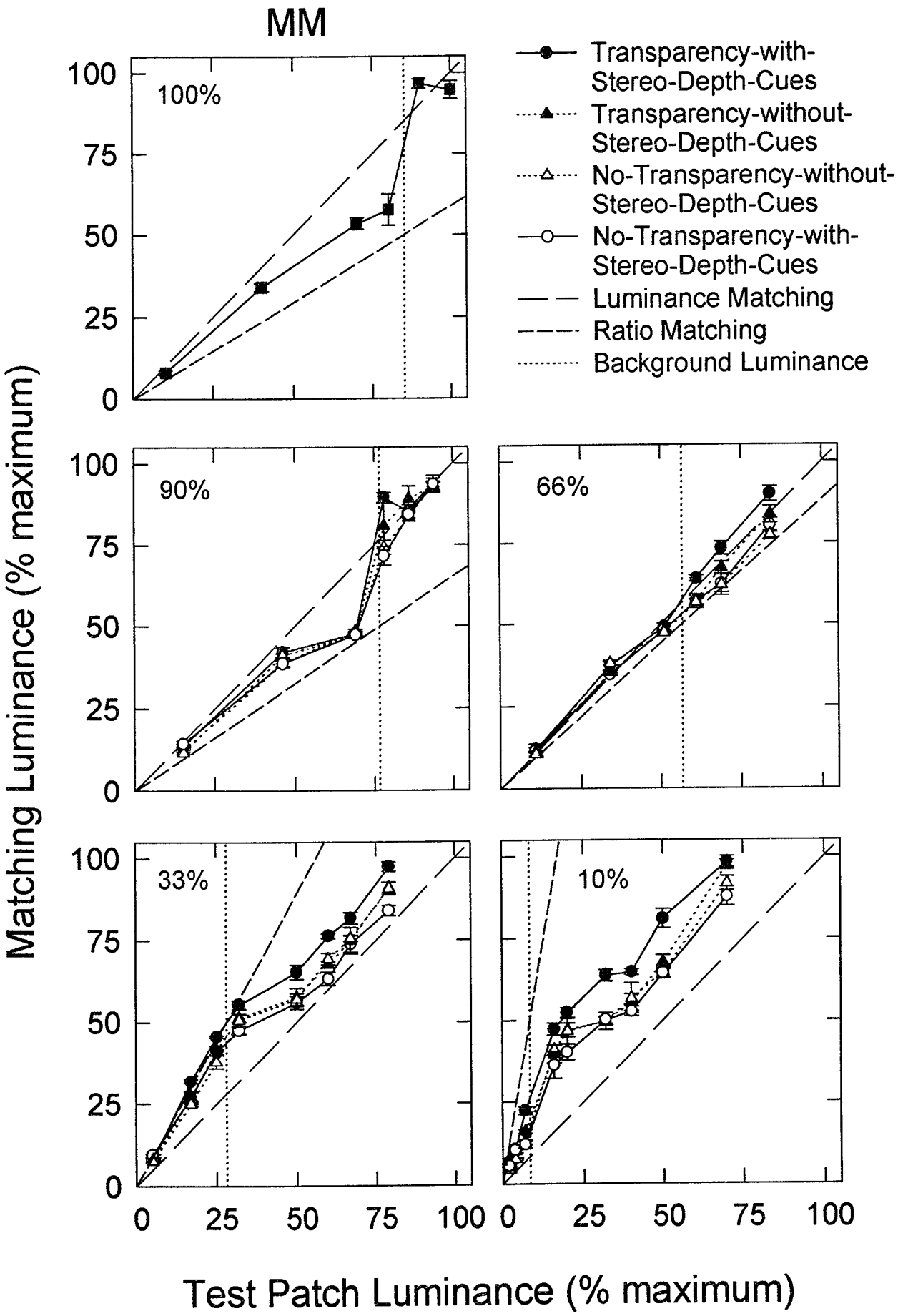
MM
Transparency-with-Stereo-Depth-Cues
Transparency-without-Stereo-Depth-Cues
No-Transparency-without-Stereo-Depth-Cues
No-Transparency-with-Stereo-Depth-Cues
Luminance Matching
Ratio Matching
Background Luminance
100%
90%
66%
33%
10%
0
25
50
75
100
Matching Luminance (% maximum)
Test Patch Luminance (% maximum)

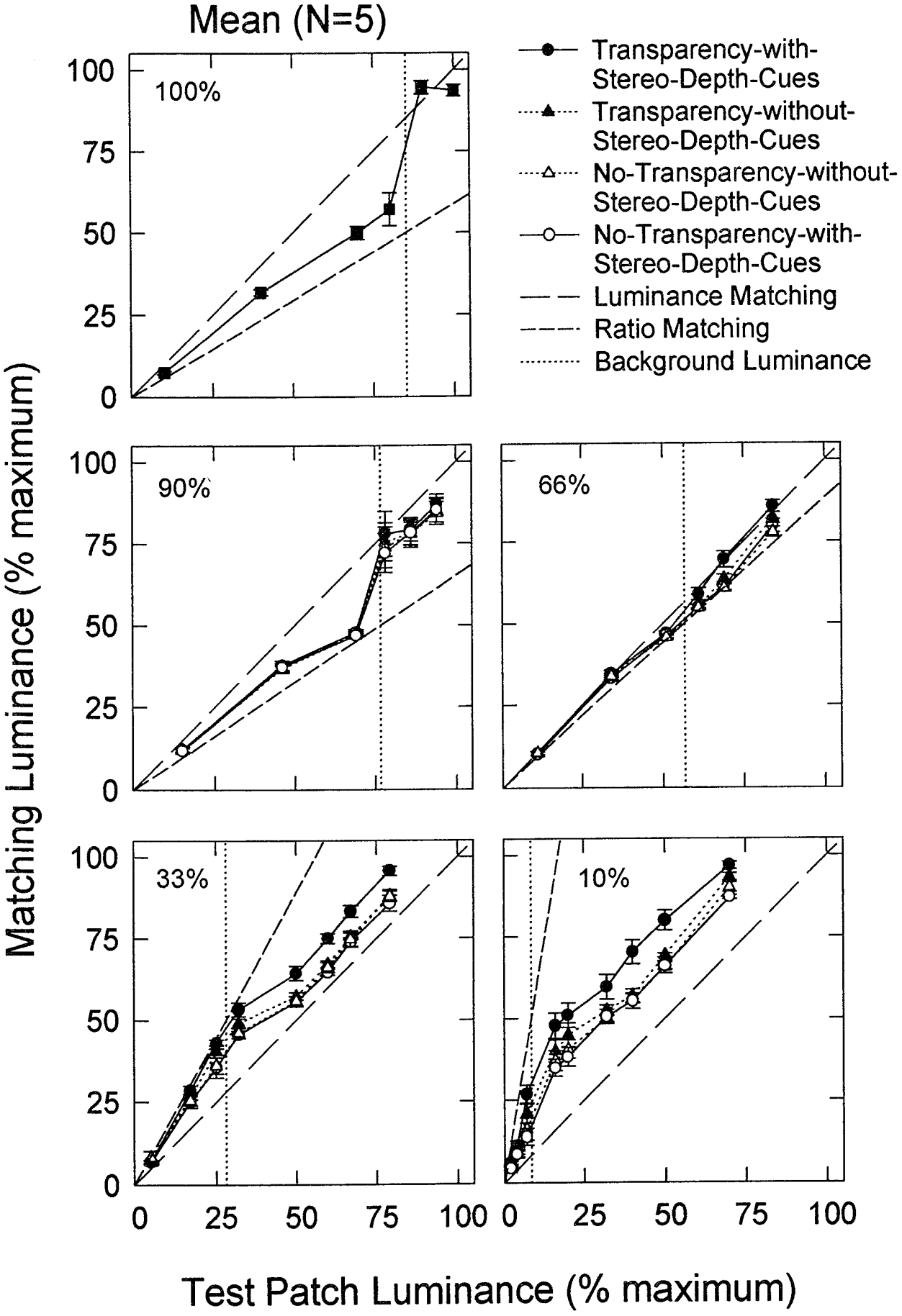
Mean (N=5)
Transparency-with-Stereo-Depth-Cues
Transparency-without-Stereo-Depth-Cues
No-Transparency-without-Stereo-Depth-Cues
No-Transparency-with-Stereo-Depth-Cues
Luminance Matching
Ratio Matching
Background Luminance
100%
90%
66%
33%
10%
Matching Luminance (% maximum)
Test Patch Luminance (% maximum)
0
25
50
75
100

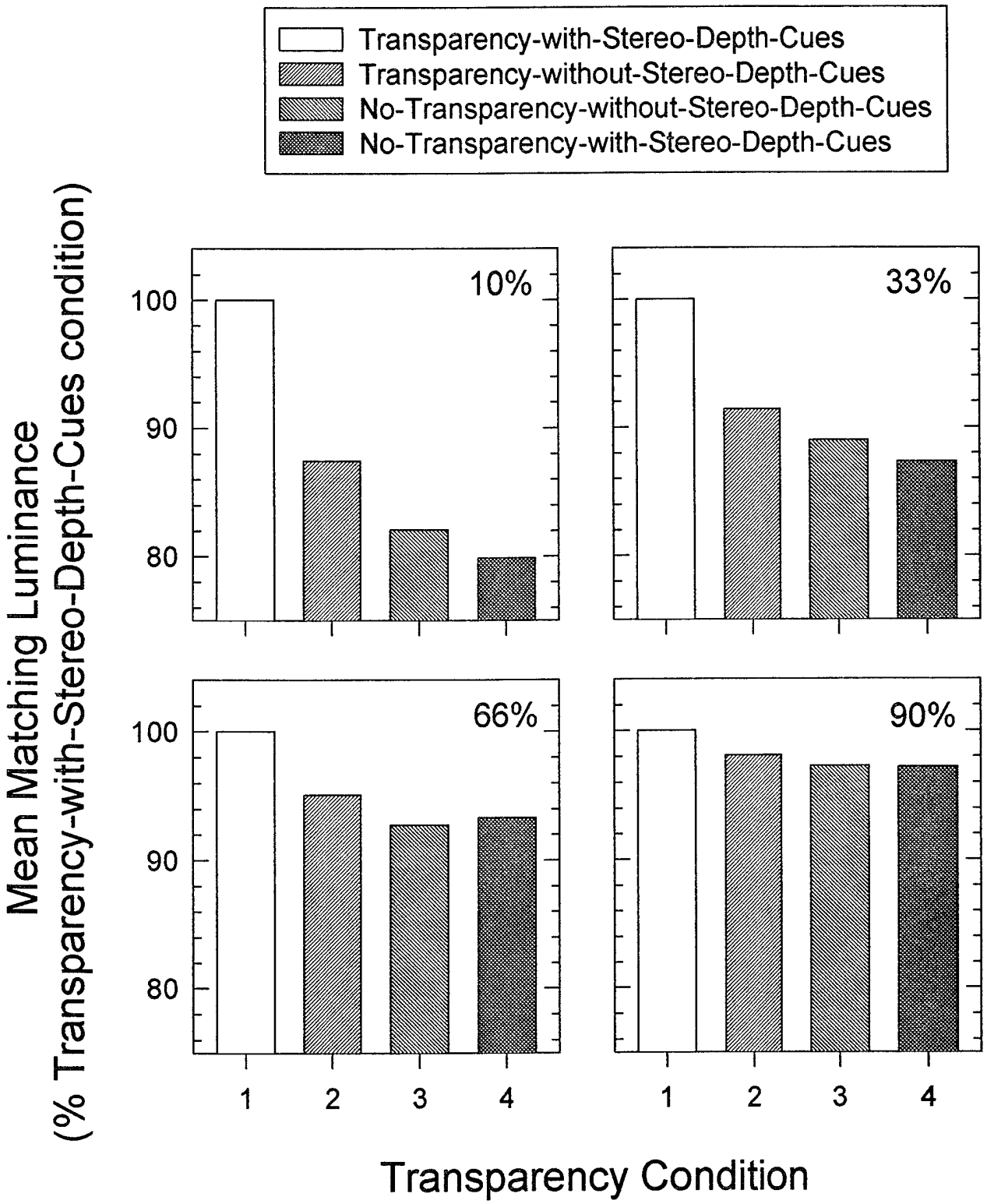
Transparency-with-Stereo-Depth-Cues
Transparency-without-Stereo-Depth-Cues
No-Transparency-without-Stereo-Depth-Cues
No-Transparency-with-Stereo-Depth-Cues
10%
33%
66%
90%
100
90
80
1
2
3
4
Mean Matching Luminance
(% Transparency-with-Stereo-Depth-Cues condition)
Transparency Condition

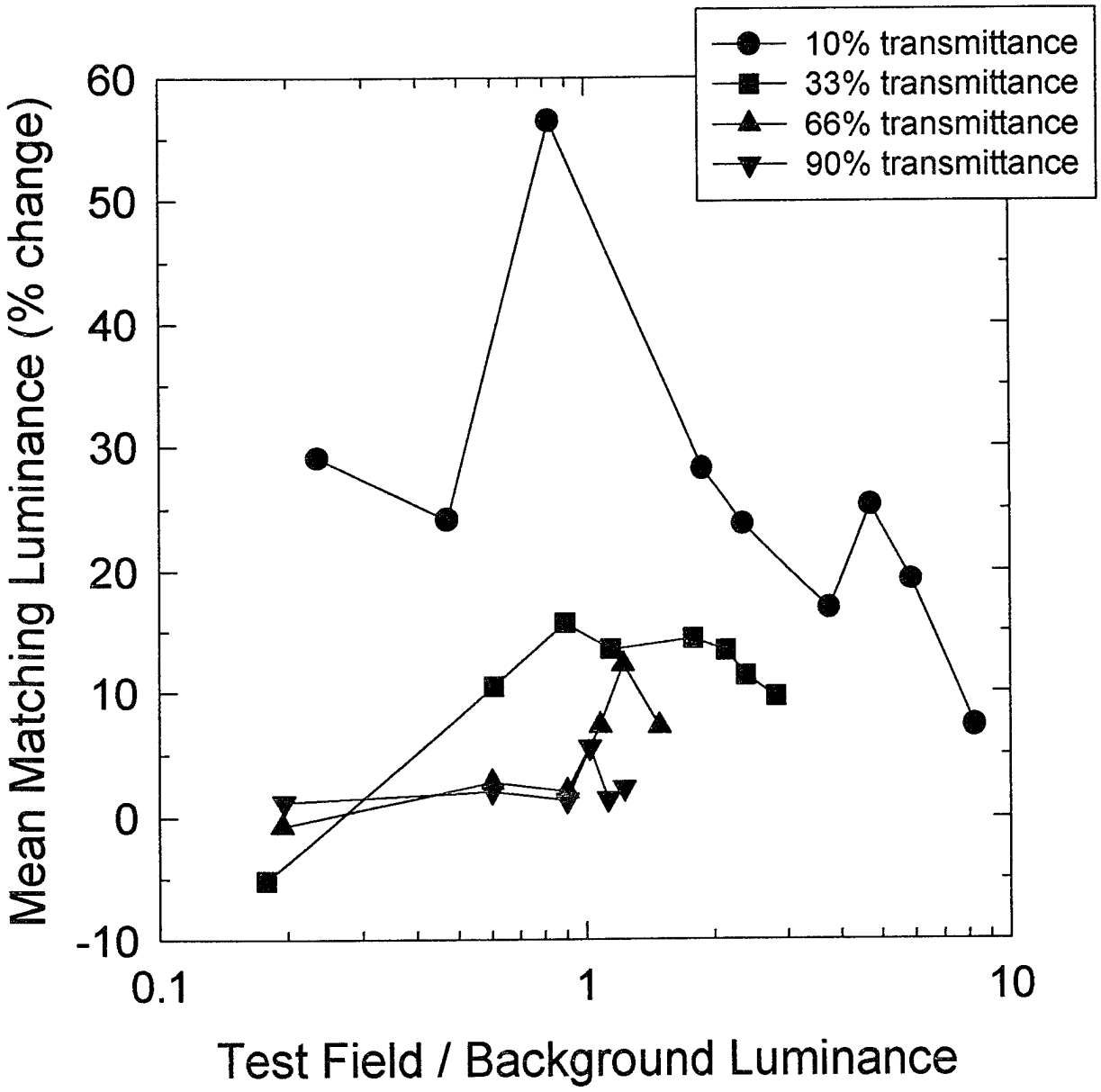
Transparency-with-Stereo-Depth-Cues
versus Other Three Conditions (mean)
10% transmittance
33% transmittance
66% transmittance
90% transmittance
Mean Matching Luminance (% change)
60
50
40
30
20
10
0
-10
0.1
1
10
Test Field / Background Luminance

LETTER TO THE EDITOR

In defence of "lateral inhibition" as the underlying cause of simultaneous brightness contrast. A reply to Spehar, Gilchrist & Arend.

by

Frederick A. A. Kingdom,* Mark E. McCourt† and Barbara Blakeslee†

*McGill Vision Research Unit
687 Pine Av. W. Rm. H4-14
Montreal, Quebec, H3A 1A1
Canada
[*Email* fred@jiffy.vision.mcgill.ca]

†Department of Psychology
North Dakota State University
Fargo, ND, 58105-5075
USA

Vision Research
(in press)

Illusory, or induced, brightness phenomena have for many years interested vision scientists because they offer the potential to reveal fundamental truths concerning the mechanisms of brightness and contrast processing. The traditional idea that such phenomena reflect the operation of "lateral inhibition", a term which predates and is cognate to the modern usage of "bandpass filtering", has recently come under attack from a number of quarters. It has been shown for instance, in the classic demonstration of simultaneous contrast in which two identical grey patches appear markedly different in brightness depending on the luminance of their backgrounds, that the magnitude of the brightness difference between the grey patches depends on whether the viewer perceives the backgrounds to be of different reflectance (identically illuminated), or of identical reflectance (differently illuminated) (Gilchrist, 1977; 1979; see also Knill & Kersten, 1991, and Adelson, 1993). Such important demonstrations reveal that low-level brightness percepts are susceptible to modification by secondary (presumably higher order, but poorly-understood) visual processes which, for example, are invoked to establish whether intensity variations within scenes are based on reflectance or illumination changes. These demonstrations do not, however, discredit the substantial body of evidence which links simultaneous contrast phenomena to early visual filtering operations.

One of the strongest such links concerns the variety of simultaneous contrast known as the grating induction effect (McCourt, 1982). This effect refers to the illusory, "induced", grating observed in a uniform test stripe that runs orthogonal to the orientation of the bars of a real, "inducer", grating. We have recently shown that the detection of real gratings can be facilitated by induced gratings, under some circumstances to a degree identical to that found for a real grating with the same spatial characteristics and perceived contrast (Kingdom & McCourt, 1993; McCourt & Kingdom, 1995). The fact that the induced brightness variations could act as almost

perfect metamers of real luminance variations is simply not consistent with the view that the simultaneous contrast effects revealed in grating induction reflect the operation of high level perceptual processes. Instead it shows that the same mechanisms which transduce real luminance variations (i.e., contrast) are transducing the illusory luminance variations as well. These mechanisms are generally understood to be retinal and cortical neurons whose receptive fields perform bandpass spatial filtering operations on the distribution of luminance in scenes.

It is therefore of particular interest when new evidence is brought forward and interpreted to challenge this traditional view, and the recent study by Spehar, Gilchrist and Arend (Vision Research, 1995, 35, 2603-2614) is such a case in point. Spehar et al. measured the magnitude of brightness induction in two previously quite well-studied effects: White's effect (White, 1979) and grating induction. The simplest and arguably best understood of these two varieties of simultaneous brightness contrast is grating induction, and we will therefore concentrate our response on Spehar et al's. claims concerning this phenomenon, although our analysis may apply to White's effect as well. Spehar et al. reported that the perceived contrast of induced gratings depended on the luminance of the test stripe relative to that of the mean of the inducer grating. When test stripe luminance was either higher or lower than the mean of the inducer grating, the perceived contrast of the induced grating was reduced compared with the situation when the test stripe was at the mean luminance of the inducer (see their Figure 3). Spehar et al. regard as critical however their finding that when the luminance of the test stripe exceeds the peak of the inducer, or falls below that of the trough, no induced grating was observed. Spehar et al. concluded that ".....we have demonstrated the importance of qualitative boundaries in the luminance relationships that support the appearance

of both White's effect and Foley and McCourt's grating induction: the luminance of the test patches must lie within the range of luminances of the grating stripes ..... when this constraint is violated the effects are not observed. None of the existing models can readily accommodate these findings" (p 2163). Because previous models of grating induction have emphasised the role of early bandpass filters to account for grating induction (Foley & McCourt, 1985; Moulden & Kingdom, 1991) Spehar et al. clearly regard their results as constituting an important challenge to such an approach.

In this communication we show that the findings of Spehar et al. are in fact precisely what one would expect from the operation of bandpass filters normally associated with signalling real luminance contrast. We begin with a simple demonstration to refute Spehar et al's assertion that, when test stripe luminance is greater than the peak, or less than the trough luminance of the grating, no grating induction is ever found. Figure 1 shows that this is not the case when the inducer grating is of a low spatial frequency. An induced grating is observed in all three test stripes in Figure 1 yet only the luminance of the middle stripe, B (set to the mean luminance of the inducing grating) lies within the luminance range of the grating. The apparent contrast of induced gratings in test fields A and C (43% above and below mean luminance, respectively), are reduced relative to that seen in B, and especially in C, but are visible nonetheless.

The obvious question is: Why was this induction not observed by Spehar et al.? As explanation we begin by noting that they used sub-optimal stimuli and hence produced only weak grating induction in the first place. For instance, they employed square-wave rather than sinewave inducing gratings. The former are known to produce much (up to 40%) weaker levels of induction than sinewaves of identical

spatial frequency (McCourt, 1982; McCourt & Foley, 1985). In addition, their inducer possessed a relatively high spatial frequency, and their test fields were rather large -- the exact values of which are not reported, but inspection of their Figure 3 reveals that they might have been approximately 0.25 c/d, and 2 deg, respectively. Grating induction magnitude is a lowpass function of spatial frequency and is inversely related to test field height, falling, for example, to half-maximum amplitude for a 2 deg test field at a spatial frequency as low as 0.15 c/d (McCourt, 1982). Because the magnitude of grating induction in the stimulus displays of Spehar et. al. was initially so low, we do not regard it as particularly surprising or significant that the effect of setting test stripe luminance to lie outside the luminance range of the inducer grating was to render the induced brightness variations invisible to their observers in that particular stimulus condition. In other words, we believe Spehar et. al. have overinterpreted their negative results, mistaking what is essentially a basement effect for a real effect of test field luminance. The amplitude of grating induction does diminish as the luminance of the test stripe departs from the mean luminance of the inducer, but not in the categorical way suggested by Spehar et al. The results of an extensive series of quantitative pointwise brightness matching experiments (McCourt, 1994) confirms both the earlier work of Foley & McCourt (1985) and McCourt (1982), and the demonstrations of both our Fig. 1, and Fig. 3 of Spehar et al.

Why then does the magnitude of grating induction diminish as the test stripe luminance increasingly departs from that of the mean of the inducer ? A strong clue to the answer to this question is given by inspection of Figure 2, which shows the analogous situation for real grating stimuli. Instead of an induced grating, each test stripe in Figure 2 contains a real grating of the same amplitude (14% of maximum luminance), and the three test stripes are now shown on a uniform background

rather than on one containing an inducer grating. The amplitude of the real grating in Figure 2 has been set by inspection to give roughly the same resultant apparent contrasts as those of the induced gratings in Figure 1. The pattern of apparent contrasts of the real gratings in Figure 2 is virtually identical to that of the induced gratings in Figure 1, suggesting that the reduced visibility of the outer test stripes in both Figures has a similar underlying cause. A simple explanation now immediately lends itself. It is widely believed from studies of contrast discrimination (Legge & Foley, 1980; Wilson, 1980; Greenlee & Heitger, 1988; Kingdom & Whittle, 1995), contrast magnitude estimation (Gottesman, Rubin & Legge, 1981), contrast or brightness scaling (Whittle, 1993) and contrast matching (Swanson, Wilson &Giese, 1984) that contrast transduction involves a compressive nonlinearity which depends on contrast, at least over much of the suprathreshold range*. Such a contrast-dependent compressive nonlinearity can explain the reduced visibility of the gratings in the outer test stripes of Figure 2. In the outer test stripes the grating is effectively sitting on a "pedestal" contrast produced by the luminance difference between the test stripe and the background. This pedestal serves to push the response of the mechanisms sensitive to the luminance variations of the grating into the compressed part of the response range, thus reducing the apparent contrast of the grating compared to that in the middle stripe where no pedestal is present.

If this is accepted as the explanation of the reduced visibility of the real gratings in the outer test stripes of Figure 2, then a simple filtering model incorporating the

---

* There are alternative explanations for the results of contrast discrimination studies to that of a compressive contrast transducer function. For example Legge, Kersten & Burgess (1987) have shown that contrast discrimination thresholds can be modelled in terms of a linear, rather than compressive contrast transducer function with multiplicative, rather than additive internal noise, and Foley (1994) has modelled contrast discrimination thresholds using the notion of divisive inhibition. Two points are worth mentioning in the light of these alternatives. First, our demonstrations involve suprathreshold levels of "ΔC" with respect to "pedestal" contrast C, if C is considered to be the contrast of the test stripe and ΔC the modulation of the grating within it. Thus our findings are not necessarily cognate with those from contrast discrimination experiments which by definition involve threshold levels of ΔC. Second, even if they are, a compressive nonlinearity is still an adequate mathematical model for our purpose even if not necessarily correct physiologically.

compressive nonlinearity will account for the appearance of the induced gratings in Figure 1, as well as the real gratings in Figure 2. The model is illustrated schematically in Figure 3. The essential idea is that both the induced and real gratings in the test stripes are signalled by a bandpass filter with a conventional centre-surround receptive field organisation, whose receptive field centre fits just within the width of the test stripe, and whose surround falls outside the stripe. Such a filter is optimal for signalling, within the test stripe, the presence of either an inducer outside the test stripe, or a real grating within it, provided that the gratings have a cycle width significantly larger than the height of the test stripe. The filter shown in Figure 3 is oriented, though a circularly symmetric filter would suffice just as well, as we have shown previously (Foley & McCourt, 1985; Moulden & Kingdom, 1991).

Figure 3 shows the model as applied to the illusory gratings of Figure 1, but is essentially identical in its predictions for the real gratings in Figure 2, though for this the luminance profile in Figure 3a needs to be phase-reversed. In the Figure, A, B and C refer respectively to the test stripes greater than, equal to and less than the luminance of the background. Figure 3a shows the luminance profile of the inducer in Figure 1 (phase reversed for the real gratings in Figure 2) with the dashed lines representing the luminance of the three test stripes. Figure 2b shows an oriented filter sitting within each test stripe, the arrows indicating that the filter is being convolved with the stimulus along the length of the test stripe. Assuming linear spatial summation, the resulting convolution outputs are shown in Figure 3c, with the dotted lines showing the zero response levels. Notice that the responses are 180 degrees out of phase with the inducer grating (Figure 3a) in accordance with the percept, because it is the inhibitory surround of the filter that is stimulated directly by the inducer grating. If applied to the stimulus in Figure 2, the excitatory centre of the

filters would be stimulated directly, producing in-phase modulation. Notice also that whereas in the case of B the response modulation is about zero, in A it is modulated about a positive dc response level, and in C around a negative dc response level. These dc levels can be thought of as"pedestal" levels of response. In Figure 3d we simply assume there is a compressive nonlinearity on the *absolute* response, while preserving its sign, and as shown this has the effect of reducing the amplitude of the response modulations in A and C compared with B. It is this reduction in response amplitude which we argue is the cause of the reduced visibility of the gratings in the outer stripes in Figures 1 and 2. The model incidentally also accounts for the rapid fall off in the magnitude of grating induction with inducer spatial frequency for a constant test height, as has been previously demonstrated by Moulden & Kingdom (1991), at least for circularly symmetric filters.

Although we have illustrated only the operation of an ON-centre oriented filter in Figure 3, it is of course widely believed that the below zero components of the convolution responses shown in the Figure would likely be carried by filters tuned to other phases, such as OFF-centre filters, with the outputs of all classes of filter being half-wave rectified. If modelled in such a way it would not have been necessary to apply the compressive nonlinearity to the absolute responses while at the same time preserving the sign of the response. We have used the single class of filter however for simplicity of exposition. We also wish to emphasize that we are not asserting or implying that only one receptive field size of filter is involved in grating induction. Doubtless filters not optimally tuned to the test stripe height will contribute to some degree or other to grating induction (e.g. see Moulden & Kingdom, 1991). Figure 3 is meant to illustrate how *in principle* the appearance of the gratings within the test stripes in Figures 1 and 2 can be simply explained using well-established notions about the mechanisms involved in signalling periodic luminance variations. We

are also well aware that higher level processes will undoubtedly modify the magnitude of the induced gratings produced by the early filtering mechanisms that we have postulated. In particular, the mechanisms which are believed to be involved in integrating local contrast information across luminance boundaries to establish, generally, a more veridical representation of the reflectance of surfaces (Arend, Buehler & Lockhead, 1971; Arend, 1973; Arend & Goldstein, 1987; Arend, 1994; Gilchrist, 1979, 1994; Kingdom & Moulden, 1988; Kingdom & Moulden, 1992), undoubtedly act in some circumstances to reduce the magnitude of grating induction. McCourt & Blakeslee's (1993) finding that removing the high spatial frequencies from grating induction figures enhances the effect is pertinent to this issue, since it is likely that such integrative mechanisms principally employ the high spatial frequency information at the sharp edge boundaries of the test stripes.

In conclusion we have shown how a simple model consisting of a bandpass filter with a contrast-dependent compressive nonlinearity can account for the appearance of the illusory gratings in the study of Spehar et al. In so far as bandpass filters can be said to exhibit what is traditionally referred to as "lateral inhibition", we assert that lateral inhibition is the simplest and still most plausible explanation of grating induction. Furthermore, since White's effect and other forms of simultaneous brightness contrast have many properties in common with grating induction, we suggest that such an explanation is likely applicable to these phenomena as well.

Acknowledgements

This study was supported by a grant from the Medical Research Council of Canada (MT 11554) given to Fred Kingdom, and grants from the National Eye Institute (EY-1-

13301) and the Air Force Office of Scientific Research (F49620-94-1-0445) given to Mark McCourt and Barbara Blakeslee.

References

Arend, L. E. (1973). Spatial differential and integral operations in human vision: implications of stabilized retinal image fading. Psychological Review, 80, 374-395.

Arend, L. E., Buehler, J. N. & Lockhead, G. R. (1971). Difference information in brightness perception. *Perception & Psychophysics, 9,* 367-370.

Arend, L. E. and Goldstein, R. (1987). Lightness models, gradient illusions, and curl. *Perception & Psychophysics, 42,* 65-80.

Arend, L. E. (1994). Surface colors, illumination, and surface geometry: Intrinsic-image models of human color perception. In Gilchrist (Ed.), *Lightness, Brightness, and Transparency,* (pp. 159-213). Hillsdale: Erlbaum.

Adelson, E. H. (1993). Perceptual organization and the judgement of brightness. *Science, 262,* 2042-2044.

Foley, J. M. (1994). Human luminance pattern-vision mechanisms: masking experiments require a new model. *Journal of the Optical Society of America, A, 11,* 1710-1719.

Foley, J. M. & McCourt, M. E. (1985). Visual grating induction. *Journal of the Optical Society of America, A, 2,* 1220-1230.

Gilchrist, A. L. (1977). Perceived lightness depends on perceived spatial arrangement. *Science, 195,* 185-187.

Gilchrist, A. L. (1979). The perception of surface blacks and whites. *Scientific American, 240,* 112-123.

Gilchrist, A. L. (1994). Absolute versus relative theories of lightness perception. In Gilchrist (Ed.), *Lightness, Brightness, and Transparency,* (pp. 1-33). Hillsdale: Erlbaum.

Gottesman, J., Rubin, G. S. & Legge, G. E. (1981). A power law for perceived contrast in human vision. *Vision Research, 21,* 791-799.

Greenlee, M. W. & Heitger, F. (1988). The functional role of contrast adaptation. *Vision Research, 28,* 791-797.

Kingdom, F. A. A. & McCourt. M. E. (1993). Do illusory gratings behave like real gratings ? *Perception, 22,* A5.

Kingdom, F. & Moulden, B. (1988). Border effects on brightness: A review of findings, models and issues. *Spatial Vision, 3,* 225-262.

Kingdom, F. & Moulden, B. (1992). A multi-channel approach to brightness coding. *Vision Research, 32,* 1565-1582.

Kingdom, F. A. A. & Whittle, P. (1995). Contrast discrimination at high contrasts reveals the influence of local light adaptation on contrast processing. *Vision Research,* In Press.

Knill, D. C.. and Kersten, D. (1991). Apparent surface curvature affects lightness perception. *Nature, 351,* 228-230.

Legge, G. E. & Foley, J. M. (1980). Contrast masking in human vision. *Journal of the Optical Society of America, 70,* 1458-1471.

Legge, G. E. Kersten, D. & Burgess, A. E. (1987). Contrast discrimination in noise. *Journal of the Optical Society of America, A., 4,* 391-404

McCourt, M. E. (1992). A spatial frequency dependent grating-induction effect. *Vision Research, 22,* 119-134.

McCourt, M. E.. (1994). Grating induction: a new explanation for stationary visual phantoms. *Vision Research, 34,* 1609-1618.

McCourt, M. E. & Blakeslee, B. (1993). The effect of edge blur on grating induction magnitude. *Vision Research, 33,* 2499-2508.

McCourt, M. E.. and Foley, J. M. (1985). Spatial frequency interference on grating-induction. *Vision Research, 25,* 1507-1518.

McCourt, M. E. & Kingdom, F. A. A. (1995). Facilitation of luminance grating detection by illusory gratings. *Vision Research,* In Press.

Moulden, B. and Kingdom, F. (1991). The local border mechanism in grating induction. *Vision Research, 31,* 1999-2008.

Spehar, B., Gilchrist, A. & Arend, L. (1995). The critical role of relative luminance relations in White's effect and grating induction. *Vision Research, 35,* 2603-2614.

Swanson, W. H., Wilson, H. R. and Giese, S. C. (1984). Contrast matching data predicted from increment thresholds. *Vision Research, 28,* 457-459.

White, M. (1979). A new effect of pattern on perceived lightness. *Perception, 8,* 413-416.

Whittle, P. (1993). Brightness, discriminability and the "crispening effect". *Vision Research, 32,* 1493-1507

Wilson, H. R. (1980). A transducer function for threshold and suprathreshold human vision. *Biological Cybernetics, 38,* 171-178.

Figure Legends

Figure 1. Grating induction with a low spatial frequency sine-wave inducer. The luminances of the three uniform test stripes are from top to bottom: A greater than the peak, B at the mean, and C less than the trough of the inducer. The contrast of the inducer on the monitor surface was 60%, making its peak 80% and trough 20% of maximum luminance. A, B and C were 7%, 50% and 97% of maximum luminance respectively. Note that due to the limitations of photographic reproduction these values may be slightly inaccurate in the actual Figure.

Figure 2. The effect of test stripe luminance with real gratings. A sine-wave with an amplitude of 14% of maximum luminance has been added to each of the three test stripes, whose luminances are the same as in Figure 1. The background is uniform and of the same mean luminance as in Figure 1.

Figure 3. Schematic representation of a simple model for the appearance of the gratings in the test stripes in Figures 1 and 2. For explanation see text.

Figure 1

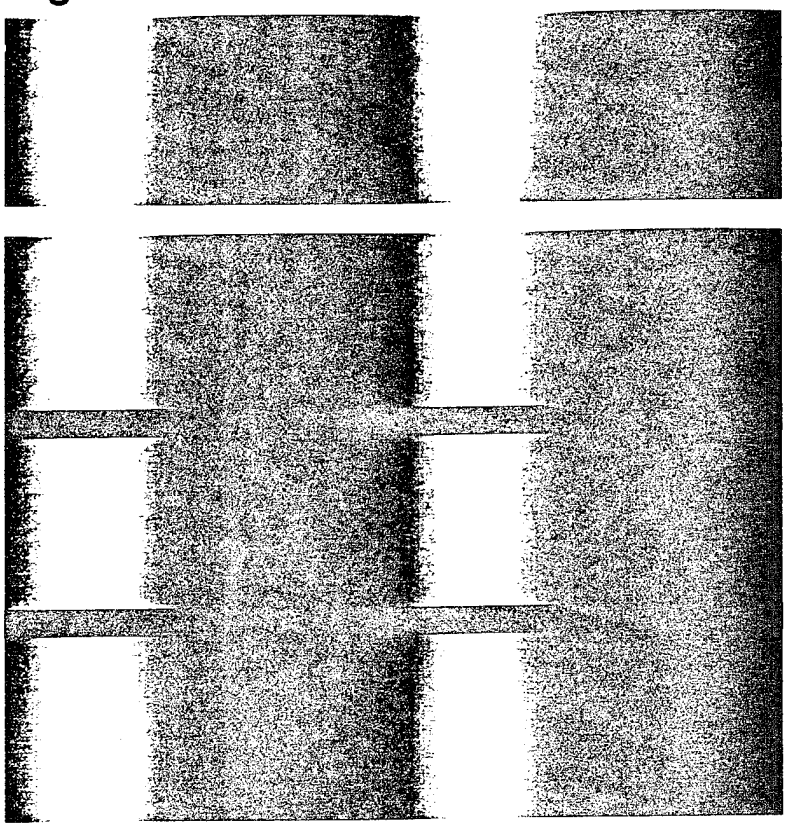

Figure 2

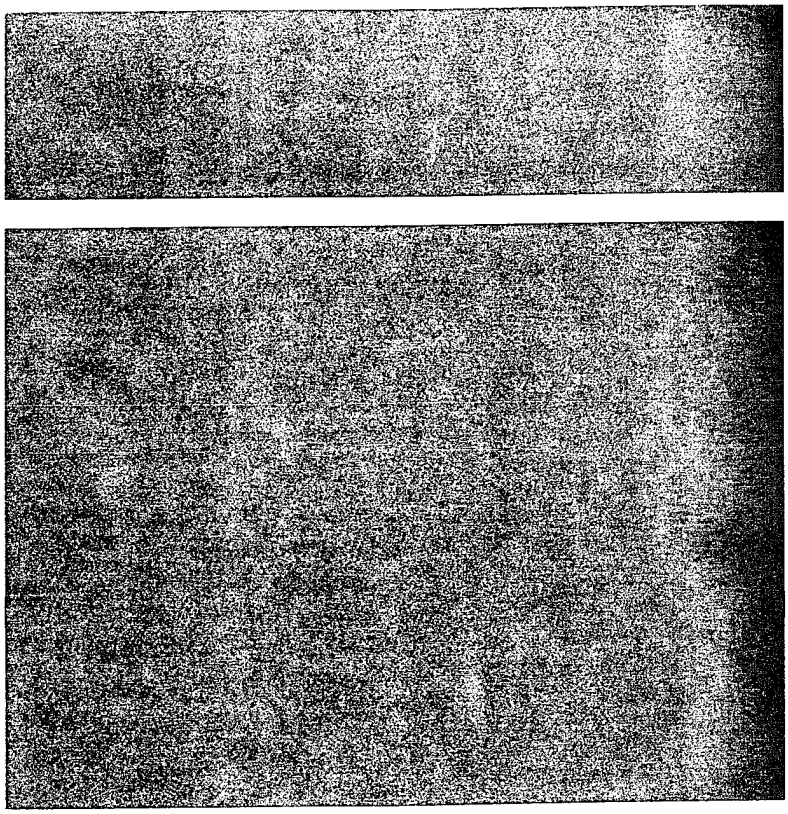

FIG.

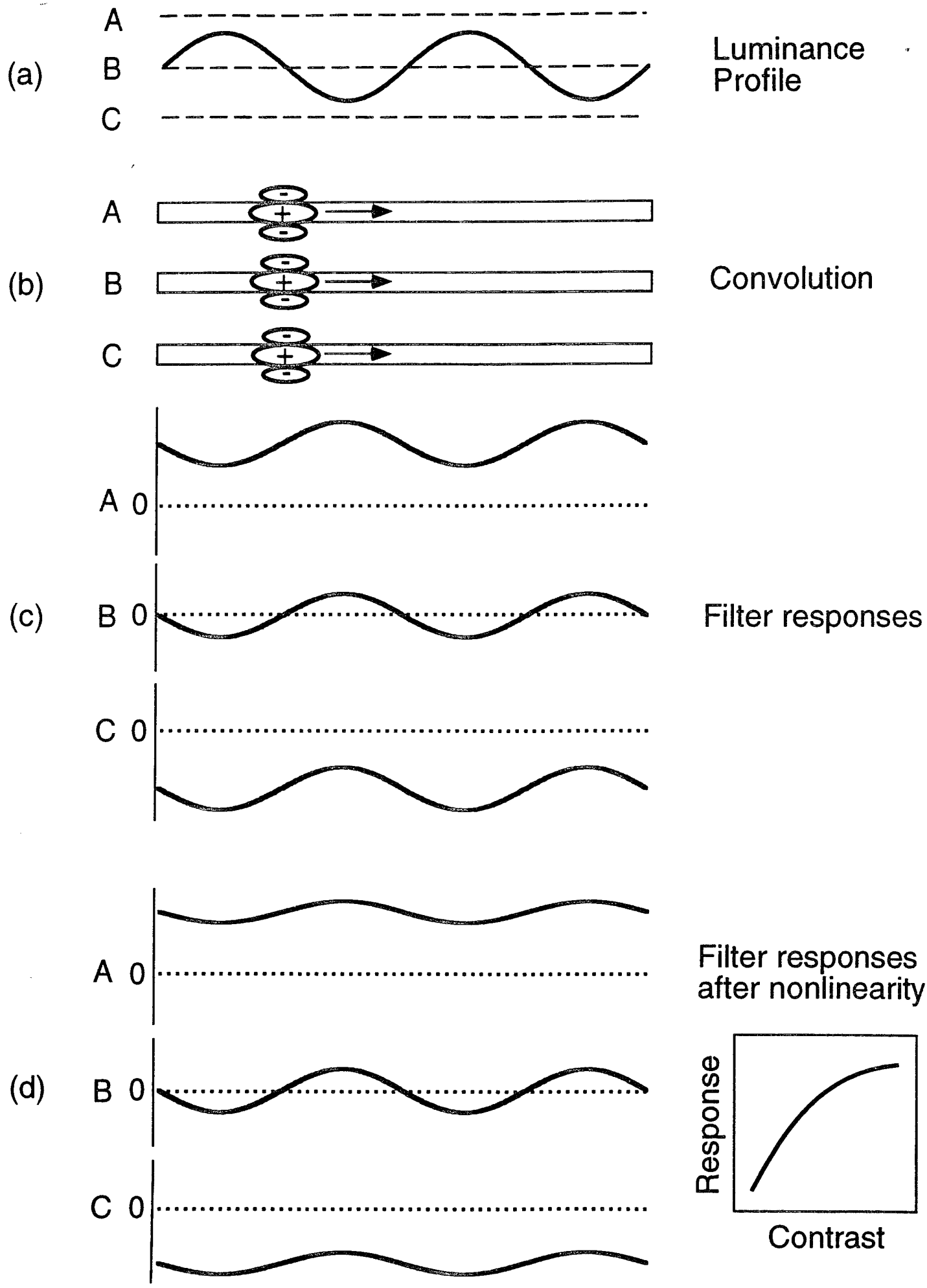
(a)
A
B
C
Luminance Profile
(b)
A
B
C
Convolution
A 0
(c)
B 0
C 0
Filter responses
A 0
(d)
B 0
C 0
Filter responses after nonlinearity
Response
Contrast